# Appendix E
# FCT Document Cover Sheet

| | |
|---|---|
| Name/Title of Deliverable/Milestone/Revision No. | Update UNF-ST&DARDS criticality report - M3SF-19OR0204050160 |
| Work Package Title and Number | Commercial SNF Characterization – ORNL, SF-19OR02040501 |
| Work Package WBS Number | 1.08.02.04.05 |
| Responsible Work Package Manager | Kaushik Banerjee |
| | (Name/Signature) |

Date Submitted 09/20/2019

| Quality Rigor Level for Deliverable/Milestone | ☒ QRL-3 | ☐ QRL-2 | ☐ QRL-1<br>☐ Nuclear Data | ☐ Lab Participant QA Program (No additional FCT QA requirements) |
|---|---|---|---|---|

This deliverable was prepared in accordance with ORNL
*(Participant/National Laboratory Name)*

QA program which meets the requirements of
☐ DOE Order 414.1 ☐ NQA-1-2000 ☒ NQA-1-2008

**This Deliverable was subjected to:**

☒ Technical Review

**Technical Review (TR)**
**Review Documentation Provided**
☐ Signed TR Report or,
☒ Signed TR Concurrence Sheet or,
☐ Signature of TR Reviewer(s) below

**Name and Signature of Reviewers**

☐ Peer Review

**Peer Review (PR)**
**Review Documentation Provided**
☐ Signed PR Report or,
☐ Signed PR Concurrence Sheet or,
☐ Signature of PR Reviewer(s) below

**NOTE 1:** *Appendix E should be filled out and submitted with the deliverable. Or, if the PICS:NE system permits, completely enter all applicable information in the PICS:NE Deliverable Form. The requirement is to ensure that all applicable information is entered either in the PICS:NE system or by using the FCT Document Cover Sheet.*

**NOTE 2**: *In some cases there may be a milestone where an item is being fabricated, maintenance is being performed on a facility, or a document is being issued through a formal document control process where it specifically calls out a formal review of the document. In these cases, documentation (e.g., inspection report, maintenance request, work planning package documentation or the documented review of the issued document through the document control process) of the completion of the activity, along with the Document Cover Sheet, is sufficient to demonstrate achieving the milestone. If QRL 1, 2, or 3 is not assigned, then the Lab / Participant QA Program (no additional FCT QA requirements) box must be checked, and the work is understood to be performed and any deliverable developed in conformance with the respective National Laboratory /Participant, DOE or NNSA-approved QA Program.*

## Documents

| | |
|---|---|
| Internal Document | PB1901109_Clarity_Criticality_to_JOHN.pdf |
| Published Document | PB1901109_Clarity_Criticality_to_JOHN.pdf |

## Reviewers

Requested Release Date: Sep 18, 2019

| Workflow | Reviewer | Duration (avg.) | |
|---|---|---|---|
| Derivative Classifier<br>*Added by keywords* |  Ellen Saylor | 2 days | charge number |
| Technical Editor<br>*Required by Reactor & Nuclear Systems Division* |  Rose Raney | 4 days | 35304D78 |
| Technical Reviewer |  Bret Brickner | 7 days | |
| Technical Reviewer<br>*Required by Reactor & Nuclear Systems Division* |  Georgeta Radulescu | 7 days | |
| Supervisor |  Douglas Bowen | 3 days | |
| Program Manager<br>*Required by Reactor & Nuclear Systems Division* |  John Scaglione | 1 days | |
| Export Control<br>*Added by keywords* |  Edward Graham | 2 days | |
| Administrative Check<br>*Required by Reactor & Nuclear Systems Division* |  Marsha Henley | 1 days | |
| Division Approver |  Jeremy Busby | 3 days | |
| Releasing Official |  Leesa Laymance | 3 days | |

DRAFT

# *Criticality Process, Modeling and Status for UNF-ST&DARDS*

## Fuel Cycle Research & Development

*Prepared for*
*US Department of Energy*
*Integrated Waste Management*

*Oak Ridge National Laboratory:*
*J. B. Clarity, K. Banerjee, and L. P. Miller*

*September 20, 2019*

**M3SF-19OR0204050160**
**FCRD-NFST-2015-000440, Rev. 2**
**ORNL/TM-2015/362, Rev. 2 (ORNL/SPR-2019-1318)**

**DISCLAIMER**

This information was prepared as an account of work sponsored by an agency of the U.S. Government. Neither the U.S. Government nor any agency thereof, nor any of their employees, makes any warranty, expressed or implied, or assumes any legal liability or responsibility for the accuracy, completeness, or usefulness, of any information, apparatus, product, or process disclosed, or represents that its use would not infringe privately owned rights. References herein to any specific commercial product, process, or service by trade name, trade mark, manufacturer, or otherwise, does not necessarily constitute or imply its endorsement, recommendation, or favoring by the U.S. Government or any agency thereof. The views and opinions of authors expressed herein do not necessarily state or reflect those of the U.S. Government or any agency thereof.

Revision History

| Version | Description |
|---|---|
| FCRD-NFST-2015-000440 | Initial Release |
| FCRD-NFST-2016-000440, Rev. 1 | This revision updates or adds three items to the report. In the order that they appear in the report, the three changes are (1) an update to Table 22 in Section 5, which documents the status of the sites that have been analyzed, (2) replacement of the tabular $k_{eff}$ results presented in Appendix B with a query that is capable of retrieving the results from the Unified Database, and (3) the addition of Appendix C, which justifies the BWR burnup credit approach for as-loaded criticality analysis within UNF-ST&DARDS. Changes in the main body are identified by a black vertical line in the margin. |
| FCRD-NFST-2016-000440, Rev. 2/ M3SF-19OR0204050160 | This revision updates or adds three items: (1) and update to Table 22 in Section 5, which documents the status of the sites that have been analyzed, (2) addition of the Appendices sections A.13 and A.14 to document the CSAS6 models of the NUHOMS® 61BT/BTH-DSC and NUHOMS® 32PTH/PTH1 DSC canisters, and (3) an update to the query provided in Appendix B to extract results. The query has been updated to accommodate the more recent updates to the UDB table names. |

# SUMMARY

This report documents the Used Nuclear Fuel – Storage, Transportation & Disposal Analysis Resource and Data System (UNF-ST&DARDS) criticality analysis process development effort through fiscal year (FY) 2019. Included in this work are descriptions of the UNF-ST&DARDS components, safety analysis codes, templates, and analytical approaches used in the criticality analysis process. Special attention is paid to describing the templates used in the criticality analysis process, the information they require, and how the templates relate to one another. A detailed description of each of the canister-specific criticality analysis templates that have been developed and an assessment of the sites that have been analyzed are also provided. A database query that can be used to extract the criticality analysis results from the Unified Database (UDB) is provided in Appendix B. Finally, the approach used to take burnup credit for Boiling Water Reactor (BWR) fuel for as-loaded criticality analysis is also presented.

This page is intentionally left blank.

# CONTENTS

# LIST OF FIGURES

# LIST OF TABLES

# ACRONYMS

| | |
|---|---|
| BWR | boiling water reactor |
| CSAS6 | Criticality Safety Analysis Sequence using Keno-VI |
| CY-MPC | Connecticut Yankee Multipurpose Canisters |
| DFC | damaged fuel can |
| DSC | Dry Shield Canister |
| FC | Fuel and Component |
| FCRD | Fuel Cycle Research and Development |
| FF | Failed Fuel |
| FO | Fuel Only |
| FY | fiscal year |
| FSAR | final safety analysis report |
| HB | Humboldt Bay |
| HI | Holtec International |
| JSON | JavaScript Object Notation |
| LACBWR | La Crosse Boiling Water Reactor |
| MPC | Multipurpose Canisters |
| MTU | Metric Tons of Uranium |
| NFST | Nuclear Fuels Storage and Transportation Planning Project |
| NRC | Nuclear Regulatory Commission |
| ORIGAMI | ORIGEN Assembly Isotopics |
| ORIGEN | Oak Ridge Isotope Generation and Depletion Code |
| ORNL | Oak Ridge National Laboratory |
| PWR | pressurized water reactor |
| RW-859 | Office of Civilian Radioactive Waste Management 859 database |
| SAR | safety analysis report |
| SNF | spent nuclear fuel |
| STC | storable transport cask |
| TRITON | Transport Rigor Implemented with Time-dependent Operations for Neutronic depletion |
| UDB | Unified Database |
| UNF | used nuclear fuel |
| UNF-ST&DARDS | Used Nuclear Fuel – Storage, Transportation & Disposal Analysis Resource and Data System |

This page is intentionally left blank.

# CRITICALITY PROCESS, MODELING, AND STATUS FOR UNF-ST&DARDS

## 1. INTRODUCTION

This report documents work performed supporting the US Department of Energy (DOE) Office of Nuclear Energy (NE) Spent Fuel and Waste Disposition (SFWD) Integrated Waste Management under work breakdown structure element 1.08.02.04.05, "Commercial SNF Characterization." In particular, this report fulfills milestone M3SF-19OR0204050160, "Update UNF-ST&DARDS criticality report" as Revision 2 to FCRD-NFST-2016-000440, "Criticality Process, Modeling and Status for UNF-ST&DARDS," within work package SF-19OR02040501, "Commercial SNF Characterization – ORNL."

This report discusses the criticality analysis process within Used Nuclear Fuel – Storage, Transportation & Disposal Analysis Resource and Data System (UNF-ST&DARDS) [1]. The UNF-ST&DARDS criticality analysis process performs full (actinides and fission products) burnup credit calculations for as-loaded storage and transportation canisters using an automated template-based process. The codes, methods, and flow of information necessary to develop canister-specific criticality analysis models are discussed in this report.

The safety analysis cases for the current generation of multipurpose canisters (MPC) are developed by the cask vendors to demonstrate that the storage and transportation casks will remain subcritical under normal, off-normal, and accident conditions of spent fuel storage, and normal and accident conditions of transportation. The vendors have implemented a simplified and conservative approach in demonstrating compliance with the regulations including use of a fresh fuel assumption, or a very conservative implementation of burnup credit. Additionally, the licensing basis is also able to accommodate a variety of fuel designs and operating conditions within a single licensing application. The models used to support these licensing applications provide flexibility, but also result in large margins of safety for an actual as-loaded canister system.

UNF-ST&DARDS is being developed to perform as-loaded analysis of spent nuclear fuel (SNF) storage, transportation, and disposal systems. UNF-ST&DARDS provides a comprehensive and unified domestic SNF system database integrated with analysis tools to perform automated nuclear safety-related analyses. The information flow within UNF-ST&DARDS is illustrated in Fig. 1. As depicted in Fig. 1, data are collected from available sources (e.g., open literature, vendor-provided data); verified; and incorporated into the UDB for subsequent use by integrated nuclear safety and systems analysis tools. Data and analysis tool integration is a powerful UNF-ST&DARDS feature that enables assembly- and cask-specific nuclear safety assessments based on actual assembly characteristics of as-loaded SNF (e.g., fuel assembly burnup, enrichment, decay time). Integration of these tools helps to quantify realistic safety margins associated with actual fuel loading compared with the regulatory licensing limits. All of these processes are streamlined within UNF-ST&DARDS using the consolidated data from the UDB, a suite of SNF application input templates processed by an application-agnostic template engine, and the computational processes tailored for analysis of SNF.

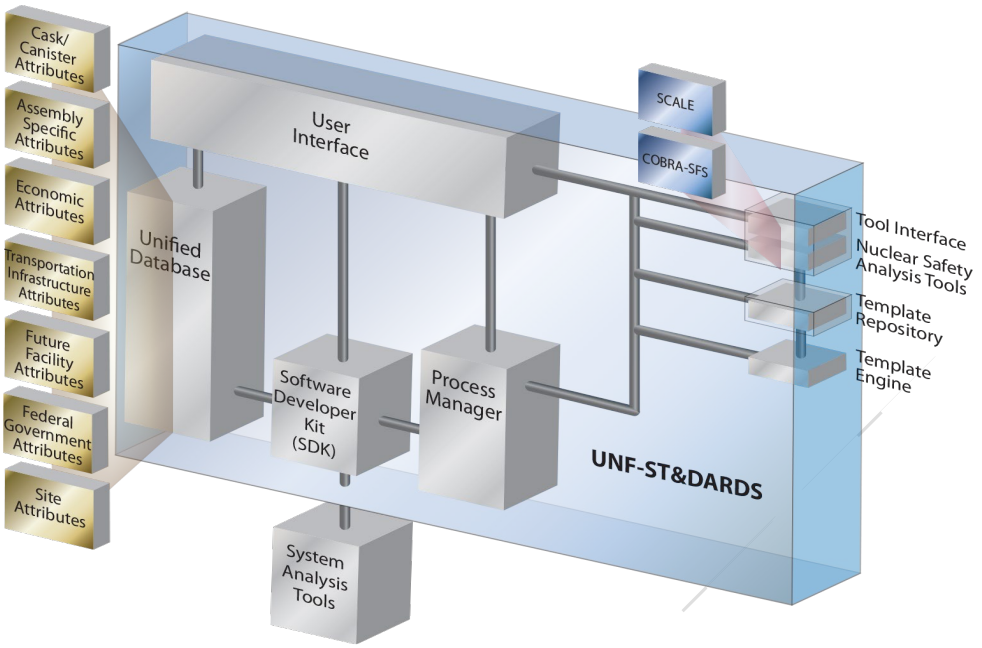


**Fig. 1. UNF-ST&DARDS structure. Source: Adapted from K. Banerjee et al., Safety Analysis Capabilities of the Used Nuclear Fuel Storage, Transportation and Disposal Analysis Resource and Data System, FCRD-NFST-2014-000360/ORNL/LTR-2014/414, Oak Ridge National Laboratory, Oak Ridge, Tenn., September 2014.**

This report provides documentation of the development of the criticality analysis capabilities with UNF-ST&DARDS to date. Section 2 briefly discusses the criticality analysis modeling approach. Section 3 provides an overview of the codes and process used for criticality analysis. Section 4 provides a detailed discussion of the depletion, decay, and criticality analysis templates and their connection to one another. Section 5 discusses the status of the criticality models and sites that have been analyzed through the end of FY 2015. Appendix A contains detailed information with respect to the model dimensions and verification, and Appendix B contains the calculated $k_{eff}$ values for the analyzed sites not included in Ref 1.

# 2. UNF-ST&DARDS CRITICALITY ANALYSIS APPROACH

This section provides a brief discussion the modeling approaches implemented in UNF-ST&DARDS for as-loaded criticality calculations using full (actinides and fission products) burnup credit. Each of the listed items below addresses an important aspect of a burnup credit criticality evaluation. Additionally, appropriate references to other sections or documents are provided to augment the information provided below.

1. Burnup credit analysis for intact fuel assemblies using fuel assembly isotopic concentrations corresponding to actual fuel assembly average initial enrichment, discharge burnup, and post-irradiation cooling time.
2. Axial burnup profiles demonstrated to be conservative for criticality evaluations are used to calculate fuel assembly isotopic concentrations (see Section 4.1.2).
3. The isotopic concentrations are generated with a set of depletion parameters demonstrated to be conservative with respect to criticality. For pressurized water reactor (PWR) fuel, the depletion calculations use bounding values for the burnable absorber rod insertion, soluble boron concentrations, and moderator densities. For boiling water reactor (BWR) fuel bounding, values for control blade insertion and moderator density are used. For further information, see Reference [3].
4. The isotope set, credited in the UNF-ST&DARDS criticality calculations is selected based on the burnup credit isotopes recommended by NUREG/CR-7108 and -7109 [7,8]. for the UNF storage and transportation. The credited isotopes are listed in Table 3 of Ref [1].
5. The nominal design dimensions of the actual fuel assembly type or a representative fuel assembly type are used in the criticality model for intact assemblies.
6. Damaged fuel modeling employs a more conservative modeling approach than is used for intact fuel and is consistent with the modeling techniques in the final safety analysis reports (FSAR) for storage and/or safety analysis reports (SAR) for transportation licensing evaluations. These fuel assembly models typically use a special fuel pin arrangement pattern to account for possible fuel lattice deformation and ignore credit for decreased enrichment of increased burnup relative to the design basis. The damaged fuel assumptions are handled on a canister or site specific basis and are discussed in more detail in each of the subsection of Appendix A.
7. Inclusion of fuel assembly components stored in the guide tubes of fuel assemblies such as burnable absorbers and control rods is under development.
8. Radially and axially centered fuel assemblies within the basket cells of the canister are used in the criticality models.
9. The canister models use water moderator and a 50-cm water reflector, both at a mass density of 1 g/cm$^3$ and temperature of 300 K.
10. Boron-10 concentration (areal density) in canister absorber plates is taken from FSAR/SAR.
11. Nominal canister dimensions are taken from the FSAR/SAR.
12. Model verification is performed for each canister model. Model verification is accomplished by attempting to replicate a case specified in the SAR or FSAR. Typically, SAR cases are used because they correspond to transport conditions, which is the primary application of UNF-ST&DARDS criticality analysis. However, storage cases are used in the event that the canister is not licensed for transportation or no non-burnup credit cases are available in the SAR. Once the case is selected and the appropriate fuel type, enrichment, and possible basket deformation is modeled the results are compared to those in the SAR or FSAR. Replication of the licensing

results can be affected by a paucity of information related to the case being modeled, differences in the code sets and cross sections used. Therefore, the calculated $k_{eff}$s are expected to be slightly different that in the FSAR/SAR. An attempt is generally made to explain the differences between licensing and calculated $k_{eff}$ values when the difference is large.

13. Bias and bias uncertainty associated with the isotopic concentrations used in the models is not currently considered (i.e., all $k_{eff}$ values reported in this report do not include bias and bias uncertainty in the isotopic concentrations).
14. Bias and bias uncertainty associated with the criticality code is not currently considered (i.e., all $k_{eff}$ values reported in this report do not include bias and bias uncertainty associated with the criticality code).
15. Criticality results from UNF-ST&DARDS are presented as margin to the licensing basis rather than as raw $k_{eff}$ values as is discussed in Ref 1. The margin values are calculated as the difference in $k_{eff}$ from model verification calculations based on the SAR to the value calculated by UNF-ST&DARDS with full burnup credit. Reporting the margin results alleviates the need to consider the isotopic or criticality code benchmarking because the purpose is to show the amount of uncredited margin is available.

# 3. UNF-ST&DARDS CRITICALITY ANALYSIS CODES AND PROCESS

This section discusses the process used to perform criticality calculations with UNF-ST&DARDS. Included in the discussion of the criticality analysis process are the relevant nuclear analysis codes, UNF-ST&DARDS software components, and the processes which relate each of the components.

## 3.1 Codes

The codes used in the UNF-ST&DARDS criticality analysis process are part of the SCALE computer code system [2], pre-release version 6.2. This section describes the codes used to perform depletion calculations to generate Oak Ridge Isotope Generation and Depletion Code (ORIGEN) cross section libraries, to produce discharge and decayed isotopic concentrations, and to perform three dimensional criticality calculations. The SCALE computer codes/sequences relevant to criticality process are Transport Rigor Implemented with Time-dependent Operations for Neutronic depletion (TRITON) for ORIGEN library generation, ORIGEN Assembly Isotopics (ORIGAMI) for development of discharge and decayed isotopic concentrations, and the Criticality Safety Analysis Sequence using Keno-VI (CSAS6) to determine canister $k_{eff}$ values. Each of the aforementioned codes is briefly discussed in the subsections below.

### 3.1.1 TRITON

The TRITON two-dimensional (2-D) depletion sequence ([2], Sect. T01) is used to perform depletion calculations that generate cross section libraries for generic assembly/reactor-specific classes and a range of fuel operating conditions, which subsequently can be used by ORIGAMI for rapid processing of problem-dependent cross sections. TRITON was used to generate a series of ORIGEN libraries for a variety of fuel assembly types in Reference [3]; these ORIGEN libraries are used for subsequent ORIGAMI depletion and decay calculations.

### 3.1.2 ORIGAMI

Assembly-specific isotopic inventories are generated with ORIGAMI, which is a SCALE 6.2 sequence dedicated to calculating nuclide inventories, decay heat, and radiation source terms for SNF assemblies with axial and radial burnup variations. This code performs fast ORIGEN depletion and decay calculations using pre-generated fuel assembly–specific ORIGEN one-group cross section libraries. UNF-ST&DARDS contains pre-generated ORIGEN cross section libraries for representative fuel assemblies within the fuel classes identified in the Office of Civilian Radioactive Waste Management (RW)-859 database [4], as discussed in Section 3.1.1.

### 3.1.3 CSAS6

Keno-VI as automated by CSAS6 is an extension of the Keno Monte Carlo criticality program developed for use in the SCALE system. Keno-VI contains all features currently in KENO V.a plus a more flexible geometry package known as the SCALE Generalized Geometry Package. The geometry package in Keno-VI is capable of modeling any volume that can be constructed using quadratic equations. In addition, such features as geometry intersections, body rotations, hexagonal and dodecahedral arrays, and array boundaries have been included to make the code more flexible.

Keno-VI Monte Carlo code with the continuous-energy ENDF/B-VII.0 cross section library was used to determine the effective neutron multiplication factor, $k_{eff}$, on a canister-specific basis. Note that a pre-released version of SCALE 6.2, which is under development, is used for continuous-energy criticality calculations. Currently, CSAS6 criticality calculations are typically performed with 800 active generations of 20000 neutrons per generation, with the initial 300 generations discarded (total of 1100 generations). Appropriate fission source convergence methodology will be implemented in UNF-ST&DARDS in future.

## 3.2 UNF-ST&DARDS COMPONENTS

UNF-ST&DARDS has subcomponent pieces of software that are used in the criticality safety analysis process. The principal components of concern to this report are the UDB, the Template Engine, the analysis templates, and the pre-generated ORIGEN libraries used to characterize the SNF assemblies. Each of those components is described in the subsections below.

### 3.2.1 Unified Database

The UDB provides a comprehensive, controlled source of technical data for various waste management system analysis/evaluation tools, as well as fuel cycle system analyses and safeguards and security studies. The UDB has been designed to be flexible and expandable and to provide controlled inputs to a variety of tools and applications. Interface controls, relevant data, and data formats will continue to be identified and added as additional requirements for other tools and capabilities are identified.

The UDB contains the data necessary to model the cask and assembly geometry as well as the irradiation parameters necessary to define the SNF compositions used within the criticality analysis process. The UDB is built with MySQL, which allows for relating of the tables of information to one another with indexes or "keys." The keys allow for linking multiple tables of information to one another to pull together sets of data for analysis. Information pertinent to the UNF-ST&DARDS criticality analysis process contained in the UDB includes the canister type, the assembly identifiers loaded in the cask by position, the date the canister entered service, and the damaged or intact status of each fuel assembly. The UDB also contains the RW-859[4] fuel identifiers, enrichment, burnup, and discharge date of each of the fuel assemblies needed to model the fuel irradiation history. Once the criticality calculations are performed, the $k_{eff}$ values with statistical uncertainties are reported back to the UDB for storage.

### 3.2.2 Template Engine

The Template Engine is a template processor used to combine site-specific input parameters from the UDB with the model templates developed for the ORIGAMI and CSAS6 calculations to produce complete input files for those calculations. The Template Engine is a string substitution program designed to take advantage of repeated structures in text files. The Template Engine takes the input parameter data structures represented by a JavaScript Object Notation (JSON) parameter set and the root template file and performs attribute replacement and subtemplate imports.

### 3.2.3 JSON parameter set

The JSON parameter set contains sets of key value pairs of information necessary to perform safety analysis within UNF-ST&DARDS. The keys in the JSON file are identical to the variables in the templates. When the Template Engine encounters variables in the template, the values to which they are keyed (in the JSON file) is substituted.

### 3.2.4 UNF Templates

UNF-ST&DARDS uses templates that serve as the building blocks from which application-specific inputs are defined. The UNF-Templates repository provides UNF-ST&DARDS application-agnostic input generation. Templates allow UNF-ST&DARDS to use the same set of parameters to succinctly communicate to each application while decoupling UNF-ST&DARDS from any specific application.

In order to facilitate the criticality modeling of as-loaded canisters, it is necessary to have flexible input files that can be altered for each canister or assembly. The method of accomplishing this within UNF-ST&DARDS is to build a set of input files with tags corresponding to the JSON information discussed in Section 3.2.2. The templating process is used throughout UNF-ST&DARDS, but the templates of principal concern to the criticality process are the ORIGAMI and CSAS6 templates. These templates are discussed in detail in Sections 4.1 and 4.2.

### 3.2.5 ORIGEN Libraries

The ORIGEN libraries contain the collapsed one-group cross sections for each of the assembly types from RW-859 that have been modeled to date. The one-group cross section files are produced as an output of the assembly modeling process using the TRITON sequence of SCALE in Reference [3]. The ARP libraries are used with the ORIGAMI templates to produce depleted and decayed node-wise nuclide concentrations for each of the assemblies in the canisters that are being analyzed.

## 3.3 Criticality Process Overview

The criticality analysis process is initiated by providing UNF-ST&DARDS with a canister identifier and analysis date. The canister identifier retrieves the relevant assembly identifiers from the canister inventory located in the UDB. The assembly identifiers are then used to look up the necessary ORIGEN libraries, irradiation histories, and geometric information for the assemblies in the canister and form the discharge, decay, and criticality JSON parameter sets. The assembly-specific ORIGEN libraries and irradiation information from the discharge concentration JSON parameter set are used to expand the ORIGAMI depletion template to generate axial node-wise, assembly-specific discharge concentrations. UNF-ST&DARDS then passes discharge concentrations to the ORIGAMI decay template along with analysis-specific decay data from the decay JSON parameter set to produce the necessary isotopic concentrations for criticality analysis. A more detailed discussion of the depletion modeling for the criticality process in UNF-ST&DARDS is provided in Section 4.1.

The next step in the UNF-ST&DARDS criticality analysis process is to produce the CSAS6 criticality models. The CSAS6 models are created by pairing the base canister template, which contains the basic basket geometry with criticality JSON used to specify the fuel materials, geometry, and arrays necessary to complete the model. The expanded CSAS6 templates are then used to produce $k_{eff}$ values. The canister templates and fuel templates are discussed in greater detail in Section 4.2.

The principal output of the UNF-ST&DARDS criticality analysis process is the calculated $k_{eff}$ value for each canister at a time step, which is then imported into the UDB. Fig. 2 is a diagram of the criticality analysis process, showing how the components of UNF-ST&DARDS criticality analysis process relate to one another to perform criticality calculations.

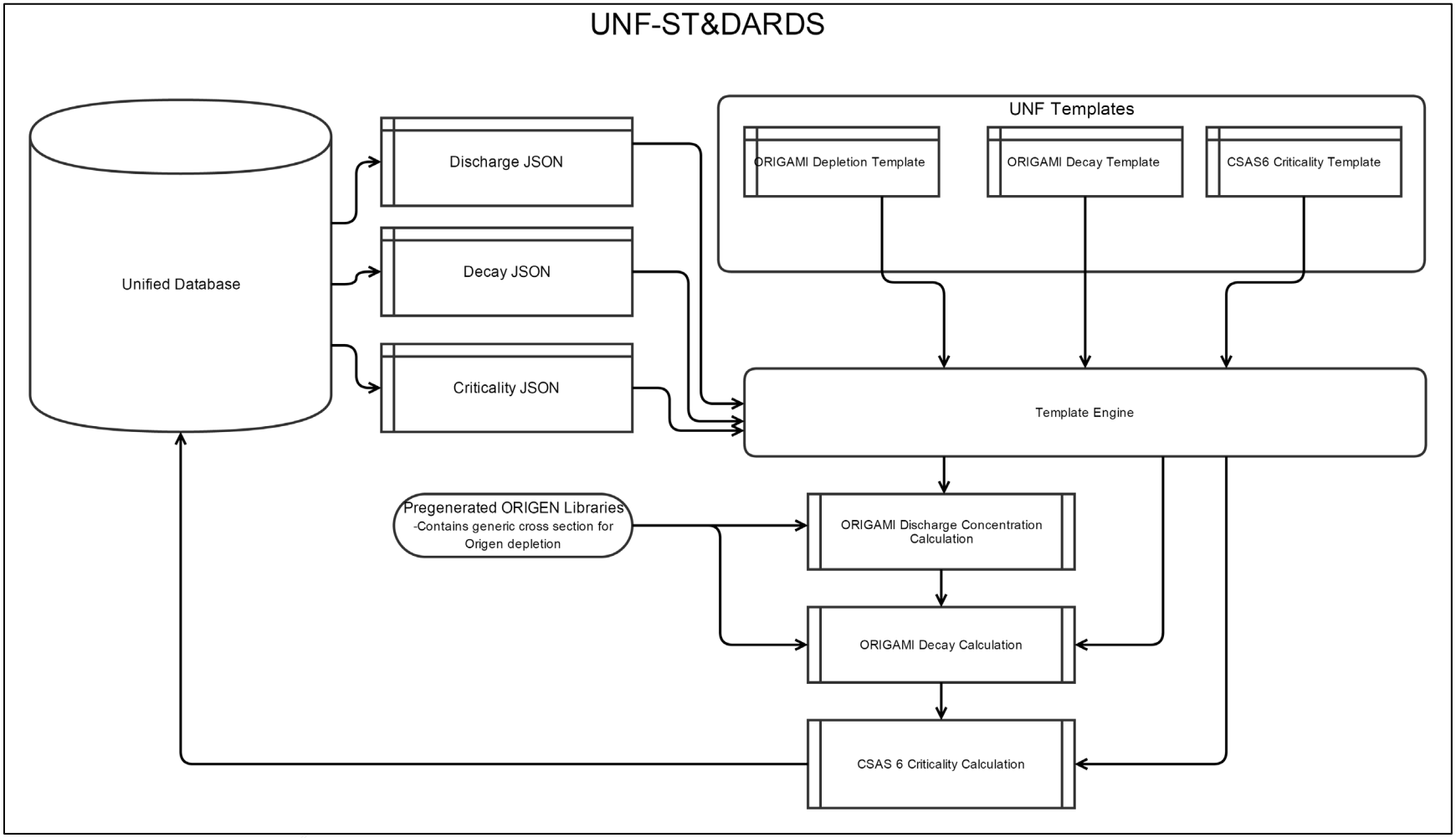


**Fig. 2. Diagram of the criticality analysis process within UNF-ST&DARD.**

# 4. MODELING PROCESS

This section of the report discusses the templates and techniques used to transform the JSON parameter set and the ORIGAMI and CSAS6 template files into depletion and criticality models. Section 4.1 discusses the ORIGAMI modeling techniques and templates, and Section 4.2 discusses the CSAS6 modeling techniques and templates.

## 4.1 ORIGAMI Modeling

As briefly discussed in Section 3.3, isotopic concentrations are calculated in a two-step process. The first step in the determination of isotopic concentrations is the depletion of fuel assemblies to the discharge burnup using the ORIGEN cross-section libraries from Reference [3] (discussed in Section 3.2.5). This section provides a more detailed description of the data and models used for the generation of isotopic concentrations in the criticality analysis process within UNF-ST&DARDS. The JSON parameter sets used for the ORIGAMI calculations, along with a description of the values in JSON are discussed in Section 4.1.1; a brief discussion of the treatment of the axial burnup profiles is provided in Section 4.1.2; and Section 4.1.3 presents the ORIGAMI templates used in the UNF-ST&DARDS criticality analysis process.

### 4.1.1 ORIGAMI JSONs

This section presents the JSON parameter sets and parameter descriptions used to develop the set isotopic concentrations used to perform as-loaded burnup credit analysis of SNF canisters. There are two JSONs currently used by UNF-ST&DARDS with the ORIGAMI templates, one for the discharge concentrations and one for the decayed concentrations. The only difference between the discharge and decay concentration JSONs is that decay concentration JSON has an additional variable to account for the post-irradiation decay time. Because the discharge JSON is a subset of the decay JSON, only the decay JSON is presented in this section. Table 1.  contains a list of the relevant parameters and their descriptions from the ORIGAMI JSON parameter sets and Table 2 contains an example decay JSON parameter set. There are additional parameters included in the Table 2 JSON that are not included in Table 1. . However, these parameters are for internal file handling within UNF-ST&DARDS and are likely to change over time; therefore, they are not discussed in this report.

**Table 1. Description of relevant JSON parameters for the ORIGAMI discharge concentration and decay cases**

| JSON Parameter[a] | Description | unf_db[b] Table |
|---|---|---|
| axial_node_count | Number of axial nodes to be depleted and used in the criticality model | - |
| moderator_density[node] | Density of the water for each node in the ORIGAMI calculation | - |
| burnup_profile[node] | Relative burnup of each node discussed. Values average to 1.0 for whole assembly. Discussed in Section 4.1.2. | - |
| arplib_name | Name of the ARP library to be used for depletion and decay calculations | - |
| assembly_id | Assembly identifier | assembly |
| reactor_id | Reactor identifier allows fuel assemblies to be uniquely identified when paired with assembly_id | assembly |
| initial_uranium | Initial mass of uranium in kg loaded in the assembly | assembly |
| initial_enrichment | Initial uranium enrichment of the fuel assembly in w/o | assembly |
| max_burnup | Assembly average burnup | assembly |
| Down | Number of post-irradiation decay time, calculated as the difference between the assembly discharge date and the analysis date. | calculated |
| Burn | The number of days that the assembly is irradiated in the reactor core | assembly |
| Power | The power level that the assembly is irradiated at in megawatts per metric ton uranium | reactor |

[a]Attribute of the fuel assembly component identified in column unf_db table.

[b]UDB (unf_db) table.

**Table 2. Example JSON parameter set for the depletion and decay of assembly A01 at Sequoyah (Reactor ID 4808) analyzed for 7/8/2016**


```
  "initial_enrichment": 2.1,
  "burnup_profile[9]": 1.188,
  "moderator_density[17]": 0.6668,
  "moderator_density[4]": 0.6668,
  "axial_node_count": 18.0,
  "burnup_profile[12]": 1.19,
  "moderator_density[6]": 0.6668,
  "burnup_profile[16]": 0.614,
  "title": "Concentration calculation for 4808 reactors, A01 assembly",
  "burn_data": [
    {
      "power": 20.423573533118383,
      "down": 0.0,
      "burn": 780.9500122070312
    }
  ],
  "moderator_density[18]": 0.6668,
  "copy_list": [
    {
      "to": "arpdata.txt",
      "from": "/projects/unf/data/../data/arplibs/bounding/arpdata.txt"
    },
    {
      "to": "./",
      "from": "/projects/unf/data/../data/arplibs/bounding/W1717WL*.arplib"
    },
    {
      "to": "assembly_restart.f71",
```

```
      "from": "/projects/unf/data/../data/discharge/4808_A01_bounding.inp.f71"
    }
  ],
  "moderator_density[3]": 0.6668,
  "cached_composition_storage": "/projects/unf/data/../data/decay/07-08-
2016_4808_A01_bounding_materials.tmpl",
  "moderator_density[14]": 0.6668,
  "burnup_profile[8]": 1.189,
  "moderator_density[10]": 0.6668,
  "burnup_profile[4]": 1.215,
  "arplib_name": "W1717WL",
  "burnup_profile[11]": 1.195,
  "moderator_density[7]": 0.6668,
  "analysis_date": "07-08-2016",
  "assembly.id": 1,
  "burnup_profile[15]": 0.756,
  "cached_decay_storage": "/projects/unf/data/../data/decay/07-08-
2016_4808_A01_bounding_decay_heat.tmpl",
  "concentration_storage": "/projects/unf/data/../data/discharge/4808_A01_bounding.inp.f71",
  "moderator_density[2]": 0.6668,
  "burnup_profile[7]": 1.197,
  "moderator_density[15]": 0.6668,
  "down": 12354,
  "burnup_profile[3]": 1.208,
  "moderator_density[11]": 0.6668
}
```


### 4.1.2 Axial Burnup Profile Treatment

One of the key parameters necessary to ensure a conservative estimate of $k_{eff}$ in a criticality evaluation is proper treatment of axial burnup distribution. As nuclear fuel burns in the reactor, neutron leakage and moderator temperature effects dictate that the ends of the fuel will accumulate less burnup than the center of the fuel assembly. The decreased burnup at the end regions of the fuel assembly cause those regions to dominate $k_{eff}$ in storage and transportation situations. The resulting effect of the asymmetric axial burning of fuel is that two fuel assemblies with the same initial enrichment and burnup could have very different reactivity. Reference [5] provides a set of PWR SNF bounding profiles based on the statistical analysis of 3,169 axial profiles taken from plant operating data covering 106 cycles of operation. The axial profiles for PWR SNF assemblies used in the UNF-ST&DARDS criticality analysis process are taken from Ref. 5 and presented in Table 3.

A uniform burnup profile was employed for the BWR fuel assemblies in this report. In this report, burnup credit is only used for BWR fuel assemblies of relatively low burnup. For the purposes of this report BWR canisters are only analyzed if the burnup of all of the fuel assemblies in a canister is less than 20 GWd/MTU. Ref. 5 determined that a uniform axial distribution is typically bounding for low burnup assemblies. However, similar conclusion has not yet been drawn for BWR assemblies. Thus far this approach has only permitted the analysis of two of the early generation BWRs (LaCrosse and Humboldt Bay).

**Table 3. Burnup dependent axial burnup profiles used for criticality calculations**

| Axial zone no. | Fraction of active fuel height | Burnup < 18 GWd/MTU | 18 ≤ Burnup < 30 GWd/MTU | Burnup ≥ 30 GWd/MTU |
|---|---|---|---|---|
| | | 1 | 2 | 3 |
| 1 | 0.0278 | 0.649 | 0.668 | 0.652 |
| 2 | 0.0833 | 1.044 | 1.034 | 0.967 |
| 3 | 0.1389 | 1.208 | 1.150 | 1.074 |
| 4 | 0.1944 | 1.215 | 1.094 | 1.103 |
| 5 | 0.2500 | 1.214 | 1.053 | 1.108 |
| 6 | 0.3056 | 1.208 | 1.048 | 1.106 |
| 7 | 0.3611 | 1.197 | 1.064 | 1.102 |
| 8 | 0.4167 | 1.189 | 1.095 | 1.097 |
| 9 | 0.4722 | 1.188 | 1.121 | 1.094 |
| 10 | 0.5278 | 1.192 | 1.135 | 1.094 |
| 11 | 0.5833 | 1.195 | 1.140 | 1.095 |
| 12 | 0.6389 | 1.190 | 1.138 | 1.096 |
| 13 | 0.6944 | 1.156 | 1.130 | 1.095 |
| 14 | 0.7500 | 1.022 | 1.106 | 1.086 |
| 15 | 0.8056 | 0.756 | 1.049 | 1.059 |
| 16 | 0.8611 | 0.614 | 0.933 | 0.971 |
| 17 | 0.9167 | 0.481 | 0.669 | 0.738 |
| 18 | 0.9722 | 0.284 | 0.373 | 0.462 |

### 4.1.3 ORIGAMI Templates

This section of the report discusses the ORIGAMI discharge concentration and decay templates used within UNF-STDARDS to develop the SNF isotopic concentrations.

The ORIGAMI discharge concentration calculations use the parameters from the JSON presented in Table 2. The discharge concentration template imports the assembly identifier, the appropriate ORIGEN library for the assembly type, the initial uranium loading and the initial enrichment. The discharge concentration templates also require the reactor power (power variable) and number of days the assembly was burned (burn variable). The axial burnup distribution discussed in Section 4.1.2 is applied to the power that is imported into the history block to develop node-wise burnups. The principal output of the discharge concentration calculation with respect to the criticality analysis process is an f71 ORIGEN library that can be subsequently decayed. The discharge concentration calculation template is presented in Table 4. .

The ORIGAMI decay calculations take the f71 output from the depletion calculations and perform decay calculations from the discharge date to the requested analysis date of the canister. The decay templates require all of the same inputs as the discharge concentration templates except the power and burn variables. Instead of the power and burn time inputs the decay template requires a down time input variable. The down time is calculated as the amount of time from the discharge date until the requested criticality analysis date. The ORIGAMI decay template is presented Table 5.

**Table 4. ORIGAMI template used to calculate fuel assembly isotopic concentrations at reactor discharge**

**/UNF-Templates/discharge_concentrations/origami.tmpl**

```
#import ../common/TemplateHeader.tmpl
=shell
#import ../common/file/link.tmpl using <copy_list>
end
=origami
title='<title>'
asmid=<assembly_id>
libs=<arplib_name>
enrich=<initial_enrichment>
param[ % problem parameters
    mtu=<initial_uranium>
    reln=yes
    nbur=15
    interp=spline
    small=yes
]
mod=[ % moderator density profile array
#repeat moderator_density_for_node.tmpl using node=1,<axial_node_count>
]
axp=[ % axial power profile array
#repeat burnup_profile_for_node.tmpl using node=1,<axial_node_count>
]
% non-fuel components
nonfuel=[ cr 3.366 mn 0.1525 fe 6.309 co 0.0302
  ni 2.366 zr 516.3 sn 8.412 ]
hist[ % irradiation/decay history array
#import power_burn_down.tmpl using <burn_data>
] % end of history array
#import gamma_groups.tmpl
#import neutron_groups.tmpl
end
=shell
#import ../common/file/copy.tmpl using {'from' :"'${OUTDIR}/${OUTBASENAME}_assembly_dump.f71'",
'to' :"'<concentration_storage>'"}
rm "'${OUTDIR}/${OUTBASENAME}_assembly_dump.f71'"
rm "'${OUTDIR}/${OUTBASENAME}_pinDumpMaster.f71'"
end
```

**Table 5. ORIGAMI template used to calculate fuel assembly isotopic concentrations at requested analysis date**

```
mod=[
#repeat ../discharge_concentrations/moderator_density_for_node.tmpl using
node=1,<axial_node_count>
 ]
axp=[
#repeat ../discharge_concentrations/burnup_profile_for_node.tmpl using
node=1,<axial_node_count>
 ]
hist[
 cycle{ down=<down> }
]
#import ../discharge_concentrations/gamma_groups.tmpl
#import ../discharge_concentrations/neutron_groups.tmpl
end
=shell
#import ../common/file/copy.tmpl using {'from':"'${OUTDIR}/${OUTBASENAME}_compBlock'",
'to':"'<cached_composition_storage>'"}
#import ../common/file/copy.tmpl using {'from':"'${OUTDIR}/${OUTBASENAME}_assembly_dump.f71'",
'to':"'<cached_composition_storage>.f71'"}
#import ../common/file/copy.tmpl using {'from':"'${OUTDIR}/${OUTBASENAME}_AxialDecayHeat'",
'to':"'<cached_decay_storage>'"}
rm "'${OUTDIR}/${OUTBASENAME}_compBlock'"
rm "'${OUTDIR}/${OUTBASENAME}_assembly_dump.f71'"
rm "'${OUTDIR}/${OUTBASENAME}_pinDumpMaster.f71'"
rm "'${OUTDIR}/${OUTBASENAME}_AxialDecayHeat'"
```

```
end
```

## 4.2 CSAS6 Modeling

This section of the report discusses the JSON parameter set, numbering scheme used to develop materials and geometry, and the templates and their relationships to one another for the CSAS6 modeling within UNF-ST&DARDS. Section 4.2.1 discusses the JSON parameter set, Section 4.2.2 discusses the scheme used to provide the material and geometry unit numbers, and Section 4.2.3 discusses the templates used for the CSAS6 materials, geometry units and arrays.

### 4.2.1 Criticality JSON

For criticality analysis the JSON file contains both general information applying to the entire canister and assembly-specific information. Canister wide information in the JSON parameter set includes the number of axial nodes used to discretize the fuel assemblies, the canister type needed to select the correct CSAS6 template, and the analysis date needed to set the amount of decay time for each ORIGAMI decay calculation. Assembly specific parameters from the JSON are found in the “assemblies” array and include data needed to retrieve the appropriate isotopic concentrations such as the fuel assembly burnup and the initial enrichment, and the information necessary to specify the materials and geometry of the fuel in the CSAS6 model such as the pin pitch, cladding material, fuel pin and non-fuel component dimensions and the dimensions of the fuel array. An explanation of the new variables used in the CSAS6 criticality analysis JSON parameter set that were not used in the ORIGAMI JSON parameter set is provided in Table 6. Table 7 contains an example JSON parameter set generated by UNF-ST&DARDS for the analysis of an MPC-32 canister located at Sequoyah. It is noted that there are 32 assemblies in the example JSON but assemblies 3 through 31 were removed to improve the readability of the document.

**Table 6. Description of relevant JSON parameters for the CSAS6 criticality calculations**

| JSON Parameter | Description | unf_db Table |
|---|---|---|
| clad_outer_radius | Outer radius of the fuel pin cladding. | fuel_pin |
| clad_inner_radius | Inner radius of the fuel pin cladding. | fuel_pin |
| clad_material | Cladding material fuel pins. | fuel_pin |
| pellet_outer_radius | Outer radius of the fuel pellet. | fuel_pin |
| stack_length | Length of the active fuel area of the fuel pin. | fuel_pin |
| Pitch | Distance between the centers of fuel pins. | fuel_pin |
| material | Material composing guide tube. | guide_tube |
| inner_radius | Guide tube inner radius. | guide_tube |
| outer_radius | Guide tube outer radius. | guide_tube |
| material | Material composition for guide tube. | instrument_tube |
| inner_radius | Instrument tube inner radius. | instrument_tube |
| outer_radius | Instrument tube outer radius. | instrument_tube |
| X | Number of fuel pins in the x dimension of the fuel pin array. | assembly_array |
| Y | Number of fuel pins in the y dimension of the fuel pin array. | assembly_array |

**Table 7. Example Criticality JSON file used in the analysis of a Sequoyah canister**

**MPC-32-TSC 092_bounding_11-11-2008.inp.json**


```
{
  "axial_node_count": 18.0,
  "assemblies": [
    {
      "assembly.max_burnup": 17588.65,
      "fuel_pin.clad_outer_radius": 0.47498,
      "guide_tube.inner_radius": 0.5715,
      "instrument_tube.outer_radius": 0.61214,
      "initial_enrichment": 2.12,
      "assembly.reactor_id": 4809,
      "instrument_tube.inner_radius": 0.5715,
      "guide_tube.outer_radius": 0.61214,
      "fuel_pin.rod_count": 264,
      "fuel_pin.pellet_radius": 0.409575,
      "assembly.assembly_id": "L41",
      "assembly": 1,
      "assembly.type": "W1717WL",
      "fuel_pin.clad_material": "Zirc4",
      "fuel_pin.total_length": 385.1529,
      "fuel_pin.bottom_gap": 4.7374,
      "initial_uranium": 0.4551,
      "assembly.pitch": 21.50364,
      "fuel_pin.clad_inner_radius": 0.41783000000000003,
      "fuel_pin.stack_length": 365.76,
      "fuel_pin.top_gap": 100000.0,
      "fuel_pin.pitch": 1.25984,
      "instrument_tube.material": "Zirc4",
      "guide_tube.material": "Zirc4",
      "assembly_array.y": 17,
      "assembly_array.x": 17
    },
```

**Table 7. Example Criticality JSON file used in the analysis of a Sequoyah canister (continued)**


```
    {
      "assembly.max_burnup": 17054.4,
      "fuel_pin.clad_outer_radius": 0.47498,
      "guide_tube.inner_radius": 0.5715,
      "instrument_tube.outer_radius": 0.61214,
      "initial_enrichment": 2.12,
      "assembly.reactor_id": 4809,
      "instrument_tube.inner_radius": 0.5715,
      "guide_tube.outer_radius": 0.61214,
      "fuel_pin.rod_count": 264,
      "fuel_pin.pellet_radius": 0.409575,
      "assembly.assembly_id": "L44",
      "assembly": 2,
      "assembly.type": "W1717WL",
      "fuel_pin.clad_material": "Zirc4",
      "fuel_pin.total_length": 385.1529,
      "fuel_pin.bottom_gap": 4.7374,
      "initial_uranium": 0.4594,
      "assembly.pitch": 21.50364,
      "fuel_pin.clad_inner_radius": 0.41783000000000003,
      "fuel_pin.stack_length": 365.76,
      "fuel_pin.pitch": 1.25984,
      "instrument_tube.material": "Zirc4",
      "guide_tube.material": "Zirc4",
      "assembly_array.y": 17,
      "assembly_array.x": 17
       },
Assemblies 3-31 deleted for ease of reading
       {
      "assembly.max_burnup": 17327.72,
      "fuel_pin.clad_outer_radius": 0.47498,
      "guide_tube.inner_radius": 0.5715,
      "instrument_tube.outer_radius": 0.61214,
      "initial_enrichment": 2.12,
      "assembly.reactor_id": 4809,
      "instrument_tube.inner_radius": 0.5715,
      "guide_tube.outer_radius": 0.61214,
      "fuel_pin.rod_count": 264,
      "fuel_pin.pellet_radius": 0.409575,
      "assembly.assembly_id": "L13",
      "assembly": 32,
      "assembly.type": "W1717WL",
      "fuel_pin.clad_material": "Zirc4",
      "fuel_pin.total_length": 385.1529,
      "fuel_pin.bottom_gap": 4.7374,
      "initial_uranium": 0.4577,
      "assembly.pitch": 21.50364,
      "fuel_pin.clad_inner_radius": 0.41783000000000003,
      "fuel_pin.stack_length": 365.76,
      "fuel_pin.top_gap": 100000.0,
      "fuel_pin.pitch": 1.25984,
      "instrument_tube.material": "Zirc4",
      "guide_tube.material": "Zirc4",
      "assembly_array.y": 17,
      "assembly_array.x": 17
    }
  ],
```

**Table 7. Example Criticality JSON file used in the analysis of a Sequoyah canister (continued)**

```
  "analysis_date": "11-11-2008",
  "canister.criticality_class": "1",
  "canister.id": "MPC-32-TSC 092",
  "canister.model": "MPC-32",
  "assembly_count": 32
}
```

### 4.2.2 Numbering System for CSAS6 Geometry and Unit Descriptions

For automated CSAS6 canister criticality input analysis, a numbering scheme is applied in the subtemplates describing the material mixtures and the geometry units needed to form the criticality input file. The unique numbers associated with different units/mixtures can be expressed by the following general format:

$$\text{Unit or Material Number} = \text{Level Constant} + \text{Variable}. \quad (1)$$

The "Number" can be either a geometry unit number or a material mixture number in the CSAS6 input file. The Level Constant is a number that is typically a multiple of 10,000 (with the exception of fuel assembly components) and is unique for each major class of units (e.g., pins, axial nodes, assemblies, or bare canister model). As an example, the units associated with the canister model are assigned to unit numbers greater than 90,000. The basket hardware (e.g., boral panels) are associated with unit numbers below greater than 97,000 and less than 97,999. The repetitive structures in the model (fuel pins, fuel nodes, etc.), contain the "Variable" part to their unit number, which is a linear function of assembly number (or, rather, the location number of a fuel assembly in the cask) and axial node number (starting at 1 for the axial node/zone at the bottom of the assembly).

The values of the Level Constants and Variables are presented in Table 8 for the material numbering scheme and Table 10 for the geometric numbering scheme. For both Table 8 and Table 10 the variable *A*, represents the index from the `<assemblies>` array in the criticality analysis JSON parameter set, the variable *N* represents the number of axial nodes specified by `axial_node_count`, and *n* represents the number of the nodes under consideration within the assembly in question. Table 8 and Table 10 also indicate the maximum number of fuel assemblies and axial nodes that may be modeled is 89 assemblies and 99 axial nodes. In addition to the *A, n,* and *N* dependences both the material and geometry numbering schemes have an *I* variable that is an arbitrary index for the non-fuel components. Because the non-fuel components vary in terms of the number of lattice locations they occupy and therefore require different geometric and material descriptions, different sets of *I* values are provided to account for the various non-fuel component geometries. Table 9 contains the values of *I* for the material specifications and Table 11 contains the values of *I* for the geometry specification.

In order to better illustrate the numbering scheme a diagram showing its implementation is provided in Fig. 3. Fig. 3 expands the numbering scheme from Table 8 and Table 10 for assemblies 1, 2, and 89 using 18 axial nodes. The number of assemblies was chosen to be 89 because that represents the maximum capacity of any canister currently being used or licensed and the maximum number of assemblies supported by the current UNF-ST&DARDS under the current numbering scheme. The number of axial nodes was selected to be 18 because that is the number of nodes used in Reference 5.

**Table 8. Materials numbering scheme for CSAS6 criticality calculations**

| Material | Level Constant | Variable | |
|---|---|---|---|
| Fuel composition | 1000 | $(A-1)\times N+n$ | Limit imposed by other variables |
| Cladding for fuel pins | 10 | $A$ | $A<89$ |
| Non-Fuel Components | $100\times I, I=1,\ldots,9$ | $A$ | $A<99$ |
| Empty Cell Location | 1000 | - | - |

*Note: A is the assembly number, N is the total number of nodes, n is the node number and I is the arbitrary non-fuel component index in Table 9.*

**Table 9. Non-fuel component material specification for CSAS6 criticality calculations**

| Value of I | Component |
|---|---|
| 1 | Guide Tube/Water Hole |
| 2 | Instrumentation Tube |
| 3 | Inert Pin/Guide Bar |
| 4 | Component |
| 5 | - |
| 6 | - |
| 7 | Channel Box |
| 8 | - |
| 9 | - |

**Table 10. Geometry numbering scheme for the CSAS6 criticality calculations**

| Component | Level Constant | Variable | Limitations |
|---|---|---|---|
| Fuel pin units a | 10,000 | $100\times A+n$ | $A<99, N<99$ |
| Non-Fuel components number a,c | $100\times I, I=1,\ldots,9$ | $A$ | $A<99$ |
| Array of pin units forming a node | 20,000 | $100\times A+n$ | $A<99, N<99$ |
| Array of node units to represent the entire assembly | 30,000 | $A$ | $A<99$ |

*Note: A is the assembly number, N is the total number of nodes, n is the node number and I is the arbitrary non-fuel component index in Table 11.*

**Table 11. Non-fuel component geometry unit specification for CSAS6 criticality calculations**

| Value of I | Single Unit Non-Fuel Components | Quad Unit Non-Fuel Components |
|---|---|---|
| 1 | Guide Tube/Water Hole | Guide Tube/Water Hole |
| 2 | Instrumentation Tube | Guide Tube/Water Hole |
| 3 | Inert Pin/Guide Bar | Guide Tube/Water Hole |
| 4 | Guide Tube with Component | Guide Tube/Water Hole |
| 5 | - | Guide Tube with Component |
| 6 | - | Guide Tube with Component |
| 7 | - | Guide Tube with Component |
| 8 | - | Guide Tube with Component |
| 9 | Empty Cell | Empty Cell |

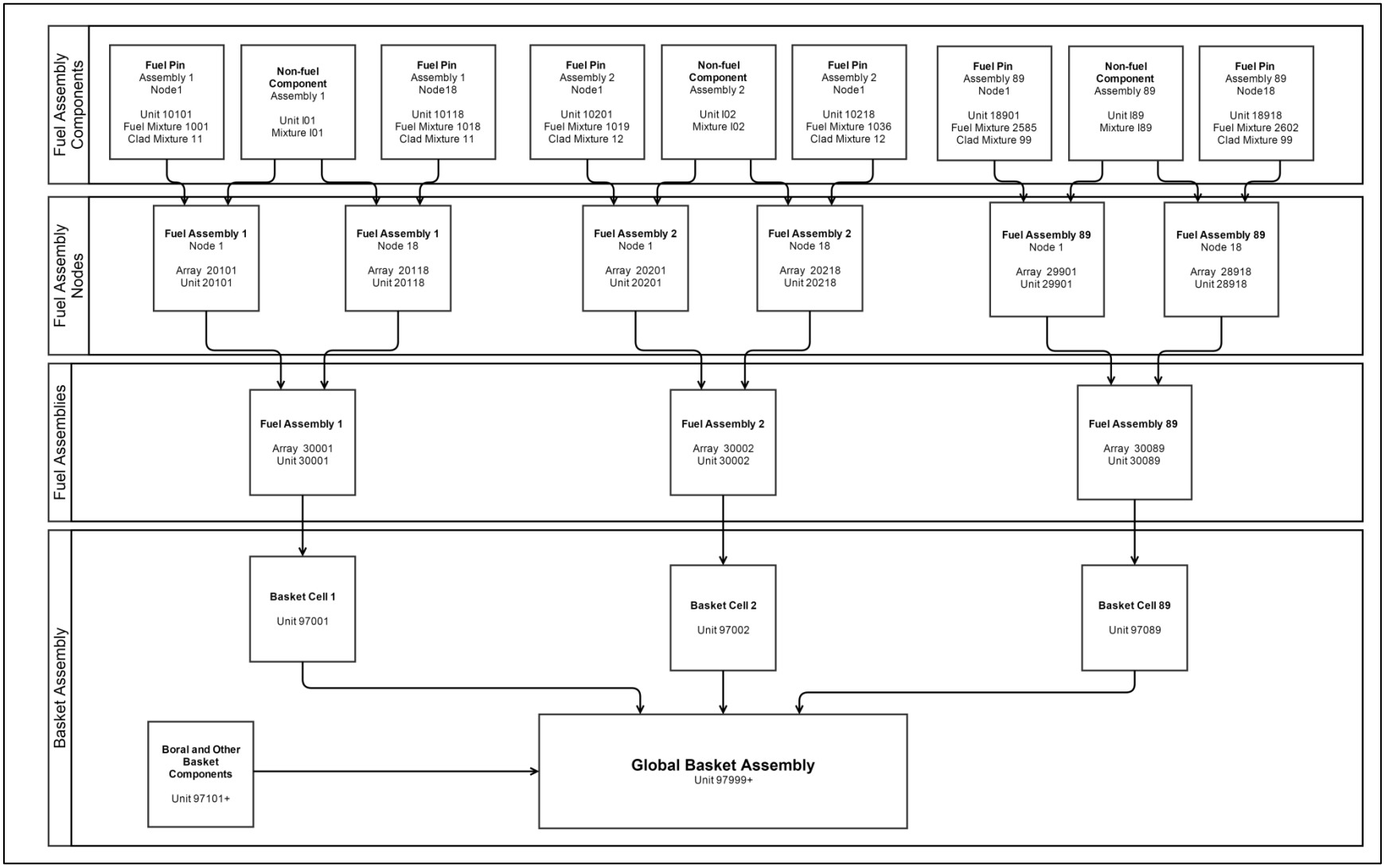


**Fig. 3. Example implementation of geometry and material numbering used for the UNF-ST&DARDS criticality analysis process.**

### 4.2.3 CSAS6 Modeling

This section discusses the CSAS6 criticality analysis templates. The CSAS6 criticality analysis modeling process is organized using a main canister template with static text for the non-variable components and insertion points for the variable components. The three main types of variable components are the fuel assembly materials, geometry, and arrays. The main canister template is discussed in more detail in Section 4.2.3.1 and the material, geometry, and array templates are discussed in Sections 4.2.3.2, 4.2.3.3, and 4.2.3.4, respectively.

#### *4.2.3.1 Main Canister Template*

In addition to the variable components discussed above, which are expanded by UNF-ST&DARDS during the analysis process, there are a number of static elements embedded in the template. Static elements of the main canister template include basic canister materials, CSAS6 control parameters, and static basket features.

The first ten material definitions are excluded from the material mixtures expanded by UNF-ST&DARDS and are used for canister components such as the structural materials, the water in the cask, and the neutron absorber material. Typical structural materials include aluminum and stainless steel used in fuel storage cell, basket, and canister wall construction. The canister is modeled as being surrounded with 50 cm water in order to produce as much reflection as possible; the canister and external water may also be modified in order to simulate the intrusion of various materials into the waste package. The neutron absorber is also modeled in the static template. The absorber material is specified as the nominal value less the percentage assumed in the SAR.

The second static item included in the canister model is the CSAS6 parameter block. Items included in the parameter block include the number of neutron histories per generation, the number of total neutron generations, and the number of generations to be skipped at the beginning of the problem. There are several additional items that may be specified in parameter block as described in Reference [2].

The final static items in the main canister template are the fuel storage cells and basket structure. The fuel storage cells modeled starting unit 97101 and incremented up through 89 basket cells. The basket cells are the used to formulate a global unit in the CSAS6 model either by arraying them or inserting them into a large block of water as holes. The appropriate basket modeling technique depends on the physical structure of the basket.

Fig. 4 contains a relationship diagram of the aforementioned templates and their subtemplates (discussed in later sections), and Table 12 contains a CSAS6 criticality main canister template for MPC-32. The insertion points for the variable subtemplates are bolded, and the number of basket cells is reduced from 32 to three in order to the improve readability of Table 12.

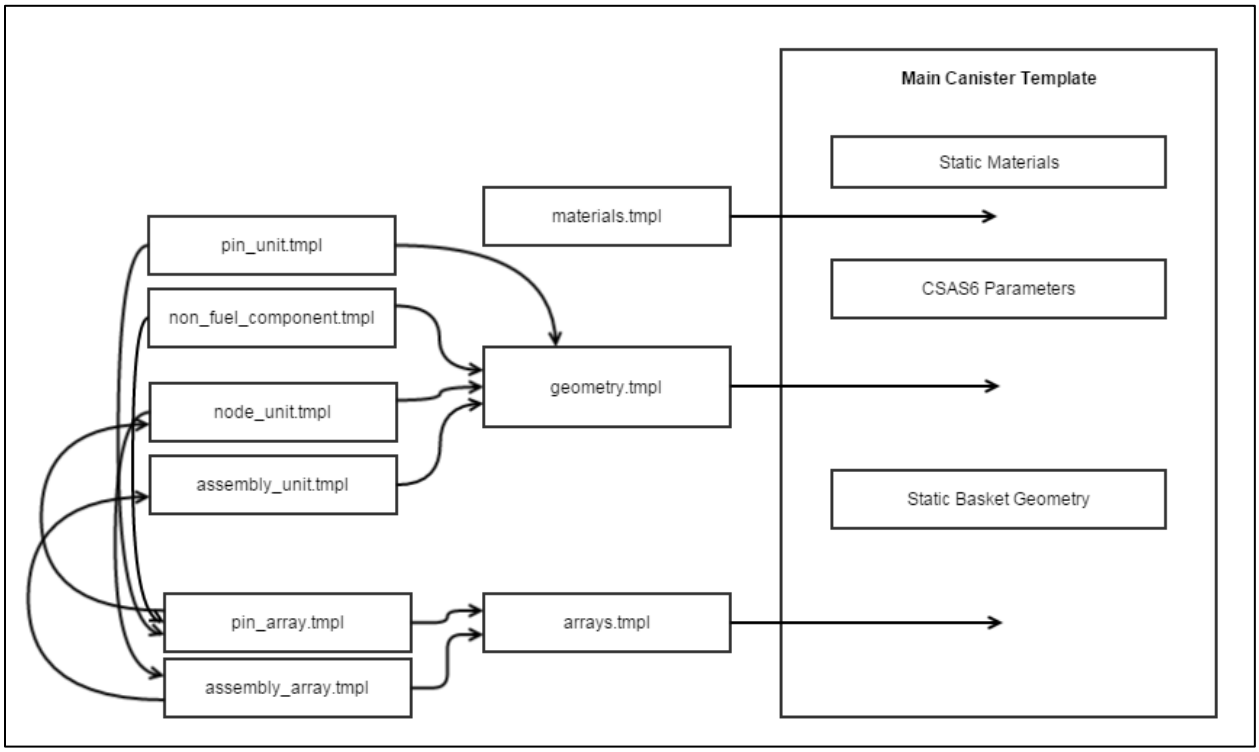


**Fig. 4. Relationship diagram of the templates used within the CSAS6 criticality models.**

**Table 12. CSAS6 canister criticality template**

**./UNF-Templates/cask/sequoyahMPC32.tmpl**

```
=csas26
Justin Clarity: October 2012. KENO-VI model of MPC-32 Sequoyah
ce_v7
' ------------------------------------------------------------------
'  References:
' 1.
' 2.
' ------------------------------------------------------------------
read comp
' Stainless steel
ss304     1                  1    300    end
' Water in cask
h2o       2    den=1.0       1    300    end
'     - Boral- B-10 loading of 0.0372 g B-10/cm2, 2.66g/cc, 0.081 inch thick (nominal)
'       information taken from Table 6.3.4 of the HI-STORM 100 FSAR Revision 9 Feb. 2010
'       The B-10 concentration reduced to 75% of the nominal value
b-10      3  0  8.071E-03   300.0  end
b-11      3  0  3.255E-02   300.0  end
c         3  0  1.015E-02   300.0  end
al        3  0  3.805E-02   300.0  end
'
'     - Al as boral clad
al        4   den=2.7      1 300.0  end
'
'
'     - water for fuel pin cell pellet/clad gap for CE calculations
h2o     1000 den=1.0      1 300.0 end
'
'
```

**Table 12. CSAS6 canister criticality template (continued)**

```
#import general_templates/assembly_materials.tmpl using
<assemblies>
end comp
'
' ------------------------------------------------------------
' Parameters
' ------------------------------------------------------------
read parm
 gen=1100 npg=20000 nsk=300 htm=no uum=no
end parm
'
' ------------------------------------------------------------
' Geometry
' ------------------------------------------------------------
read geom
'
'
'
#import general_templates/geometry.tmpl using <assemblies>
'
' No change needed in geometry beyond this point
'
'Begin Definintion of Subcell components
'
'Definition of neutron absorber components
'
unit 97001
  com='boral panel'
  cuboid 1 0.01397 0.0  9.5250 -9.5250  396.24 0.0
  cuboid 2 0.03937 0.0  9.5250 -9.5250  396.24 0.0
  cuboid 3 0.24511 0.0  9.5250 -9.5250  396.24 0.0
  cuboid 4 0.27051 0.0  9.5250 -9.5250  396.24 0.0
  cuboid 5 0.28448 0.0  9.5250 -9.5250  396.24 0.0
  cuboid 6 0.47498 0.0  9.7155 -9.7155  396.24 0.0
  media 2 1 1
  media 4 1 -1 2
  media 3 1 -2 3
  media 4 1 -3 4
  media 2 1 -4 5
  media 1 1 -5 6
  boundary  6
'
'
'BEGIN DEFINITION OF BASKET CELLS
'
 unit 97133
 com='upper left empty water cell - 33'
 cuboid 1  23.421975 0.0  23.421975 0.0  448.31 0.0
 media  2 1 1
 boundary 1
'
unit 97101
#ifdef assembly[1].undefined
 com='cell  1'
#\eval(<ioffset>+1) as ioffset#
#endif
 cuboid  1 23.421975 0.714375   22.707600 0.0  448.31 0.0
 cuboid  2 23.421975 0.0        23.421975 0.0  448.31 0.0
 media   1 1 2 -1
 media   2 1 1
#ifndef assembly[1].undefined
#ifdef #eval(getdefined(assemblies[1-<ioffset>],"assembly.assembly_id"))#
    com='assembly_id:"#eval(get(assemblies[1-<ioffset>],"assembly.assembly_id"))#"
reactor_id:#eval(get(assemblies[1-<ioffset>],"assembly.reactor_id"))# position:1'
#endif
#ifndef #eval(getdefined(assemblies[1-<ioffset>],"assembly.assembly_id"))#
    com='position:1'
#endif
```

**Table 12. CSAS6 canister criticality template (continued)**

```
 hole 30001 origin x=12.3056625 y=11.1163075 z=205.4225
#endif
 boundary 2
'
unit 97102
#ifdef assembly[2].undefined
 com='cell  2'
#\eval(<ioffset>+1) as ioffset#
#endif
 cuboid  1 23.421975 0.714375   22.707600 0.0  448.31 0.0
 cuboid  2 23.421975 0.0        23.421975 0.0  448.31 0.0
 media   1 1 2 -1
 media   2 1 1
#ifndef assembly[2].undefined
#ifdef #eval(getdefined(assemblies[2-<ioffset>],"assembly.assembly_id"))#
    com='assembly_id:"#eval(get(assemblies[2-<ioffset>],"assembly.assembly_id"))#"
reactor_id:#eval(get(assemblies[2-<ioffset>],"assembly.reactor_id"))# position:2'
#endif
#ifndef #eval(getdefined(assemblies[2-<ioffset>],"assembly.assembly_id"))#
    com='position:2'
#endif
 hole 30002 origin x=12.3056625 y=11.1163075 z=205.4225
#endif
 hole 97001 origin x=0.714375  y=11.3538  z=7.3025
 boundary 2
'
'
Basket Cells 3-31 deleted for ease of reading
'
'
unit 97132
#ifdef assembly[32].undefined
 com='cell 32'
#\eval(<ioffset>+1) as ioffset#
#endif
 cuboid  1 23.421975 0.714375   22.707600   0.0 448.31 0.0
 cuboid  2 23.421975 0.0        23.421975  -0.714375       448.31 0.0
 media   1 1 2 -1
 media   2 1 1
#ifndef assembly[32].undefined
#ifdef #eval(getdefined(assemblies[32-<ioffset>],"assembly.assembly_id"))#
    com='assembly_id:"#eval(get(assemblies[32-<ioffset>],"assembly.assembly_id"))#"
reactor_id:#eval(get(assemblies[32-<ioffset>],"assembly.reactor_id"))# position:32'
#endif
#ifndef #eval(getdefined(assemblies[32-<ioffset>],"assembly.assembly_id"))#
    com='position:32'
#endif
 hole 30032 origin x=12.3056625 y=11.1163075 z=205.4225
#endif
 hole 97001 origin x=0.714375  y=11.3538  z=7.3025
  hole 97001 origin x=12.0675475  y=22.707600  z=7.3025 rotate a1=-90
 boundary 2
'
unit 97136
 com='water cell 36'
 cuboid  1 24.13635  0.714375   23.421975  0.0    448.31  0.0
 cuboid  2 24.13635  0.0        24.136350  0.0    448.31  0.0
 media   1 1 2 -1
 media   2 1 1
 boundary 2
'
unit 97799
 com='hole for array of basket cells'
 cuboid 1 141.246225 0.0  141.246225 0.0  448.31 0.0
 array 1 1 2 place 1 1 1 0.0 0.0 0.0
 cylinder 2     85.725    448.31      0.0    origin x=70.6231125 y=70.6231125 z=0.0
 media 2 1 2 -1
 boundary 2
```

**Table 12. CSAS6 canister criticality template (continued)**

```
global unit 97800
 com='hole for array of basket cells'
 hole 97799
 cylinder 2     85.725    448.31      0.0    origin x=70.6231125 y=70.6231125 z=0.0
 cylinder 3     86.995    448.31      0.0    origin x=70.6231125 y=70.6231125 z=0.0
 cylinder 4     117.475   480.31      -60.96 origin x=70.6231125 y=70.6231125 z=0.0
 media 2 1 2
 media 1 1 3 -2
 media 2 1 4 -3
 boundary 4
'
end geom
'
read bounds
 all=vacuum
end bounds
'
'
read array
 ara=1 nux=6 nuy=6 nuz=1
 fill
  97135 97129   97130   97131   97132   97136
  97123 97124   97125   97126   97127   97128
  97117 97118   97119   97120   97121   97122
  97111 97112   97113   97114   97115   97116
  97105 97106   97107   97108   97109   97110
  97133 97101   97102   97103   97104   97134
 end fill
'
#import general_templates/arrays.tmpl using <assemblies>
end array

end data

end
```

#### 4.2.3.2 *Material Template*

The first insertion point in the main canister template is **`assembly_materials.tmpl`** template. The **`assembly_materials.tmpl`** template implements the numbering scheme for fuel and non-fuel components described in Section 4.2.2. The **`assembly_materials.tmpl`** template uses a series of **`ifdef`** statements to determine whether or not a particular material needs to be imported. The **`ifdef`** statement tests for the presence of a key parameter in the JSON parameter set and evaluates a set of templating commands if the result of the logical test is "true." The assembly_materials.tmpl template is shown in Table 13.

**Table 13. Materials template used for CSAS6 model**

**`./UNF-Templates/cask/general_templates/assembly_materials.tmpl`**

```
#ifndef assembly[<assembly:fmt=%.0f>].undefined
'
#ifndef #eval(<fuel_pin.clad_inner_radius> == 0)#
'     - <fuel_pin.clad_material> cladding for fuel pins in assembly type <assembly.type>: location #eval
fmt=%.0f (assembly)#
<fuel_pin.clad_material>      #eval fmt=%.0f (10+<assembly>)#              1 300.0  end
'
'
#endif
#ifdef guide_tube.material
'     - <guide_tube.material> cladding for guide_tubes in assembly type <assembly.type>: location #eval
```

**Table 13. Materials template used for CSAS6 model (continued)**

```
fmt=%.0f (assembly)#
<guide_tube.material>    #eval fmt=%.0f (100+<assembly>)#              1 300.0  end
'
#ifdef component_present
'    - <component.material> material for insert component in assembly type <assembly.type>: location
#eval fmt=%.0f (assembly)#
<component.material>    #eval fmt=%.0f (400+<assembly>)#              1 300.0  end
#endif
#endif
'
#ifdef instrument_tube.material
 '    - <instrument_tube.material> cladding for instrument_tubes in assembly type <assembly.type>:
location #eval fmt=%.0f (assembly)#
<instrument_tube.material>    #eval fmt=%.0f (200+<assembly>)#              1 300.0  end
#endif
'
#ifdef inert_pin.material
'    - <inert_pin.material> material for inert fuel pin <assembly.type>: location #eval fmt=%.0f
(assembly)#
<inert_pin.material>    #eval fmt=%.0f (300+<assembly>)#              1 300.0  end
#endif
'

#import <analysis_date>_<canister.id>_assembly_materials[<assembly:fmt=%.0f>].tmpl
'
#ifdef channel.material
'    - <channel.material> material for BWR fuel channel <assembly.type>: location #eval fmt=%.0f
(assembly)#
<channel.material>    #eval fmt=%.0f (700+<assembly>)#              1 300.0  end
#endif


#ifdef water_rod.material
'    - <water_rod.material> material for BWR water rod <assembly.type>: location #eval fmt=%.0f
(assembly)#
<water_rod.material>    #eval fmt=%.0f (300+<assembly>)#              1 300.0  end
#endif
#endif
```

#### *4.2.3.3 Geometry Templates*

The geometry templates are the second group of templates to be invoked from the UNF-ST&DARDS main canister template. The **`geometry.tmpl`** template is invoked following the material definitions and preceding the basket cell definitions. Like the **`assembly_materials.tmpl`** template, the **`geometry.tmpl`** template is activated by the presence of an assembly definition from the JSON file.

The purpose of the **`geometry.tmpl`** template is to invoke the assembly component geometry subtemplates based on the assembly **`assembly.type`** variable found in the JSON file. From the **`geometry.tmpl`** template four subtemplates are imported for each assembly. The subtemplates invoked are the **`non_fuel_component.tmpl`** template, the **`pin_unit.tmpl`** template, the **`node_unit.tmpl`** template, and the **`assembly_unit.tmpl`** template.

The **`non_fuel_component.tmpl`** template imports the non-fuel pin lattice components such as guide tubes with and without inserts, instrumentation tubes, water holes, and inert pins. The **`fuel_pin.tmpl`**, **`node_unit.tmpl`**, and **`assembly_unit.tmpl`** templates import the fuel pin geometry, and the container unit for the lateral array of fuel pins and non-fuel components, and the container unit for the axial array of fuel nodes. Table 14 contains the **`geometry.tmpl`** template; Table 15 contains the **`pin_unit.tmpl`** template; and Table 16 contains example **`non_fuel_component.tmpl`** templates for one-unit (W1717WO) and four-unit (C1414C) non-fuel component assembly types.

The fuel and non-fuel components discussed above are placed in an array to form an axial assembly slice, as is discussed in Section 4.2.3.4. The array forming the axial assembly slice is the placed in the **<assembly.type>.node_unit.tmpl** template for the specified assembly type. Once the node units are formed, they are, in turn, axially arrayed and placed inside the **assembly_unit.tmpl** template. It is noted that there is an **ifdef** statement included in the **assembly_unit.tmpl** template that is used to capture the presence of a fuel channel for BWR fuel. An example **< assembly.type >.node_unit.tmpl** template is shown in and the Table 17. The **assembly_unit.tmpl** template is shown in Table 18.

**Table 14. Base geometry template used for CSAS6 model**

**./UNF-Templates/cask/general_templates/geometry.tmpl**

```
#ifndef assembly[<assembly:fmt=%.0f>].undefined
#ifdef guide_tube.material
' Non-Fuel Components
'
#import ../assembly_types/<assembly.type>/<assembly.type>.non_fuel_component_unit.tmpl
#endif
'
#repeat pin_unit.tmpl using node=1,<axial_node_count>
' Nodes (pins bundled in nodes)
'
#repeat ../assembly_types/<assembly.type>/<assembly.type>.node_unit.tmpl using
node=1,<axial_node_count>
' Assemblies (nodes in assembly)
'
#import assembly_unit.tmpl
#endif
```

**Table 15. Fuel pin template used for CSAS6 model**

**./UNF-Templates/cask/general_templates/pin_unit.tmpl**

```
unit #eval fmt=%.0f (10000+100*<assembly>+<node>)#
  com='assembly_id:"<assembly.assembly_id>" reactor_id:<assembly.reactor_id> %fuel pin  in assembly
type <assembly.type>: location #eval fmt=%.0f (assembly)# node #eval fmt=%.0f (node)#'
  cuboid   1 #eval fmt=%.6f (<fuel_pin.pitch>/2) as xydist# -<xydist:fmt=%08.6f> <xydist:fmt=%08.6f>
-<xydist:fmt=%08.6f>   #eval fmt=%.6f (<fuel_pin.stack_length>/<axial_node_count>) as ztop#  0.
  cylinder 2 <fuel_pin.pellet_outer_radius:fmt=%.6f>   <ztop:fmt=%.6f>  0.
#ifndef #eval(<fuel_pin.clad_inner_radius> == 0)#
  cylinder 3 <fuel_pin.clad_inner_radius:fmt=%.6f>   <ztop:fmt=%.6f>  0.
  cylinder 4 <fuel_pin.clad_outer_radius:fmt=%.6f>   <ztop:fmt=%.6f>  0.
#endif
  media    #eval fmt=%.0f (1000+(assembly-1)*axial_node_count+node)#     1     2
#ifndef #eval(<fuel_pin.clad_inner_radius> == 0)#
  media    1000     1     3    -2
  media      #eval fmt=%.0f (10+<assembly>)#     1     4    -3
  media    1000     1     1    -4
#endif
#ifdef #eval(<fuel_pin.clad_inner_radius> == 0)#
  media    1000     1     1    -2
#endif
  boundary    1
```

**Table 16. Non-fuel component templates used for W1717WO and C1414C fuel types**

**./UNF-Templates/cask/assembly_types/W1717WO/W1717WO.non_fuel_component.tmpl**

```
#ifdef GUIDE_TUBE_UNIT
#ifdef component_present
unit #eval fmt=%.0f (400+<assembly>)#
  com='assembly_id:"<assembly.assembly_id>" reactor_id:<assembly.reactor_id> %guide tube in assembly
type <assembly.type>: location #eval fmt=%.0f (assembly)#'
  cuboid   1 #eval fmt=%.6f (<fuel_pin.pitch>/2) as xydist# -<xydist:fmt=%08.6f> <xydist:fmt=%08.6f>
```

**Table 16. Non-fuel component templates used for W1717WO and C1414C fuel types (continued)**

```
-<xydist:fmt=%08.6f> #eval fmt=%.6f (<fuel_pin.stack_length>/<axial_node_count>)# 0.
  cylinder 2 #eval fmt=%.6f (<guide_tube.inner_radius>)#                          #eval fmt=%.6f
(<fuel_pin.stack_length>/<axial_node_count>)# 0.
  cylinder 3 #eval fmt=%.6f (<guide_tube.outer_radius>)#                          #eval fmt=%.6f
(<fuel_pin.stack_length>/<axial_node_count>)# 0.
  media    1000     1     2
  hole <GUIDE_TUBE_UNIT : fmt=%.0f> origin x=0.0 y=0.0 z=0.0
  media     #eval fmt=%.0f (100+<assembly>)#     1     3    -2
  media    1000     1     1    -3
  boundary    1
#endif
#endif
unit #eval fmt=%.0f (100+<assembly>)#
  com='assembly_id:"<assembly.assembly_id>" reactor_id:<assembly.reactor_id> %guide tube in assembly
type <assembly.type>: location #eval fmt=%.0f (assembly)#'
  cuboid   1 #eval fmt=%.6f (<fuel_pin.pitch>/2) as xydist# -<xydist:fmt=%08.6f> <xydist:fmt=%08.6f>
-<xydist:fmt=%08.6f> #eval fmt=%.6f (<fuel_pin.stack_length>/<axial_node_count>)# 0.
  cylinder 2 #eval fmt=%.6f (<guide_tube.inner_radius>)#                          #eval fmt=%.6f
(<fuel_pin.stack_length>/<axial_node_count>)# 0.
  cylinder 3 #eval fmt=%.6f (<guide_tube.outer_radius>)#                          #eval fmt=%.6f
(<fuel_pin.stack_length>/<axial_node_count>)# 0.
  media    1000     1     2
  media     #eval fmt=%.0f (100+<assembly>)#     1     3    -2
  media    1000     1     1    -3
  boundary    1
unit #eval fmt=%.0f (200+<assembly>)#
  com='assembly_id:"<assembly.assembly_id>" reactor_id:<assembly.reactor_id> %instrument tube in
assembly type <assembly.type>: location #eval fmt=%.0f (assembly)#'
  cuboid   1 #eval fmt=%.6f (<fuel_pin.pitch>/2) as xydist# -<xydist:fmt=%08.6f> <xydist:fmt=%08.6f>
-<xydist:fmt=%08.6f> #eval fmt=%.6f (<fuel_pin.stack_length>/<axial_node_count>)# 0.
  cylinder 2 #eval fmt=%.6f (<instrument_tube.inner_radius>)#                          #eval
fmt=%.6f (<fuel_pin.stack_length>/<axial_node_count>)# 0.
  cylinder 3 #eval fmt=%.6f (<instrument_tube.outer_radius>)#                          #eval
fmt=%.6f (<fuel_pin.stack_length>/<axial_node_count>)# 0.
  media    1000     1     2
  media     #eval fmt=%.0f (200+<assembly>)#     1     3    -2
  media    1000     1     1    -3
  boundary    1
```

**./UNF-Templates/cask/assembly_types/C1414C/C1414C.non_fuel_component.tmpl**

```
unit #eval fmt=%.0f (300+<assembly>)#
  com='assembly_id:"<assembly.assembly_id>" reactor_id:<assembly.reactor_id> %nw guide tube in
assembly type <assembly.type>: location #eval fmt=%.0f (assembly)#'
  cuboid   1 #eval fmt=%.6f (<fuel_pin.pitch>/2) as xydist# -<xydist:fmt=%08.6f> <xydist:fmt=%08.6f>
-<xydist:fmt=%08.6f> #eval fmt=%.6f (<fuel_pin.stack_length>/<axial_node_count>)# 0.
  cylinder 2 #eval fmt=%.6f (<guide_tube.inner_radius>)#                          #eval fmt=%.6f
(<fuel_pin.stack_length>/<axial_node_count>)# 0. origin x=<xydist:fmt=%08.6f>  y=<xydist:fmt=%08.6f>
  cylinder 3 #eval fmt=%.6f (<guide_tube.outer_radius>)#                          #eval fmt=%.6f
(<fuel_pin.stack_length>/<axial_node_count>)# 0. origin x=<xydist:fmt=%08.6f>  y=<xydist:fmt=%08.6f>
  media    1000     1     1     2
  media     #eval fmt=%.0f (100+<assembly>)#     1     3     1    -2
  media    1000     1     1    -3
  boundary    1
unit #eval fmt=%.0f (400+<assembly>)#
  com='assembly_id:"<assembly.assembly_id>" reactor_id:<assembly.reactor_id> %ne guide tube in
assembly type <assembly.type>: location #eval fmt=%.0f (assembly)#'
  cuboid   1 <xydist:fmt=%08.6f> -<xydist:fmt=%08.6f> <xydist:fmt=%08.6f> -<xydist:fmt=%08.6f> #eval
fmt=%.6f (<fuel_pin.stack_length>/<axial_node_count>)# 0.
  cylinder 2 #eval fmt=%.6f (<guide_tube.inner_radius>)#                          #eval fmt=%.6f
(<fuel_pin.stack_length>/<axial_node_count>)# 0. origin x=-<xydist:fmt=%08.6f> y=<xydist:fmt=%08.6f>
  cylinder 3 #eval fmt=%.6f (<guide_tube.outer_radius>)#                          #eval fmt=%.6f
(<fuel_pin.stack_length>/<axial_node_count>)# 0. origin x=-<xydist:fmt=%08.6f> y=<xydist:fmt=%08.6f>
  media    1000     1     1     2
  media     #eval fmt=%.0f (100+<assembly>)#     1     3     1    -2
  media    1000     1     1    -3
  boundary    1
unit #eval fmt=%.0f (500+<assembly>)#
  com='assembly_id:"<assembly.assembly_id>" reactor_id:<assembly.reactor_id> %sw guide tube in
assembly type <assembly.type>: location #eval fmt=%.0f (assembly)#'
```

**Table 16. Non-fuel component templates used for W1717WO and C1414C fuel types (continued)**

```
  cuboid   1 <xydist:fmt=%08.6f> -<xydist:fmt=%08.6f> <xydist:fmt=%08.6f> -<xydist:fmt=%08.6f> #eval
fmt=%.6f (<fuel_pin.stack_length>/<axial_node_count>)# 0.
  cylinder 2 #eval fmt=%.6f (<guide_tube.inner_radius>)#                          #eval fmt=%.6f
(<fuel_pin.stack_length>/<axial_node_count>)# 0. origin x=<xydist:fmt=%08.6f>  y=-
<xydist:fmt=%08.6f>
  cylinder 3 #eval fmt=%.6f (<guide_tube.outer_radius>)#                          #eval fmt=%.6f
(<fuel_pin.stack_length>/<axial_node_count>)# 0. origin x=<xydist:fmt=%08.6f>  y=-
<xydist:fmt=%08.6f>
  media    1000     1     1     2
  media     #eval fmt=%.0f (100+<assembly>)#     1     3     1    -2
  media    1000     1     1    -3
  boundary    1
unit #eval fmt=%.0f (600+<assembly>)#
  com='assembly_id:"<assembly.assembly_id>" reactor_id:<assembly.reactor_id> %se guide tube in
assembly type <assembly.type>: location #eval fmt=%.0f (assembly)#'
  cuboid   1 <xydist:fmt=%08.6f> -<xydist:fmt=%08.6f> <xydist:fmt=%08.6f> -<xydist:fmt=%08.6f> #eval
fmt=%.6f (<fuel_pin.stack_length>/<axial_node_count>)# 0.
  cylinder 2 #eval fmt=%.6f (<guide_tube.inner_radius>)#                          #eval fmt=%.6f
(<fuel_pin.stack_length>/<axial_node_count>)# 0. origin x=-<xydist:fmt=%08.6f> y=-
<xydist:fmt=%08.6f>
  cylinder 3 #eval fmt=%.6f (<guide_tube.outer_radius>)#                          #eval fmt=%.6f
(<fuel_pin.stack_length>/<axial_node_count>)# 0. origin x=-<xydist:fmt=%08.6f> y=-
<xydist:fmt=%08.6f>
  media    1000     1     1     2
  media     #eval fmt=%.0f (100+<assembly>)#     1     3     1    -2
  media    1000     1     1    -3
  boundary    1
```

**Table 17. Lattice node unit template for CSAS6 models**

**./UNF-Templates/cask/assembly_types/C1414C/C1414C.node_unit.tmpl**

```
unit #eval fmt=%.0f (20000+100*<assembly>+<node>) as unit#
  com='assembly_id:"<assembly.assembly_id>" reactor_id:<assembly.reactor_id> % assembly  #eval
fmt=%.0f (assembly)# node #eval fmt=%.0f (node)#'
  cuboid   1   #eval fmt=%.6f (<assembly_array.x:fmt=%.0f>*<fuel_pin.pitch>/2-0.000001) as xydist# -
<xydist:fmt=%08.6f> <xydist:fmt=%08.6f> -<xydist:fmt=%08.6f>   #eval fmt=%.6f
(<fuel_pin.stack_length>/<axial_node_count>)#    0.0
  array #eval fmt=%.0f (unit)# 1  place 8    8     1 #eval fmt=%.6f (<fuel_pin.pitch>/2)#    #eval
fmt=%.6f (<fuel_pin.pitch>/2)#   0.0
  boundary    1
```

**Table 18. Assembly unit template for CSAS6 models**

**./UNF-Templates/cask/general_templates/assembly_unit.tmpl**

```
unit #eval fmt=%.0f (30000+assembly) as unit#
  com='assembly_id:"<assembly.assembly_id>" reactor_id:<assembly.reactor_id> % assembly #eval
fmt=%.0f (assembly)#'
  cuboid   1   #eval fmt=%.6f (<assembly_array.x:fmt=%.0f>*<fuel_pin.pitch>/2-0.000002) as xydist# -
<xydist:fmt=%08.6f> <xydist:fmt=%08.6f> -<xydist:fmt=%08.6f>  #eval fmt=%.6f
(<fuel_pin.stack_length>/2-0.00001)#    #eval fmt=%.6f (-<fuel_pin.stack_length>/2+0.00001)#
  array #eval fmt=%.0f (unit)# 1  place 1 1 1 0.0 0.0 #eval fmt=%.6f (-<fuel_pin.stack_length>/2)#
#ifdef channel.material
  cuboid    2   #eval fmt=%.6f    (channel.inner_dimension/2-0.000001) as chanID#  -
<chanID:fmt=%08.6f> <chanID:fmt=%08.6f> -<chanID:fmt=%08.6f>  #eval fmt=%.6f
(<fuel_pin.stack_length>/2)#    #eval fmt=%.6f (-<fuel_pin.stack_length>/2)#
  cuboid    3   #eval fmt=%.6f    (chanID + channel.thickness) as chanOD# -<chanOD:fmt=%08.6f>
<chanOD:fmt=%08.6f> -<chanOD:fmt=%08.6f>  #eval fmt=%.6f (<fuel_pin.stack_length>/2)#    #eval
fmt=%.6f (-<fuel_pin.stack_length>/2)#
  media    1000 1 2 -1
  media    #eval fmt=%.0f (300+<assembly>)# 1 3 -2
  boundary  3
#endif
#ifndef channel.material
  boundary    1
#endif
```

#### *4.2.3.4 Array Templates*

The last insertion point in the main canister template is the **arrays.tmpl** template in the read arrays block of the main CSAS6 template. The **arrays.tmpl** template is responsible for importing two subtemplates: the **<assembly.type>.pin_array.tmpl** template, which populates the fuel lattice for each axial node with fuel pins and non-fuel components, and the **node_array.tmpl** template, which is filled with units containing the axial nodes with fuel lattices in them. Similar to the guide tube portion of the **non_fuel_component.tmpl** template, **node_array.tmpl** template possesses an **ifdef** statement that can be used to alter the assembly array for the presence of inserts. The result of the expanded **node_array.tmpl** is then inserted back into the **assembly_unit.tmpl** template to form a complete fuel assembly for use in the canister criticality calculations. Table 19 shows the array insertion point template **arrays.tmpl**, Table 20 shows the nodal pin array templates for the W1717WO fuel assembly type with and without inserted components, and Table 21 shows the **node_array.tmpl** template.

**Table 19. Base array template for CSAS6 models**

**./UNF-Templates/cask/general_templates/arrays.tmpl**

```
#ifndef assembly[<assembly:fmt=%.0f>].undefined
#ifdef GUIDE_TUBE_UNIT
#ifdef component_present
#repeat  ../assembly_types/<assembly.type>/<assembly.type>.pin_array_WABA.tmpl using
node=1,<axial_node_count>
#endif
#ifndef component_present
#repeat  ../assembly_types/<assembly.type>/<assembly.type>.pin_array.tmpl using
node=1,<axial_node_count>
#endif
#endif
#ifndef GUIDE_TUBE_UNIT
#repeat  ../assembly_types/<assembly.type>/<assembly.type>.pin_array.tmpl using
node=1,<axial_node_count>
#endif
#import node_array.tmpl
#endif
```

**Table 20. Base pin array template for CSAS6 models**

**./UNF-Templates/cask/assembly_types/W1717WO/W1717WO.pin_array.tmpl**

```
  ara= #eval fmt=%.0f (20000+100*<assembly>+<node>)# nux= <assembly_array.x:fmt=%.0f> nuy=
<assembly_array.y:fmt=%.0f> nuz= 1
    fill
     #eval fmt=%.0f (10000+100*<assembly>+<node>) as funit# #eval fmt=%.0f (funit)# #eval fmt=%.0f
(funit)# #eval fmt=%.0f (funit)# #eval fmt=%.0f (funit)# #eval fmt=%.0f (funit)# #eval fmt=%.0f
(funit)# #eval fmt=%.0f (funit)# #eval fmt=%.0f (funit)# #eval fmt=%.0f (funit)# #eval fmt=%.0f
(funit)# #eval fmt=%.0f (funit)# #eval fmt=%.0f (funit)# #eval fmt=%.0f (funit)# #eval fmt=%.0f
(funit)# #eval fmt=%.0f (funit)# #eval fmt=%.0f (funit)#
     #eval fmt=%.0f (funit)# #eval fmt=%.0f (funit)# #eval fmt=%.0f (funit)# #eval fmt=%.0f (funit)#
#eval fmt=%.0f (funit)# #eval fmt=%.0f (funit)# #eval fmt=%.0f (funit)# #eval fmt=%.0f (funit)#
#eval fmt=%.0f (funit)# #eval fmt=%.0f (funit)# #eval fmt=%.0f (funit)# #eval fmt=%.0f (funit)#
#eval fmt=%.0f (funit)# #eval fmt=%.0f (funit)# #eval fmt=%.0f (funit)# #eval fmt=%.0f (funit)#
#eval fmt=%.0f (funit)#
     #eval fmt=%.0f (funit)# #eval fmt=%.0f (funit)# #eval fmt=%.0f (funit)# #eval fmt=%.0f (funit)#
#eval fmt=%.0f (funit)#   #eval fmt=%.0f (100+<assembly>) as gunit# #eval fmt=%.0f (funit)# #eval
fmt=%.0f (funit)#   #eval fmt=%.0f (gunit)# #eval fmt=%.0f (funit)# #eval fmt=%.0f (funit)#   #eval
fmt=%.0f (gunit)# #eval fmt=%.0f (funit)# #eval fmt=%.0f (funit)# #eval fmt=%.0f (funit)# #eval
fmt=%.0f (funit)# #eval fmt=%.0f (funit)#
     #eval fmt=%.0f (funit)# #eval fmt=%.0f (funit)# #eval fmt=%.0f (funit)#   #eval fmt=%.0f
(gunit)# #eval fmt=%.0f (funit)# #eval fmt=%.0f (funit)# #eval fmt=%.0f (funit)# #eval fmt=%.0f
(funit)# #eval fmt=%.0f (funit)# #eval fmt=%.0f (funit)# #eval fmt=%.0f (funit)# #eval fmt=%.0f
(funit)# #eval fmt=%.0f (funit)#   #eval fmt=%.0f (gunit)# #eval fmt=%.0f (funit)# #eval fmt=%.0f
(funit)# #eval fmt=%.0f (funit)#
     #eval fmt=%.0f (funit)# #eval fmt=%.0f (funit)# #eval fmt=%.0f (funit)# #eval fmt=%.0f (funit)#
#eval fmt=%.0f (funit)# #eval fmt=%.0f (funit)# #eval fmt=%.0f (funit)# #eval fmt=%.0f (funit)#
```

```
#eval fmt=%.0f (funit)# #eval fmt=%.0f (funit)# #eval fmt=%.0f (funit)# #eval fmt=%.0f (funit)#
#eval fmt=%.0f (funit)# #eval fmt=%.0f (funit)# #eval fmt=%.0f (funit)# #eval fmt=%.0f (funit)#
```

**Table 20. Base pin array template for CSAS6 models (continued)**

```
#eval fmt=%.0f (funit)#
     #eval fmt=%.0f (funit)# #eval fmt=%.0f (funit)#   #eval fmt=%.0f (gunit)# #eval fmt=%.0f
(funit)# #eval fmt=%.0f (funit)#   #eval fmt=%.0f (gunit)# #eval fmt=%.0f (funit)# #eval fmt=%.0f
(funit)#   #eval fmt=%.0f (gunit)# #eval fmt=%.0f (funit)# #eval fmt=%.0f (funit)#   #eval fmt=%.0f
(gunit)# #eval fmt=%.0f (funit)# #eval fmt=%.0f (funit)#   #eval fmt=%.0f (gunit)# #eval fmt=%.0f
(funit)# #eval fmt=%.0f (funit)#
     #eval fmt=%.0f (funit)# #eval fmt=%.0f (funit)# #eval fmt=%.0f (funit)# #eval fmt=%.0f (funit)#
#eval fmt=%.0f (funit)# #eval fmt=%.0f (funit)# #eval fmt=%.0f (funit)# #eval fmt=%.0f (funit)#
#eval fmt=%.0f (funit)# #eval fmt=%.0f (funit)# #eval fmt=%.0f (funit)# #eval fmt=%.0f (funit)#
#eval fmt=%.0f (funit)# #eval fmt=%.0f (funit)# #eval fmt=%.0f (funit)# #eval fmt=%.0f (funit)#
#eval fmt=%.0f (funit)#
     #eval fmt=%.0f (funit)# #eval fmt=%.0f (funit)# #eval fmt=%.0f (funit)# #eval fmt=%.0f (funit)#
#eval fmt=%.0f (funit)# #eval fmt=%.0f (funit)# #eval fmt=%.0f (funit)# #eval fmt=%.0f (funit)#
#eval fmt=%.0f (funit)# #eval fmt=%.0f (funit)# #eval fmt=%.0f (funit)# #eval fmt=%.0f (funit)#
#eval fmt=%.0f (funit)# #eval fmt=%.0f (funit)# #eval fmt=%.0f (funit)# #eval fmt=%.0f (funit)#
#eval fmt=%.0f (funit)#
     #eval fmt=%.0f (funit)# #eval fmt=%.0f (funit)#   #eval fmt=%.0f (gunit)# #eval fmt=%.0f
(funit)# #eval fmt=%.0f (funit)#   #eval fmt=%.0f (gunit)# #eval fmt=%.0f (funit)# #eval fmt=%.0f
(funit)#   #eval fmt=%.0f (200+<assembly>)# #eval fmt=%.0f (funit)# #eval fmt=%.0f (funit)#   #eval
fmt=%.0f (gunit)# #eval fmt=%.0f (funit)# #eval fmt=%.0f (funit)#   #eval fmt=%.0f (gunit)# #eval
fmt=%.0f (funit)# #eval fmt=%.0f (funit)#
     #eval fmt=%.0f (funit)# #eval fmt=%.0f (funit)# #eval fmt=%.0f (funit)# #eval fmt=%.0f (funit)#
#eval fmt=%.0f (funit)# #eval fmt=%.0f (funit)# #eval fmt=%.0f (funit)# #eval fmt=%.0f (funit)#
#eval fmt=%.0f (funit)# #eval fmt=%.0f (funit)# #eval fmt=%.0f (funit)# #eval fmt=%.0f (funit)#
#eval fmt=%.0f (funit)# #eval fmt=%.0f (funit)# #eval fmt=%.0f (funit)# #eval fmt=%.0f (funit)#
#eval fmt=%.0f (funit)#
     #eval fmt=%.0f (funit)# #eval fmt=%.0f (funit)# #eval fmt=%.0f (funit)# #eval fmt=%.0f (funit)#
#eval fmt=%.0f (funit)# #eval fmt=%.0f (funit)# #eval fmt=%.0f (funit)# #eval fmt=%.0f (funit)#
#eval fmt=%.0f (funit)# #eval fmt=%.0f (funit)# #eval fmt=%.0f (funit)# #eval fmt=%.0f (funit)#
#eval fmt=%.0f (funit)# #eval fmt=%.0f (funit)# #eval fmt=%.0f (funit)# #eval fmt=%.0f (funit)#
#eval fmt=%.0f (funit)#
     #eval fmt=%.0f (funit)# #eval fmt=%.0f (funit)#   #eval fmt=%.0f (gunit)# #eval fmt=%.0f
(funit)# #eval fmt=%.0f (funit)#   #eval fmt=%.0f (gunit)# #eval fmt=%.0f (funit)# #eval fmt=%.0f
(funit)#   #eval fmt=%.0f (gunit)# #eval fmt=%.0f (funit)# #eval fmt=%.0f (funit)#   #eval fmt=%.0f
(gunit)# #eval fmt=%.0f (funit)# #eval fmt=%.0f (funit)#   #eval fmt=%.0f (gunit)# #eval fmt=%.0f
(funit)# #eval fmt=%.0f (funit)#
     #eval fmt=%.0f (funit)# #eval fmt=%.0f (funit)# #eval fmt=%.0f (funit)# #eval fmt=%.0f (funit)#
#eval fmt=%.0f (funit)# #eval fmt=%.0f (funit)# #eval fmt=%.0f (funit)# #eval fmt=%.0f (funit)#
#eval fmt=%.0f (funit)# #eval fmt=%.0f (funit)# #eval fmt=%.0f (funit)# #eval fmt=%.0f (funit)#
#eval fmt=%.0f (funit)# #eval fmt=%.0f (funit)# #eval fmt=%.0f (funit)# #eval fmt=%.0f (funit)#
#eval fmt=%.0f (funit)#
     #eval fmt=%.0f (funit)# #eval fmt=%.0f (funit)# #eval fmt=%.0f (funit)#   #eval fmt=%.0f
(gunit)# #eval fmt=%.0f (funit)# #eval fmt=%.0f (funit)# #eval fmt=%.0f (funit)# #eval fmt=%.0f
(funit)# #eval fmt=%.0f (funit)# #eval fmt=%.0f (funit)# #eval fmt=%.0f (funit)# #eval fmt=%.0f
(funit)# #eval fmt=%.0f (funit)#   #eval fmt=%.0f (gunit)# #eval fmt=%.0f (funit)# #eval fmt=%.0f
(funit)# #eval fmt=%.0f (funit)#
     #eval fmt=%.0f (funit)# #eval fmt=%.0f (funit)# #eval fmt=%.0f (funit)# #eval fmt=%.0f (funit)#
#eval fmt=%.0f (funit)#   #eval fmt=%.0f (gunit)# #eval fmt=%.0f (funit)# #eval fmt=%.0f (funit)#
#eval fmt=%.0f (gunit)# #eval fmt=%.0f (funit)# #eval fmt=%.0f (funit)#   #eval fmt=%.0f (gunit)#
#eval fmt=%.0f (funit)# #eval fmt=%.0f (funit)# #eval fmt=%.0f (funit)# #eval fmt=%.0f (funit)#
#eval fmt=%.0f (funit)#
     #eval fmt=%.0f (funit)# #eval fmt=%.0f (funit)# #eval fmt=%.0f (funit)# #eval fmt=%.0f (funit)#
#eval fmt=%.0f (funit)# #eval fmt=%.0f (funit)# #eval fmt=%.0f (funit)# #eval fmt=%.0f (funit)#
#eval fmt=%.0f (funit)# #eval fmt=%.0f (funit)# #eval fmt=%.0f (funit)# #eval fmt=%.0f (funit)#
#eval fmt=%.0f (funit)# #eval fmt=%.0f (funit)# #eval fmt=%.0f (funit)# #eval fmt=%.0f (funit)#
#eval fmt=%.0f (funit)#
     #eval fmt=%.0f (funit)# #eval fmt=%.0f (funit)# #eval fmt=%.0f (funit)# #eval fmt=%.0f (funit)#
#eval fmt=%.0f (funit)# #eval fmt=%.0f (funit)# #eval fmt=%.0f (funit)# #eval fmt=%.0f (funit)#
#eval fmt=%.0f (funit)# #eval fmt=%.0f (funit)# #eval fmt=%.0f (funit)# #eval fmt=%.0f (funit)#
#eval fmt=%.0f (funit)# #eval fmt=%.0f (funit)# #eval fmt=%.0f (funit)# #eval fmt=%.0f (funit)#
#eval fmt=%.0f (funit)#
```

```
    end fill
./UNF-Templates/cask/assembly_types/W1717WO/W1717WO.pin_array_WABA.tmpl
  ara= #eval fmt=%.0f (20000+100*<assembly>+<node>)# nux= <assembly_array.x:fmt=%.0f> nuy=
<assembly_array.y:fmt=%.0f> nuz= 1
    fill
     #eval fmt=%.0f (10000+100*<assembly>+<node>) as funit# #eval fmt=%.0f (funit)# #eval fmt=%.0f
(funit)# #eval fmt=%.0f (funit)# #eval fmt=%.0f (funit)# #eval fmt=%.0f (funit)# #eval fmt=%.0f
(funit)# #eval fmt=%.0f (funit)# #eval fmt=%.0f (funit)# #eval fmt=%.0f (funit)# #eval fmt=%.0f
(funit)# #eval fmt=%.0f (funit)# #eval fmt=%.0f (funit)# #eval fmt=%.0f (funit)# #eval fmt=%.0f
(funit)# #eval fmt=%.0f (funit)# #eval fmt=%.0f (funit)#
     #eval fmt=%.0f (funit)# #eval fmt=%.0f (funit)# #eval fmt=%.0f (funit)# #eval fmt=%.0f (funit)#
#eval fmt=%.0f (funit)# #eval fmt=%.0f (funit)# #eval fmt=%.0f (funit)# #eval fmt=%.0f (funit)#
#eval fmt=%.0f (funit)# #eval fmt=%.0f (funit)# #eval fmt=%.0f (funit)# #eval fmt=%.0f (funit)#
#eval fmt=%.0f (funit)# #eval fmt=%.0f (funit)# #eval fmt=%.0f (funit)# #eval fmt=%.0f (funit)#
#eval fmt=%.0f (funit)#
     #eval fmt=%.0f (funit)# #eval fmt=%.0f (funit)# #eval fmt=%.0f (funit)# #eval fmt=%.0f (funit)#
#eval fmt=%.0f (funit)#   #eval fmt=%.0f (600+<assembly>) as waba# #eval fmt=%.0f (funit)# #eval
fmt=%.0f (funit)#   #eval fmt=%.0f (100+<assembly>) as gunit# #eval fmt=%.0f (funit)# #eval fmt=%.0f
(funit)#   #eval fmt=%.0f (waba)# #eval fmt=%.0f (funit)# #eval fmt=%.0f (funit)# #eval fmt=%.0f
(funit)# #eval fmt=%.0f (funit)# #eval fmt=%.0f (funit)#
     #eval fmt=%.0f (funit)# #eval fmt=%.0f (funit)# #eval fmt=%.0f (funit)#   #eval fmt=%.0f
(waba)# #eval fmt=%.0f (funit)# #eval fmt=%.0f (funit)# #eval fmt=%.0f (funit)# #eval fmt=%.0f
(funit)# #eval fmt=%.0f (funit)# #eval fmt=%.0f (funit)# #eval fmt=%.0f (funit)# #eval fmt=%.0f
(funit)# #eval fmt=%.0f (funit)#   #eval fmt=%.0f (waba)# #eval fmt=%.0f (funit)# #eval fmt=%.0f
(funit)# #eval fmt=%.0f (funit)#
     #eval fmt=%.0f (funit)# #eval fmt=%.0f (funit)# #eval fmt=%.0f (funit)# #eval fmt=%.0f (funit)#
#eval fmt=%.0f (funit)# #eval fmt=%.0f (funit)# #eval fmt=%.0f (funit)# #eval fmt=%.0f (funit)#
#eval fmt=%.0f (funit)# #eval fmt=%.0f (funit)# #eval fmt=%.0f (funit)# #eval fmt=%.0f (funit)#
#eval fmt=%.0f (funit)# #eval fmt=%.0f (funit)# #eval fmt=%.0f (funit)# #eval fmt=%.0f (funit)#
#eval fmt=%.0f (funit)#
     #eval fmt=%.0f (funit)# #eval fmt=%.0f (funit)#   #eval fmt=%.0f (waba)# #eval fmt=%.0f
(funit)# #eval fmt=%.0f (funit)#   #eval fmt=%.0f (gunit)# #eval fmt=%.0f (funit)# #eval fmt=%.0f
(funit)#   #eval fmt=%.0f (waba)# #eval fmt=%.0f (funit)# #eval fmt=%.0f (funit)#   #eval fmt=%.0f
(gunit)# #eval fmt=%.0f (funit)# #eval fmt=%.0f (funit)#   #eval fmt=%.0f (waba)# #eval fmt=%.0f
(funit)# #eval fmt=%.0f (funit)#
     #eval fmt=%.0f (funit)# #eval fmt=%.0f (funit)# #eval fmt=%.0f (funit)# #eval fmt=%.0f (funit)#
#eval fmt=%.0f (funit)# #eval fmt=%.0f (funit)# #eval fmt=%.0f (funit)# #eval fmt=%.0f (funit)#
#eval fmt=%.0f (funit)# #eval fmt=%.0f (funit)# #eval fmt=%.0f (funit)# #eval fmt=%.0f (funit)#
#eval fmt=%.0f (funit)# #eval fmt=%.0f (funit)# #eval fmt=%.0f (funit)# #eval fmt=%.0f (funit)#
#eval fmt=%.0f (funit)#
     #eval fmt=%.0f (funit)# #eval fmt=%.0f (funit)# #eval fmt=%.0f (funit)# #eval fmt=%.0f (funit)#
#eval fmt=%.0f (funit)# #eval fmt=%.0f (funit)# #eval fmt=%.0f (funit)# #eval fmt=%.0f (funit)#
#eval fmt=%.0f (funit)# #eval fmt=%.0f (funit)# #eval fmt=%.0f (funit)# #eval fmt=%.0f (funit)#
#eval fmt=%.0f (funit)# #eval fmt=%.0f (funit)# #eval fmt=%.0f (funit)# #eval fmt=%.0f (funit)#
#eval fmt=%.0f (funit)#
     #eval fmt=%.0f (funit)# #eval fmt=%.0f (funit)#   #eval fmt=%.0f (gunit)# #eval fmt=%.0f
(funit)# #eval fmt=%.0f (funit)#   #eval fmt=%.0f (waba)# #eval fmt=%.0f (funit)# #eval fmt=%.0f
(funit)#   #eval fmt=%.0f (200+<assembly>)# #eval fmt=%.0f (funit)# #eval fmt=%.0f (funit)#   #eval
fmt=%.0f (waba)# #eval fmt=%.0f (funit)# #eval fmt=%.0f (funit)#   #eval fmt=%.0f (gunit)# #eval
fmt=%.0f (funit)# #eval fmt=%.0f (funit)#
     #eval fmt=%.0f (funit)# #eval fmt=%.0f (funit)# #eval fmt=%.0f (funit)# #eval fmt=%.0f (funit)#
#eval fmt=%.0f (funit)# #eval fmt=%.0f (funit)# #eval fmt=%.0f (funit)# #eval fmt=%.0f (funit)#
#eval fmt=%.0f (funit)# #eval fmt=%.0f (funit)# #eval fmt=%.0f (funit)# #eval fmt=%.0f (funit)#
#eval fmt=%.0f (funit)# #eval fmt=%.0f (funit)# #eval fmt=%.0f (funit)# #eval fmt=%.0f (funit)#
#eval fmt=%.0f (funit)#
     #eval fmt=%.0f (funit)# #eval fmt=%.0f (funit)# #eval fmt=%.0f (funit)# #eval fmt=%.0f (funit)#
#eval fmt=%.0f (funit)# #eval fmt=%.0f (funit)# #eval fmt=%.0f (funit)# #eval fmt=%.0f (funit)#
#eval fmt=%.0f (funit)# #eval fmt=%.0f (funit)# #eval fmt=%.0f (funit)# #eval fmt=%.0f (funit)#
#eval fmt=%.0f (funit)# #eval fmt=%.0f (funit)# #eval fmt=%.0f (funit)# #eval fmt=%.0f (funit)#
#eval fmt=%.0f (funit)#
     #eval fmt=%.0f (funit)# #eval fmt=%.0f (funit)#   #eval fmt=%.0f (waba)# #eval fmt=%.0f
(funit)# #eval fmt=%.0f (funit)#   #eval fmt=%.0f (gunit)# #eval fmt=%.0f (funit)# #eval fmt=%.0f
(funit)#   #eval fmt=%.0f (waba)# #eval fmt=%.0f (funit)# #eval fmt=%.0f (funit)#   #eval fmt=%.0f
(gunit)# #eval fmt=%.0f (funit)# #eval fmt=%.0f (funit)#   #eval fmt=%.0f (waba)# #eval fmt=%.0f
(funit)# #eval fmt=%.0f (funit)#
     #eval fmt=%.0f (funit)# #eval fmt=%.0f (funit)# #eval fmt=%.0f (funit)# #eval fmt=%.0f (funit)#
#eval fmt=%.0f (funit)# #eval fmt=%.0f (funit)# #eval fmt=%.0f (funit)# #eval fmt=%.0f (funit)#
#eval fmt=%.0f (funit)# #eval fmt=%.0f (funit)# #eval fmt=%.0f (funit)# #eval fmt=%.0f (funit)#
#eval fmt=%.0f (funit)# #eval fmt=%.0f (funit)# #eval fmt=%.0f (funit)# #eval fmt=%.0f (funit)#
#eval fmt=%.0f (funit)#
```

```
     #eval fmt=%.0f (funit)# #eval fmt=%.0f (funit)# #eval fmt=%.0f (funit)#   #eval fmt=%.0f
(waba)# #eval fmt=%.0f (funit)# #eval fmt=%.0f (funit)# #eval fmt=%.0f (funit)# #eval fmt=%.0f
(funit)# #eval fmt=%.0f (funit)# #eval fmt=%.0f (funit)# #eval fmt=%.0f (funit)# #eval fmt=%.0f
(funit)# #eval fmt=%.0f (funit)#   #eval fmt=%.0f (waba)# #eval fmt=%.0f (funit)# #eval fmt=%.0f
(funit)# #eval fmt=%.0f (funit)#
     #eval fmt=%.0f (funit)# #eval fmt=%.0f (funit)# #eval fmt=%.0f (funit)# #eval fmt=%.0f (funit)#
#eval fmt=%.0f (funit)#   #eval fmt=%.0f (waba)# #eval fmt=%.0f (funit)# #eval fmt=%.0f (funit)#
#eval fmt=%.0f (gunit)# #eval fmt=%.0f (funit)# #eval fmt=%.0f (funit)#   #eval fmt=%.0f (waba)#
#eval fmt=%.0f (funit)# #eval fmt=%.0f (funit)# #eval fmt=%.0f (funit)# #eval fmt=%.0f (funit)#
#eval fmt=%.0f (funit)#
     #eval fmt=%.0f (funit)# #eval fmt=%.0f (funit)# #eval fmt=%.0f (funit)# #eval fmt=%.0f (funit)#
#eval fmt=%.0f (funit)# #eval fmt=%.0f (funit)# #eval fmt=%.0f (funit)# #eval fmt=%.0f (funit)#
#eval fmt=%.0f (funit)# #eval fmt=%.0f (funit)# #eval fmt=%.0f (funit)# #eval fmt=%.0f (funit)#
#eval fmt=%.0f (funit)# #eval fmt=%.0f (funit)# #eval fmt=%.0f (funit)# #eval fmt=%.0f (funit)#
#eval fmt=%.0f (funit)#
     #eval fmt=%.0f (funit)# #eval fmt=%.0f (funit)# #eval fmt=%.0f (funit)# #eval fmt=%.0f (funit)#
#eval fmt=%.0f (funit)# #eval fmt=%.0f (funit)# #eval fmt=%.0f (funit)# #eval fmt=%.0f (funit)#
#eval fmt=%.0f (funit)# #eval fmt=%.0f (funit)# #eval fmt=%.0f (funit)# #eval fmt=%.0f (funit)#
#eval fmt=%.0f (funit)# #eval fmt=%.0f (funit)# #eval fmt=%.0f (funit)# #eval fmt=%.0f (funit)#
#eval fmt=%.0f (funit)#
    end fill
```

**Table 21. Node array template for CSAS6 models**

**./UNF-Templates/cask/general_templates/node_array.tmpl**

```
  ara=  #eval fmt=%.0f (30000+assembly)# nux= 1 nuy= 1 nuz=#eval fmt=%.0f (axial_node_count)#
    fill
    #func fmt=%.0f (node=1,<axial_node_count>) 20000+100*assembly+node#
    end fill
```

This page is intentionally left blank.

# 5. PROJECT STATUS THROUGH FY19

The UNF-ST&DARDS criticality analysis status for FY15 was provided in the initial version of this report. The report was updated in FY16 to include the BWR burnup credit approach and to add data on more canisters. This section provides an update of the criticality analysis status through FY19. As discussed throughout the report, the ability to carry out criticality analyses with UNF-ST&DARDS requires a set of CSAS6 templates, ORIGEN cross section libraries, as well as fuel irradiation information and canister loading maps from the UDB.

Assessment of the as-loaded criticality analysis status involves comparison of the number of canisters analyzed to date with the total number of canisters loaded at the various reactor sites throughout the United States. The number of loaded canisters present at reactor sites was determined by reviewing the *StoreFuel* [6] publication from August 2019. *StoreFuel* is a monthly newsletter that provides current information with regard to development, licensing, and loading of SNF canisters. Table 15 of the August 2019 issue of *StoreFuel* [6] lists the number of canisters at the various sites. This list is organized by cask vendor, canister design, and cask system. Relevant data from *StoreFuel* are periodically imported to the UDB.

A list of the currently deployed canisters by site, vendor, and storage system, derived from Table 15 of *StoreFuel* [6], is presented Table 22. Table 22 also includes information such as whether or not a criticality model is available in UNF-ST&DARDS, how many loading maps are available in the UDB, and the number of canisters that have been analyzed. In most cases, the limiting item is the lack of availability of canister loading maps, although canister models are still needed for some of the newer canister designs and a few of the older TN canisters. Furthermore, calculations have not been performed for Big Rock Point, for which there is a model and loading map, but further assessment is required to determine how to perform KENO calculations with the two-story basket design.

The FY19 effort analyzed an additional 92 total canisters, 68 of which are PWR canisters, and 24 of which are BWR canisters. To date, the total number of loaded canisters for which criticality analysis has been completed is 708 canisters at 33 sites. A query capable of accessing all $k_{eff}$ results from the UDB is presented in Appendix B.

## Table 22. FY19 UNF-ST&DARDS criticality analysis status assessment

| Canister | Model Available | Reactor | Vendor | Cask system | EOFY19 | | |
|---|---|---|---|---|---|---|---|
| | | | | | Loaded | Maps | Analyzed |
| **PWR** | | | | | | | |
| TSC-24 | Yes | Maine Yankee | NAC | UMS | 60 | 60 | 60 |
| | | Catawba | | | 24 | 24 | 24 |
| | | Palo Verde | | | 152 | 0 | 0 |
| | | McGuire | | | 28 | 0 | 0 |
| TSC-37 | Yes | Zion | | MAGNASTOR | 61 | 61 | 61 |
| | | Catawba | | | 20 | 0 | 0 |
| | | McGuire | | | 23 | 0 | 0 |
| | | Kewaunee | | | 24 | 24 | 24 |
| CY-MPC 26 | Yes | Haddam Neck | | NAC-MPC | 37 | 37 | 37 |
| CY-MPC 24 | Yes | | | | 3 | 3 | 3 |
| Yankee-MPC | Yes | Yankee Rowe | | | 15 | 15 | 15 |
| I-28 | No | Surry | | N/A | 2 | 0 | 0 |
| MPC-24E/EF | Yes | Trojan | Holtec | TranStor Cask | 34 | 34 | 34 |
| MPC-24 | Yes | ANO | | HI-STORM | 36 | 20 | 20 |
| MPC-32 | Yes | Sequoyah | | | 44 | 27 | 27 |
| | | Indian Point | | | 49 | 18 | 18 |
| | | ANO | | | 32 | 17 | 17 |
| | | Comanche Peak | | | 36 | 9 | 9 |
| | | Salem | | | 32 | 16 | 7 |
| | | Waterford | | | 23 | 9 | 9 |
| | | D. C. Cook | | | 44 | 12 | 12 |
| | | Byron | | | 31 | 0 | 0 |
| | | Braidwood | | | 29 | 0 | 0 |
| | | Diablo Canyon | | | 58 | 0 | 0 |
| | | Farley | | | 51 | 21 | 21 |
| | | Vogtle | | | 34 | 0 | 0 |
| MPC-37 | No | V. C. Summer | | | 8 | 0 | 0 |
| | | Sequoyah | | | 15 | 0 | 0 |
| | | Callaway | | | 18 | 0 | 0 |
| | | Palisades | | | 11 | 0 | 0 |
| | | SONGS 2&3 | | | 31 | 0 | 0 |
| | | Sequoyah | | | 15 | 0 | 0 |
| | | South Texas Project | | | 12 | 0 | 0 |
| | | Watts Bar | | | 14 | 0 | 0 |
| FO-DSC | Yes | Rancho Seco | TN | NUHOMS | 2 | 2 | 2 |
| FC-DSC | Yes | | | | 18 | 18 | 18 |
| FF-DSC | Yes | | | | 1 | 1 | 1 |
| DSC-32PT | Yes | Kewaunee | | | 14 | 14 | 14 |
| | | Millstone | | | 34 | 18 | 18 |
| | | Palisades | | | 11 | 11 | 11 |
| | | Ginna | | | 10 | 6 | 6 |
| | | Point Beach | | | 34 | 0 | 0 |
| | | Fort Calhoun | | | 10 | 0 | 0 |
| DSC-32PTH | Yes | North Anna | | | 40 | 0 | 0 |
| | | Surry | | | 38 | 0 | 0 |
| | | Seabrook | | | 22 | 0 | 0 |
| | | St. Lucie | | | 48 | 0 | 0 |
| | | Turkey Point | | | 28 | 0 | 0 |
| DSC-32PTH1 | Yes | Crystal River | | | 39 | 39 | 39 |
| | | Davis-Besse | | | 4 | 0 | 0 |
| DSC-37PTH | No | Beaver Valley | | | 10 | 0 | 0 |
| DSC-24P | No | Oconee | | | 84 | 0 | 0 |
| | | Calvert Cliffs | | | 48 | 0 | 0 |
| | | Davis-Besse | | | 3 | 0 | 0 |
| DSC-32P | No | Calvert Cliffs | | | 30 | 0 | 0 |
| DSC-32PHB | No | Calvert Cliffs | | | 11 | 0 | 0 |
| DSC-24PHB | No | Oconee | | | 64 | 0 | 0 |
| DSC-24PTH | No | Robinson | | | 23 | 0 | 0 |
| | | Palisades | | | 13 | 13 | 13 |
| | | Oconee | | | 11 | 0 | 0 |
| DSC-24PT1 | Yes | SONGS | | | 18 | 18 | 17 |
| DSC-24PT4 | No | SONGS | | | 33 | 33 | 0 |
| DSC-7P | No | Robinson | | | 8 | 0 | 0 |
| TN-32 | No | North Anna | | TN-Metal | 28 | 0 | 0 |
| | | Surry | | | 26 | 0 | 0 |
| | | McGuire | | | 10 | 0 | 0 |

| | | | | | | | |
|---|---|---|---|---|---|---|---|
| TN-40 | No | Prairie Island | | | 29 | 15 | 0 |
| TN-40HT | No | Prairie Island | | | 15 | 2 | 0 |
| VSC-24 | No | ANO | ES | N/A | 24 | 24 | 0 |
| | | Palisades | | | 18 | 18 | 0 |
| | | Point Beach | | | 16 | 0 | 0 |
| X33 | No | Surry | Castor | N/A | 1 | 0 | 0 |
| V21 | No | Surry | | N/A | 25 | 0 | 0 |
| MC-10 | No | Surry | Westinghouse | N/A | 1 | 0 | 0 |

**Table 22. FY19 UNF-ST&DARDS criticality analysis status assessment (continued)**

| Canister | Model Available | Reactor | Vendor | Cask system | EOFY19 | | |
|---|---|---|---|---|---|---|---|
| | | | | | Loaded | Maps | Analyzed |
| **BWR** | | | | | | | |
| MPC-LACBWR | Yes | Lacrosse | NAC | NAC-MPC | 5 | 5 | 5 |
| MPC-HB | Yes | Humboldt Bay | Holtec | HI-STAR | 5 | 5 | 5 |
| W150 | Yes | Big Rock Point | BFS/ES | Fuel Solutions | 8 | 8 | 0 |
| MPC-68 | Yes | Grand Gulf | Holtec | HI-STORM | 28 | 22 | 22 |
| | | Vermont Yankee | | | 23 | 13 | 13 |
| | | Dresden | | | 64 | 0 | 0 |
| | | Hatch | | | 63 | 0 | 0 |
| | | Browns Ferry | | | 45 | 40 | 40 |
| | | Columbia | | | 36 | 27 | 27 |
| | | Fermi | | | 18 | 0 | 0 |
| | | Fitzpatrick | | | 21 | 21 | 21 |
| | | Hope Creek | | | 29 | 0 | 0 |
| | | LaSalle | | | 24 | 0 | 0 |
| | | Perry | | | 20 | 0 | 0 |
| | | Pilgrim | | | 17 | 0 | 0 |
| | | Quad Cities | | | 39 | 0 | 0 |
| | | River Bend | | | 31 | 19 | 19 |
| MPC-68M | No | Hatch | | | 22 | 0 | 0 |
| | | Dresden | | | 18 | 0 | 0 |
| | | Fitzpatrick | | | 5 | 0 | 0 |
| | | Columbia | | | 9 | 0 | 0 |
| | | Grand Gulf | | | 6 | 0 | 0 |
| | | La Salle | | | 14 | 0 | 0 |
| | | Quad Cities | | | 16 | 0 | 0 |
| | | Vermont Yankee | | | 35 | 0 | 0 |
| MPC-89 | No | Browns Ferry | | | 33 | 0 | 0 |
| | | Clinton | | | 11 | 0 | 0 |
| DSC-52B | No | Susquehanna | TN | NUHOMS | 27 | 0 | 0 |
| DSC-61BT | Yes | Limerick | | | 19 | 0 | 0 |
| | | Nine Mile Point | | | 16 | 10 | 10 |
| | | Oyster Creek | | | 8 | 0 | 0 |
| | | Duane Arnold | | | 20 | 0 | 0 |
| | | Cooper | | | 8 | 8 | 8 |
| | | Susquehanna | | | 48 | 0 | 0 |
| | | Monticello | | | 10 | 10 | 10 |
| DSC-61BTH | Yes | Brunswick | | | 40 | 0 | 0 |
| | | Limerick | | | 27 | 0 | 0 |
| | | Oyster Creek | | | 26 | 0 | 0 |
| | | Cooper | | | 22 | 0 | 0 |
| | | Susquehanna | | | 27 | 0 | 0 |
| | | Monticello | | | 20 | 0 | 0 |
| | | Nine Mile Point | | | 26 | 0 | 0 |
| TN-68 | No | Peach Bottom | | TN Metal | 92 | 0 | 0 |

# 6. REFERENCES

1. K. Banerjee et al., *Safety Analysis Capabilities of the Used Nuclear Fuel Storage, Transportation and Disposal Analysis Resource and Data System*, FCRD-NFST-2014-000360 (ORNL/LTR-2014/414), Oak Ridge National Laboratory, Oak Ridge, Tenn., September 2014.
2. *SCALE: A Comprehensive Modeling and Simulation Suite for Nuclear Safety Analysis and Design,* ORNL/TM-2005/39, Version 6.1, Oak Ridge National Laboratory, Oak Ridge, Tenn., June 2011. Available from Radiation Safety Information Computational Center at Oak Ridge National Laboratory as CCC-785.
3. H. Smith, J. Peterson, and J. Hu, "Fuel Assembly Modeling for the Modeling and Simulation Toolset," ORNL/LTR-2012-555, Oak Ridge National Laboratory, Oak Ridge, Tenn., November 2012.
4. *RW-859 Nuclear Fuel Data*, Energy Information Administration, Washington, D.C., October 2004.
5. J. C. Wagner, M. D. Dehart, and C. V. Parks, *Recommendations for Addressing Axial Burnup in PWR Burnup Credit Analyses*, NUREG/CR-6801 (ORNL/TM-2001/273), prepared for the US Nuclear Regulatory Commission by Oak Ridge National Laboratory, Oak Ridge, Tenn., March 2003.
6. *StoreFuel*, Vol. 21 , No. 252, UxC Consulting Compay, Roswell, Ga. August 6, 2019
7. G. Radulescu et al., *An Approach for Validating Actinide and Fission Product Burnup Credit Criticality Safety Analyses–Isotopic Composition Predictions*, NUREG/CR-7108 (ORNL/TM-2011/514), prepared for the US Nuclear Regulatory Commission by Oak Ridge National Laboratory, Oak Ridge, Tenn., April 2012.
8. J. M. Scaglione et al. *An Approach for Validating Actinide and Fission Product Burnup Credit Criticality Safety Analyses–Criticality ($k_{eff}$) Predictions*, NUREG/CR-7109 (ORNL/TM-2011/514), prepared for the US Nuclear Regulatory Commission by Oak Ridge National Laboratory, Oak Ridge, Tenn., April 2012.

This page is intentionally left blank.

# Appendix A

# Description of CSAS6 Canister Criticality Models

## A-1. TSC-24

### A-1.1 Canister

The TSC-24 canisters have 24 locations that can host intact spent fuel assemblies, consolidated fuel assemblies, damaged fuel assemblies, fuel debris, or control element assemblies. There are two classes of the TSC-24 denoted Class 1 and Class 2; they differ in terms of their height. Table A-1.1 has all of the common dimensions for both canister classes, and Table A-1.2 has the canister dimensions that differ between the two canister designs. Figure A-1.1 shows the plan and isometric views of the SCALE model loaded with CE14×14 fuel assemblies together with the storage location numbering conventions [1, 2, 3, and 4]. Shown on this picture are the radial positioning of the 8 tie rods and the drain tube. The latter is shown as a reference for the numbering convention of the 24 fuel locations (also shown on this figure).

The difference between the two classes is negligible from the criticality point of view, but they differ through their height, the number of support disks (30 for Class 1 and 32 for Class 2), and the number of heat transfer disks (29 for Class 1 and 31 for Class 2). Certain restrictions can apply on loading the used fuel in a Class 1 or Class 2 canister. For example, if the fuel (consolidated fuel, damaged fuel, fuel debris, but also intact fuel) is loaded in a Maine Yankee Fuel Can, then this can may only be stored in a Class 1 canister while, if the canister contains a Control Element Assembly (CEA), then this canister can only be a Class 2 canister. Also, the difference in height between the two classes (Class 2 is taller) might be important for thermal evaluations.

The criticality control of the cask is achieved using a neutron flux trap configuration with individual pressurized water reactor (PWR) assemblies surrounded by 4 neutron absorber sheets (Boral) with a minimum loading of 0.025g $^{10}B/cm^2$. The Boral composition used in the SCALE/KENO-VI evaluations is obtained from the cask material composition at page 210 of [1].

### A-1.2 Damaged Fuel

The design basis fuel assembly for the TSC-24 is a 4.2 w/o W1717WO fuel assembly and should be used for all calculations at sites other than Maine Yankee. The site-specific fuel assembly for Maine Yankee is a modified version of the C1414C fuel assembly with rods removed to form a diamond pattern. The Maine Yankee site-specific fuel also uses and enrichment of 4.2 w/o and is designated as the C1414CMY.

### A-1.3 Model Verification

A verification calculation was performed with the TSC-24 uniformly loaded with fresh W1717WO fuel assemblies enriched to 4.2 w/o. The canister was modeled as being in the nominal configuration, with the fuel assemblies radially centered in the basket cells. The results of this calculation along with the calculated $k_{eff}$ found in Table 6.4-5 of Reference [6] are presented in Table A-1.3 and show good agreement.

## A-1.4 References

1. NAC International, Submittal of Replacement Pages to Update the NAC-UMS FSAR from Rev. 3 to Rev. 4, November 19, 2004.
2. NAC International, Submittal of Replacement Pages to Update the NAC-UMS FSAR from Rev. 4 to Rev. 5, October 11, 2005.
3. Appendix B Approved Contents and Design Features for the NAC-UMS System Amendment 5, December 2009.
4. NAC International, Submittal of NAC-UMS FSAR Amendment 1, May 11, 2001, Docket No. 72-1015.
5. NAC-UMS, Final Safety Analyses Report, Revision 3, 2004.
6. Safety Analysis Report – UMS Universal Transport Cask, NAC International, Revision 1, Norcross, Georgia, December 2002.

**Table A-1.1. SCALE criticality model dimensions for the TSC-24. (Class 2 dimensions shown only when different from Class 1.)**

| | Size (cm) Class 1 | Size (cm) Class 2 | Reference and NAC International Drawing Number |
|---|---|---|---|
| **Canister** | | | |
| Inner canister radius | 83.5787 | | 2, page 71 (Drawing 582, R12) |
| Outer canister radius | 85.1662 | | 2, page 71 (Drawing 582, R12) |
| Inner canister height (cavity, top baseplate to bottom lid) | 414.782 | 437.896 | 2, page 71 (Drawing 582, R12) |
| Bottom plate thickness | 4.445 | | 2, page 71 (Drawing 582, R12) |
| Lid thickness | 25.4 | | 2, page 74 (Drawing 584, R19) |
| Total height (bottom baseplate to top lid) | 444.627 | 467.741 | C-2, page 71 (Drawing 582, R12) |
| **UMS-24 fuel can** | | | |
| Inner size (square) | 22.352 | | 1, page 112 (Drawing 581, R12) |
| Internal cavity height | 387.604 | 405.384 | 1, page 112 (Drawing 581, R12) |
| Outer size (square) | 22.5044 | | 1, page 112 (Drawing 581, R12) |
| Can wall thickness (18 gauge) | 0.121412 | | 1, page 112 (Drawing 581, R12) |
| Cladding thickness (26 gauge) | 0.045466 | | 1, page 112 (Drawing 581, R12) |
| Cladding height | 384.302 | 402.082 | 1, page 112 (Drawing 581, R12) |
| **Boral** | | | |
| Boral core thickness | 0.126992 | | Calculated based on 0.025g $^{10}B/cm^2$ |
| Boral thickness | 0.1905 | | 1, page 112 (Drawing 581, R12) |
| Boral width | 20.9042 | | 1, page 113 (Drawing 581, R12) |
| Boral height | 382.27 | 400.05 | 1, page 113 (Drawing 581, R12) |
| Sheathing thickness | 0.045466 | | 1, page 112 (Drawing 581, R12) |
| Sheathing width | 20.99513 | | 1, page 112 (Drawing 581, R12) |
| Sheathing height | 382.3609 | 400.1409 | 1, page 112 (Drawing 581, R12) |
| Distance from bottom of basket to bottom of boral plate | | | Boral plate positioned vertically symmetric on the can surface |
| **Basket** | | | |
| Bottom weldment disk radius | 83.185 | | 5, page 329 (Drawing 591, R6) |
| Bottom weldment disk thickness | 2.54 | | 5, page 329 (Drawing 591, R6) |
| Support disk radius | 83.2739 | | 5, page 332 (Drawing 593, R7) |
| Support disk thickness | 1.27 | | 5, page 332, (Drawing 593, R7) |

**Table A-1.2. SCALE criticality model dimensions for the TSC-24. (Class 2 dimensions shown only when different from Class 1.)**

| | | | |
|---|---|---|---|
| Heat transfer disk radius | 82.9564 | | 5, page 334 (Drawing 594, R2) |
| Heat transfer disk thickness | 1.27 | | 5, page 334 (Drawing 594, R2) |
| Top weldment disk radius | 83.185 | | 5, page 331, (Drawing 592, R8) |
| Top weldment disk thickness | 3.175 | | 5, page 331 (Drawing 592, R8) |
| **Tie Rod** | | | |
| Rod Radius (modeled with split spacers) | 3.6576 | | 5, page 333 (Drawing 593, R7) |
| Rod Height | 401.828 | 419.608 | 5, page 333 (Drawing 593, R7) |
| **Drain Pipe** | | | |
| Outer radius | 1.27 | | 5, page 319 (Drawing 583, R8) |
| Wall thickness | 0.0889 | | 5, page 319 (Drawing 583, R8) |

**Table A-1.3. Model Verification results the TSC-24**

| Reference 6 $k_{eff}$ | Calculated $k_{eff} \pm \sigma$ | $\Delta k_{eff}$ |
|---|---|---|
| 0.9192 | 0.91871 ± 0.00017 | 0.00050 |

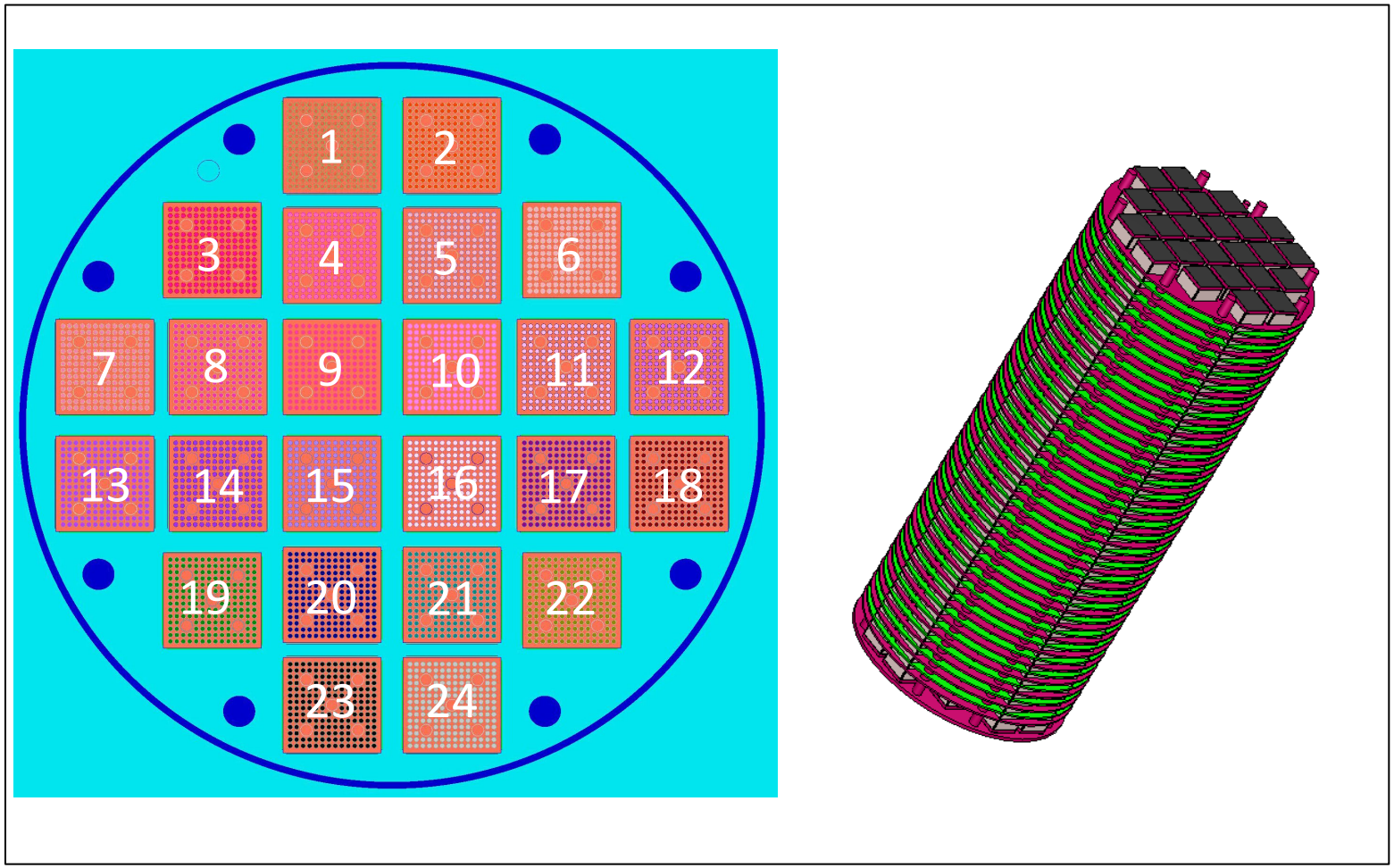


**Fig. A-1.1. Plan view (left) and isometric view (right) of the NAC TSC-24.**

# A-2. TSC-37

## A-2.1 Canister

The TSC-37 canister uses 21 fuel tubes that form 16 developed cells to accommodate up to 37 Zion fuel assemblies. The TSC-37 basket assembly consists of 21 fuel tubes that are connected by 31 weld rods that support the fuel tubes. Each fuel tube contains an inner lining of borated aluminum neutron absorber that is held between sheets of aluminum and wrapped with a stainless steel sheath. All fuel tubes contain borated aluminum neutron absorber, except for the developed cells, which have no neutron absorber.

There are two different varieties of the TSC-37 canister, the undamaged PWR TSC-37 and damaged PWR TSC-37. The primary difference between the two is that the PWR TSC-37 has four corner fuel tubes that have an increased inner cavity width to accommodate damaged fuel cans (DFCs). Both designs have been chosen for incorporation into the UNF-ST&DARDS database to model canisters containing damaged fuel.

The dimensions of the model are presented in TableA-2.1. Figure A-2.1 shows plan and isometric views of an undamaged fuel TSC-37 canister. Figure A-2.2 shows plan and isometric views of a damaged fuel TSC-37 canister.

## A-2.2 Damaged Fuel

Damaged fuel is modeled canned with a larger rod pitch, no cladding, and no burnup credit taken. This is to model the hypothetical loss of cladding and separation of the fuel rods into the most reactive configuration. Each assembly design has an associated most reactive damaged fuel surrogate [pg. 300, 1]. The damaged fuel surrogate of the Westinghouse 15 × 15 design used at Zion has a rod pitch of 1.43002 cm.

## A-2.3 Model Verification

Verification of the TSC-37 CSAS6 model was performed by comparison to the FSAR analysis corresponding to the 17×17H1 case from Table 6.7.2-1 [1]. The case was modeled using the fuel dimensions from Table 6.4.3-1 at 5.0 wt% enrichment and fully flooded canister with 2500 ppm borated water. The results of the model verification calculation are presented along with those from Reference [1] in Table A.2-2 and show good agreement with the FSAR value.

## A-2.4 References

1. *MAGNASTOR Final Safety Analysis Report*, ADAMS Accession Number: ML102420568, NAC International, 2010.

**Table A-2.1. SCALE criticality model dimensions for the TSC-37**

| Canister | Size (cm) | Reference 1 Location |
|---|---|---|
| Inner Canister Radius | 90.18 | Figure 6.3.3-2 |
| Outer Canister Radius | 81.44 | Figure 6.3.3-2 |
| Canister Cavity Height | 457.2 | Figure 6.3.3-2 |
| **Basket** | | |
| Inner Cell Dimension – Standard Cell | 22.504 | DWG 551 Sheet 2 |
| Cell Thickness – Standard Cell | 0.79502 | DWG 551 Sheet 1 |
| Cell Height – Standard Cell | 440.69 | DWG 551 Sheet 1 |
| **Borated Aluminum** | | |
| **Poison** | | |
| Thickness | 0.3175 | DWG 551 Sheet 1 |
| Width | 20.4724 | Figure 6.7.1-1 |
| Height | 440.69 | DWG W74-122 |
| **Support Structure Specifications** | | |
| Side Support Weldment Dimensions | See Reference | DWG 574 Sheet 5 |
| Side Support Weldment Material | Carbon Steel | Table 1.3-1 |
| Gusset Dimensions | See Reference | DWG 574 Sheet 4 |
| Gusset Material | Carbon Steel | Table 1.3-1 |

**Table A-2.2. Model Verification results the TSC-37**

| Reference 1 $k_{eff}$ | Calculated $k_{eff} \pm \sigma$ | $\Delta k_{eff}$ |
|---|---|---|
| 0.91897 | 0.91849 ± 0.00017 | 0.00048 |

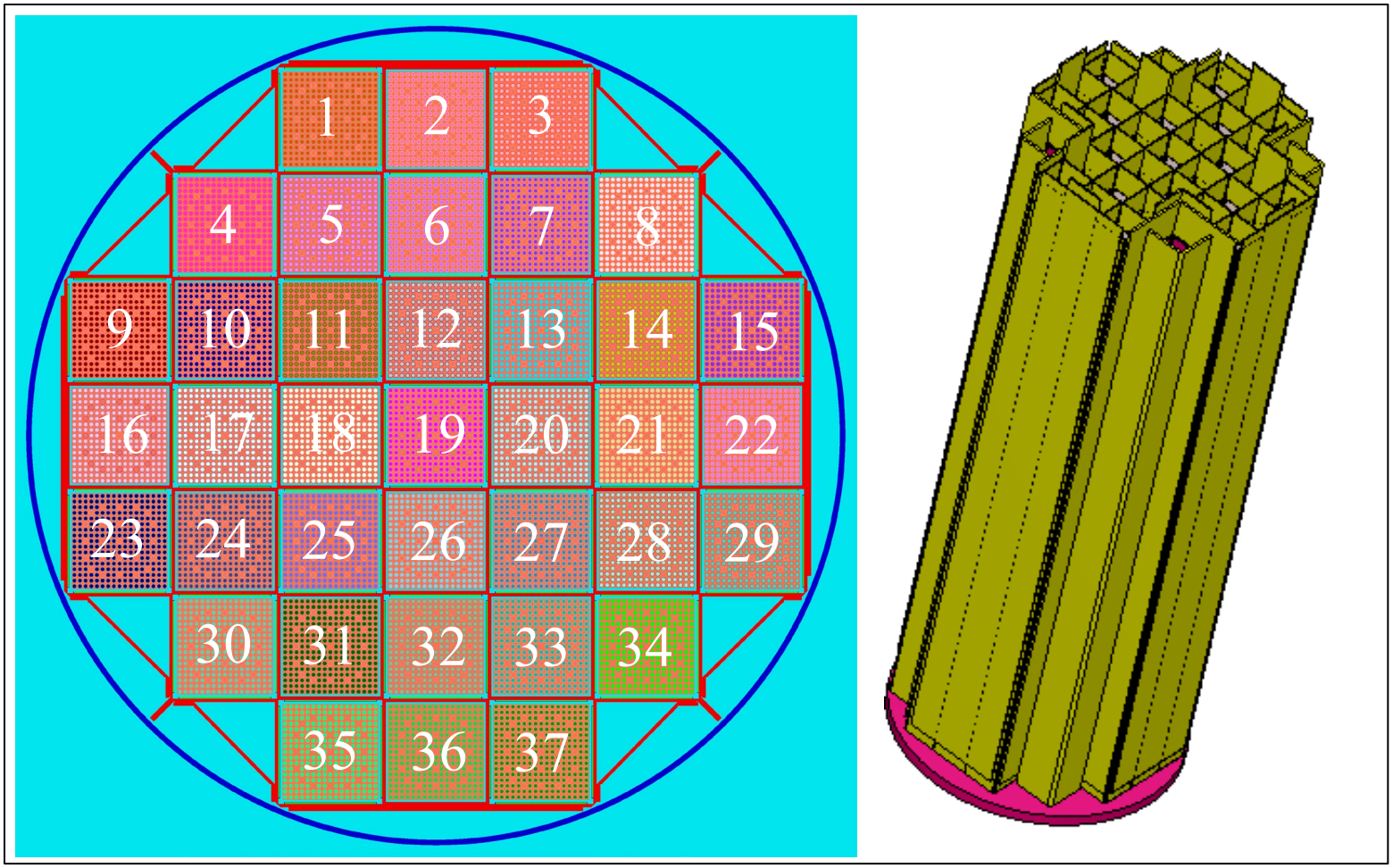


**Fig. A-2.1 Plan view (left) and isometric view (right) of the NAC TSC-37 undamaged fuel canister.**

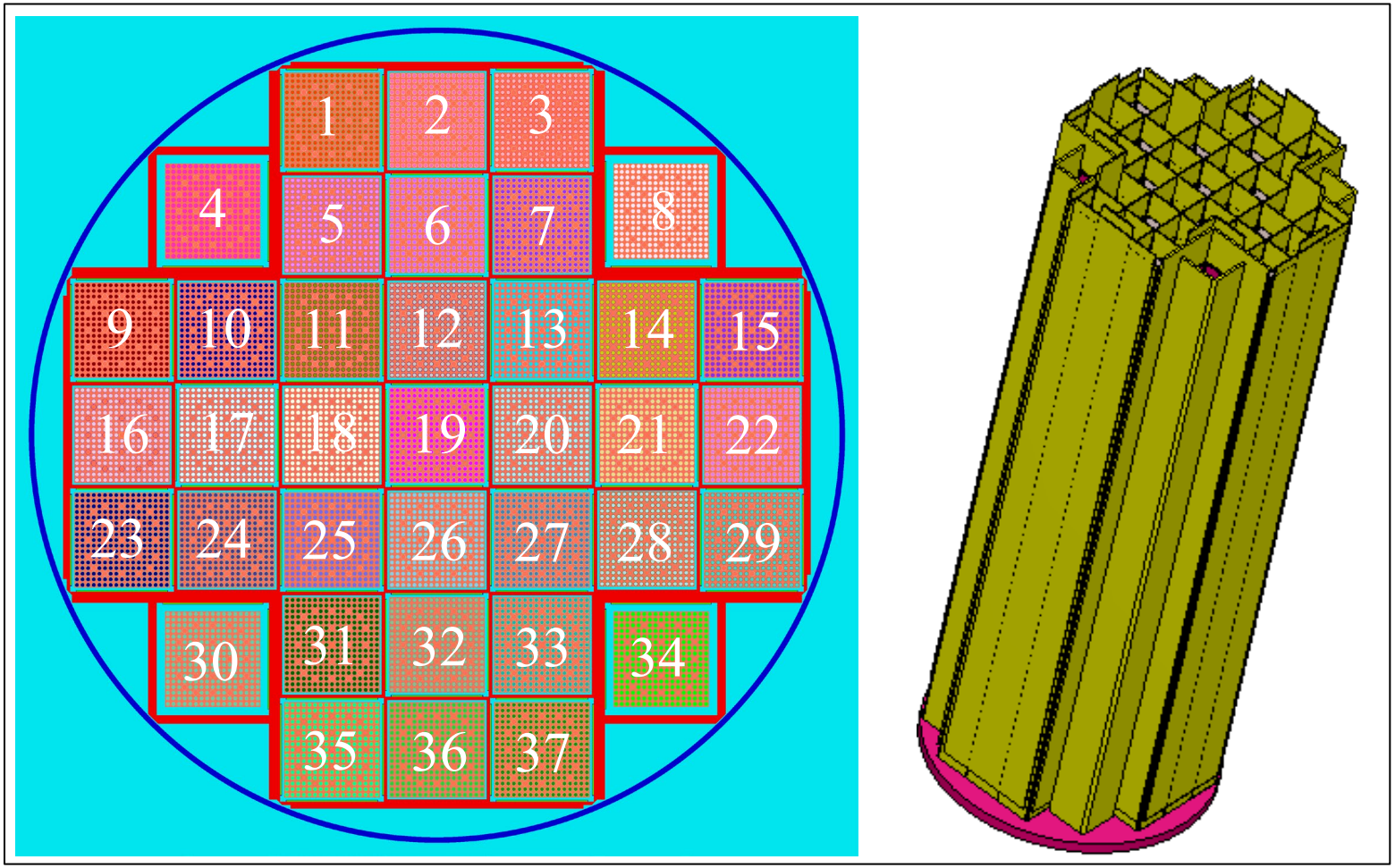


**Fig. A-2.2.Plan view (left) and isometric view (right) of the NAC TSC-37 damaged fuel canister.**

# A-3. CY-MPC-24 and CY-MPC-26

## A-3.1 Canister

The Connecticut Yankee Multipurpose Canisters (CY-MPC)-24 and -26 canisters are exclusively used at Connecticut Yankee's Haddam Neck site. NAC's CY-MPC-24 and -26 canisters are part of the storable transport cask (STC) system and can accommodate either 24 or 26 PWR spent fuel assemblies, CY-MPC reconfigured fuel assemblies, and CY-MPC DFCs. The 24-assembly basket is designed to accommodate higher enriched fuel assemblies than the 26-assembly basket. Criticality control in both baskets is primarily achieved by flux trap design. The dimensions for both 24 and 26 CY-MPCs are the same, and are presented in Table A-3.1. The only difference between the CY-MPC-26 and the CY-MPC-24 is that the CY-MPC-24 has positions 12 and 15 removed so that no fuel assembly may be placed there. Four of the loading positions (1, 4, 23, and 26) are oversized positions and are the only positions capable of accommodating reconfigured fuel assembly or DFC fuel. Plan view and isometric view layouts of the CY-MPC-26 and CY-MPC-24 are shown in Figures A-3.1 and A-3.2, respectively.

## A-3.2 Damaged Fuel

Intact fuel assemblies with missing rods are modeled with 24 fuel rods removed in a diamond pattern (Reference [1]). However, fuel assembly burnup is credited. Fuel assemblies that are damaged or reconfigured are modeled with 24 fuel rods removed in a diamond pattern (Reference [1]). Fresh design basis assemblies as defined above are used for the damaged and reconfigured assemblies.

## A-3.3 Model Verification

One verification calculation was run for the CY-MPC-24 and one was run the CY-MPC-26. Both calculations used the XHN15B fuel assemblies; the CY-MPC-24 benchmark calculation used an enrichment of 4.61 w/o, and the CY-MPC-26 calculation used an enrichment of 3.93 w/o. The results of the benchmark calculations are shown in Table A-3.2 and show reasonable agreement.

## A-3.4 References

1. *NAC-STC Safety Analysis Report*, Rev. 15, US NRC, Docket No. 71-9235, March 2004.

**Table A-3.1. SCALE criticality model dimensions for the CY-MPC-24 and CY-MPC-26**

| Canister | Size (cm) | Reference and NAC International Drawing Number) |
|---|---|---|
| Inner canister radius | 88.1253 | 1, page 197 (Drawing 870, R3) |
| Outer canister radius | 89.7128 | 1, page 197 (Drawing 870, R3) |
| Inner canister height (inner cavity length) | 360.68 | 1, page 197 (Drawing 870, R3) |
| Thickness of bottom plate | 4.445 | 1, page 197 (Drawing 870, R3) |
| Thickness of structural lid | 7.62 | 1, page 199 (Drawing 871, R5) |
| Thickness of shield lid assembly | 12.7 | 1, page 199 (Drawing 871, R5) |
| Height | 385.445 | 1, page 197 (Drawing 870, R3) |
| Drain tube length | 362.458 | 1, page 203 (Drawing 873, R2) |
| Drain tube outer radius | 2.54 | 1, page 203 (Drawing 873, R2) |
| Drain tube inner radius | 2.4511 | 1, page 203 (Drawing 873, R2) |
| Drain tube x position | 60.452 | 1, page 219 (Drawing 891, R3) |
| Drain tube y position | -47.244 | 1, page 219 (Drawing 891, R3) |
| **Standard fuel can** | | |
| Inner size (square) | 22.1488 | 1, page 106 (Drawing 881, R4) |
| Internal cavity length | 335.026 | 1, page 206 (Drawing 881, R4) |
| Thickness of can wall | 0.12192 | 1, page 206 (Drawing 881, R4) |
| **Boral (standard fuel can)** | | |
| Boral core thickness | 0.1271 | Calculated based on 0.02 g $^{10}B/cm^2$ |
| Boral thickness | 0.1905 | 1, page 206 (Drawing 881, R4) |
| Boral width | 20.828 | 1, page 207 (Drawing 881, R4) |
| Boral height | 326.39 | 1, page 207 (Drawing 881, R4) |
| Sheathing thickness | 0.04572 | 1, page 206 (Drawing 881, R4) |
| **Oversized fuel can** | | |
| Inner size (square) | 23.1648 | 1, page 106 (Drawing 882, R4) |
| Internal cavity length | 335.026 | 1, page 208 (Drawing 882, R4) |
| Thickness of can wall | 0.12192 | 1, page 106 (Drawing 882, R4) |
| **Boral (oversized fuel can)** | | |
| Boral core thickness | 0.1271 | Calculated based on 0.02g $^{10}B/cm^2$ |
| Boral thickness | 0.1905 | 1, page 208 (Drawing 882, R4) |
| Boral width | 21.844 | 1, page 209 (Drawing 882, R4) |
| Boral height | 326.39 | 1, page 209 (Drawing 882, R4) |
| Sheathing thickness | 0.04572 | 1, page 208 (Drawing 882, R4) |
| **Basket** | | |
| Bottom weldment disk radius | 87.63 | 1, page 219 (Drawing 891, R3) |
| Bottom weldment disk thickness | 1.27 | 1, page 219 (Drawing 891, R3) |

**Table A-3.1. SCALE criticality model dimensions for the CY-MPC-24 and CY-MPC-26 (cont.)**

| Canister | Size (cm) | Reference and NAC International Drawing Number |
|---|---|---|
| Support disk radius | 87.884 | 1, page 223 (Drawing 893, R2) |
| Support disk thickness | 1.27 | 1, page 223 (Drawing 893, R2) |
| Heat transfer disk radius | 87.503 | 1, page 225 (Drawing 894, R0) |
| Heat transfer disk thickness | 1.27 | 1, page 225 (Drawing 894, R0) |
| Top weldment disk radius | 87.63 | 1, page 220 (Drawing 892, R3) |
| Top weldment disk thickness | 1.27 | 1, page 220 (Drawing 892, R3) |
| **Tie rod** | | |
| Radius (with the split spacer) | 3.6576 | 1, page 224 (Drawing 893, R2) |
| Height | 348.488 | 1, page 224 (Drawing 893, R2) |
| **Drain tube** | | |
| Outer radius | 1.27 | 1, page 203 (Drawing 873, R2) |
| Wall thickness | 0.0889 | 1, page 203 (Drawing 873, R2) |

**Table A-3.2. Model verification results for CY-MPC canisters**

| Canister | Reference 1 $k_{eff}$ | Calculated $k_{eff} \pm \sigma$ | $\Delta k_{eff}$ |
|---|---|---|---|
| CY-MPC-24 | 0.9064 | 0.89911 ± 0.00029 | 0.00729 |
| CY-MPC-26 | 0.9197 | 0.91322 ± 0.00024 | 0.00648 |

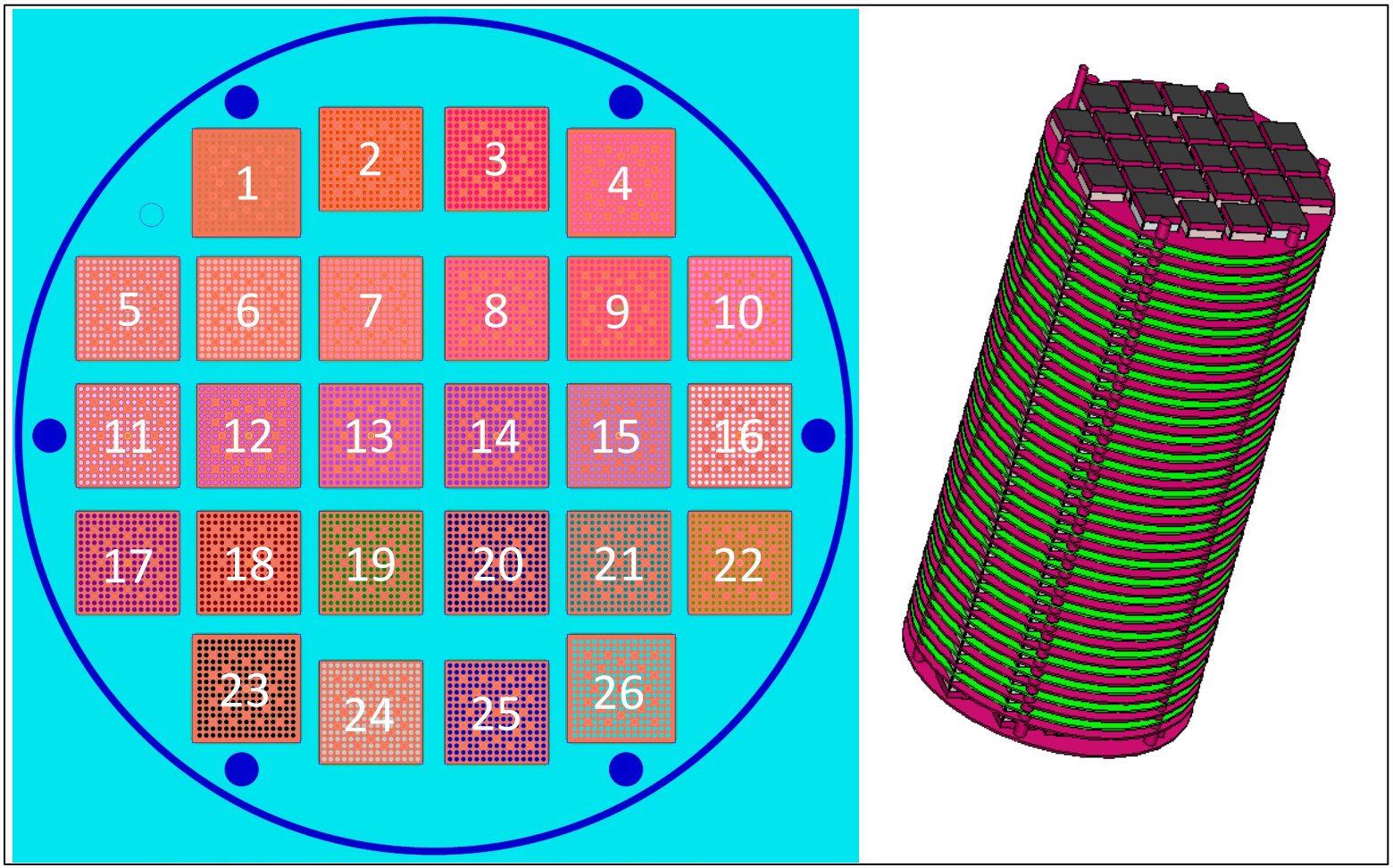


**Fig. A-3.1. Plan view (left) and isometric view (right) of the NAC CY-MPC-26 canister.**

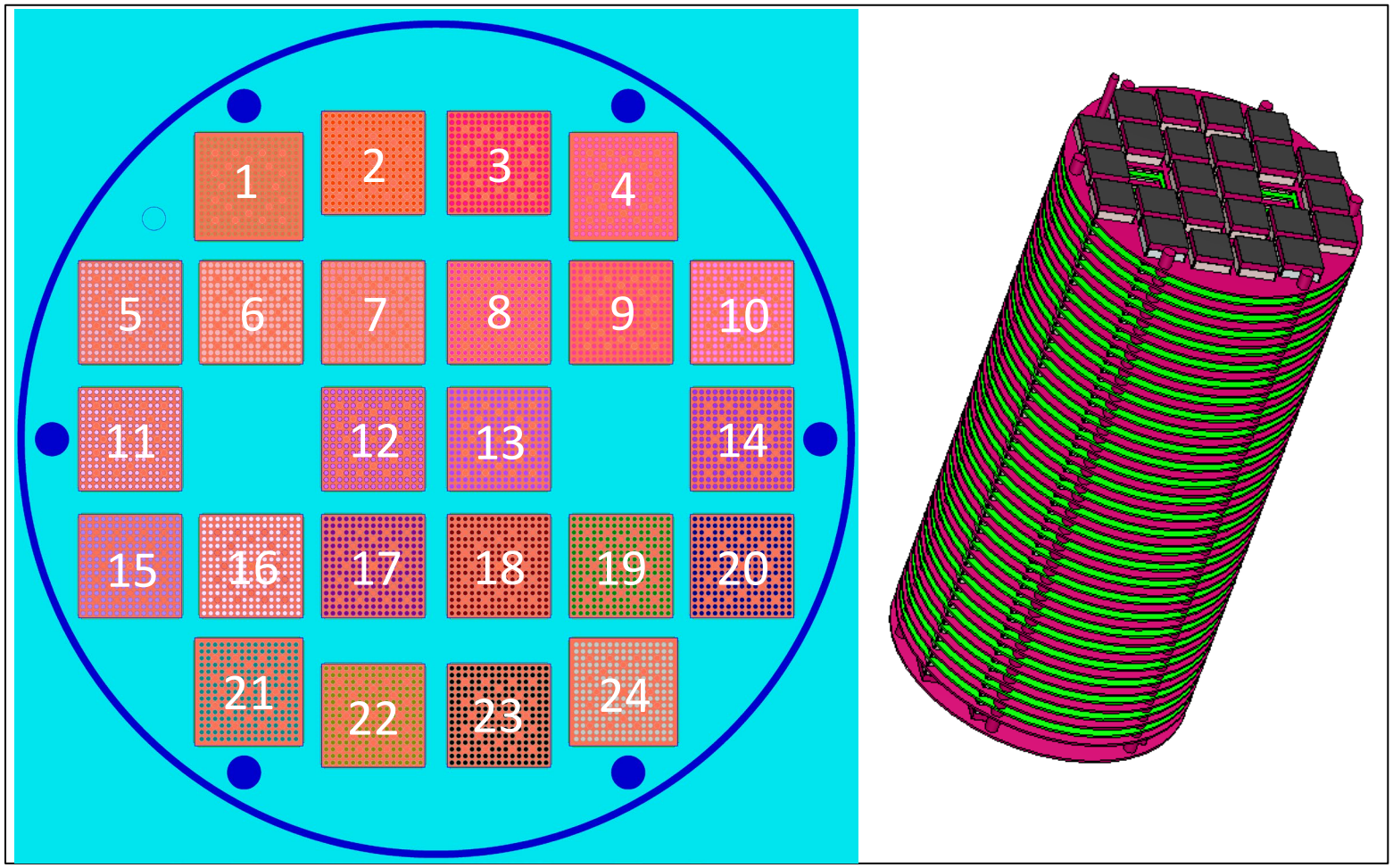


**Fig. A-3.2. Plan view (left) and isometric view (right) of the NAC CY-MPC-24 canister.**

# A-4. Yankee-MPC

## A-4.1 Canister

The Yankee Atomic Electric Company's Yankee Rowe site uses NAC's canistered STCs with Yankee-MPCs (Yankee Multipurpose Canisters) that can accommodate up to 36 fresh or spent fuel assemblies, Yankee RFAs, or re-caged fuel assemblies for a maximum content weight of 30,600 pounds. The Yankee-MPC uses a tube and disk design with support and heat transfer disks holding the fuel tubes in place. The support and heat transfer disks are joined with support rods, which connect the canister with the canister body. The dimensions for the 36-fuel assembly Yankee-MPCs are shown in Table A-4.1. A plan view with basket cell numbering scheme is provided along with an isometric view of the basket with the canister wall removed in Figure A-4.1. Four of the loading positions (4, 8, 29, and 33) may be oversized (enlarged tube) positions and are the only positions capable of accommodating RFA or DFC fuel.

## A-4.2 Damaged Fuel

No damaged fuel information is currently incorporated in UNF-ST&DARDS for the Yankee-MPC.

## A-4.3 Model Verification

No model verification has been performed to date for the Yankee-MPC canister.

## A-4.4 References

1. NAC-STC Safety Analysis Report, Revision 15, US NRC, Docket No. 71-9235, March 2004

**Table A-4.1. Dimensions used to build the SCALE criticality model for the Yankee-MPC**

| Canister | Size (cm) | Reference |
|---|---|---|
| Inner canister radius | 83.1253 | 1, page 80 |
| Outer canister radius | 89.7128 | 1, page 80 |
| Inner canister height (inner cavity length) | 306.578 | 1, page 158 |
| Thickness of bottom plate | 2.54 | 1, page 80 |
| Thickness of structural lid | 7.62 | 1, page 81 |
| Thickness of shield lid assembly | 12.7 | 1, page 81 |
| Height | 329.438 | Inferred from dimensions above |
| Drain tube length | 289.56 | 1, page 168 |
| Drain tube outer radius | 2.54 | 1, page 168 |
| Drain tube inner radius | 2.4511 | 1, page 168 |
| Drain tube x position | 69.088 | 1, page 187 |
| Drain tube y position | 46.228 | 1, page 187 |
| **Standard fuel can** | | |
| Inner size (square) | 19.812 | 1, page 169 |
| Internal cavity length | 262.89 | 1, page 169 |

**Table A-4.1. Dimensions used to build the SCALE criticality model for the Yankee-MPC (continued)**

| | | |
|---|---|---|
| Thickness of can wall | 0.121412 | 1, page 169 |
| | | |
| **Boral (standard fuel can)** | | |
| Boral core thickness | 0.06355 | Calculated based on 0.01 g $^{10}B/cm^2$ |
| Boral thickness | 0.1905 | 1, page 169 |
| Boral width | 18.288 | 1, page 170 |
| Boral height | 244.348 | 1, page 170 |
| Sheathing thickness | 0.045466 | 1, page 169 |
| **Oversized fuel can** | | |
| Inner size (square) | 20.32 | 1, page 171 |
| Internal cavity length | 262.89 | 1, page 171 |
| Thickness of can wall | 0.121412 | 1, page 171 |
| **Basket** | | |
| Bottom weldment disk radius | 87.63 | 1, page 179 |
| Bottom weldment disk thickness | 1.27 | 1, page 179 |
| Support disk radius | 87.8205 | 1, page 187 |
| Support disk thickness | 1.27 | 1, page 187 |
| Heat transfer disk radius | 87.4649 | 1, page 188 |
| Heat transfer disk thickness | 1.27 | 1, page 188 |
| Top weldment disk radius | 87.63 | 1, page 182 |
| Top weldment disk thickness | 1.27 | 1, page 182 |

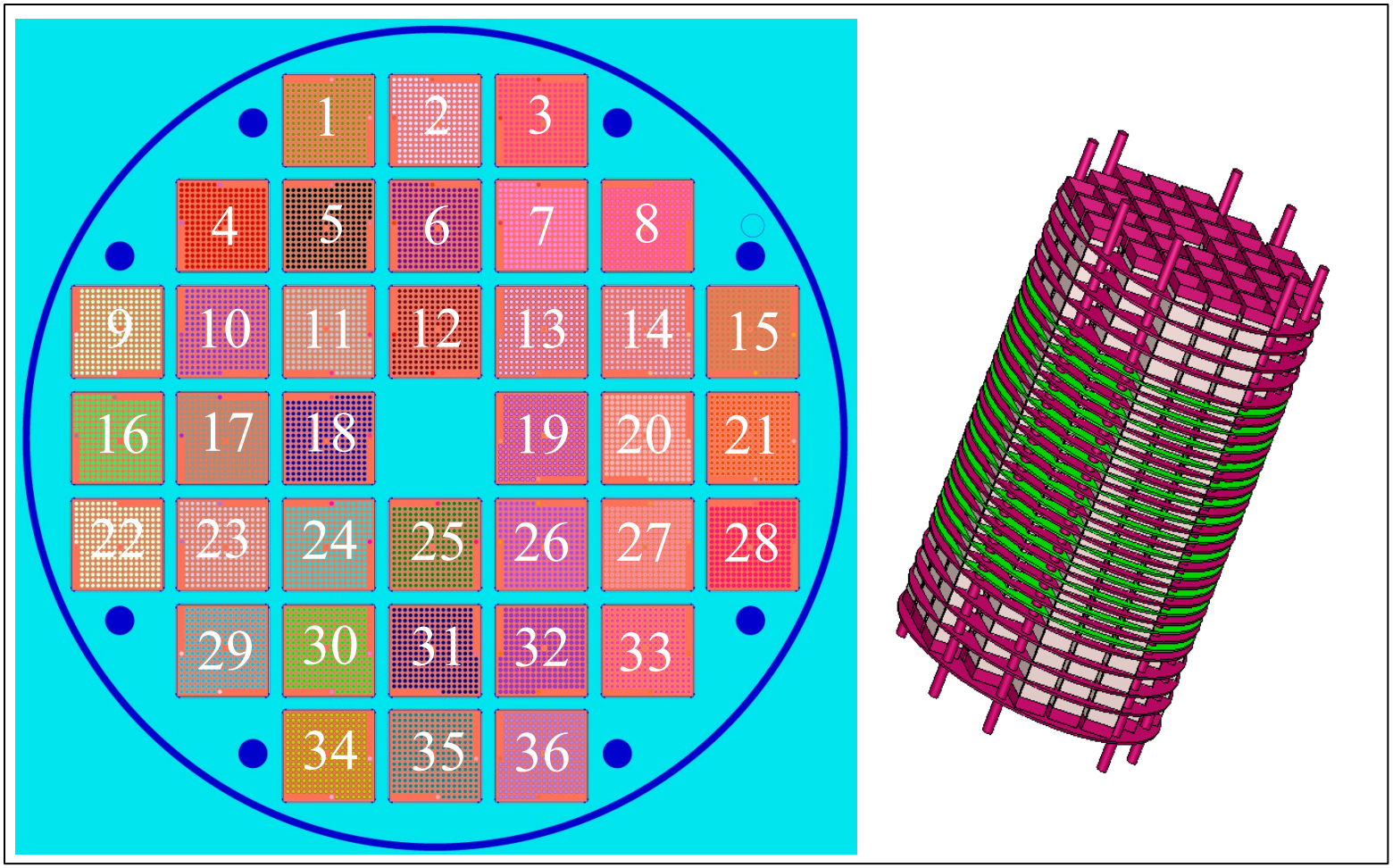


**Fig. A-4.1. Plan view (left) and isometric view (right) of the Yankee-MPC canister.**

# A-5. MPC-LACBWR

## A-5.1 Canister

MPC-LACBWR (La Crosse Boiling Water Reactor) is a right circular cylinder containing 68 fuel tubes laterally supported by a series of support disks, which are retained by spacers on radially located tie rods (neither spacers or tie rods are modeled). Damaged fuel cans (DFCs) may be placed in 32 peripheral oversized fuel tubes. The support disks are stainless steel (17-4 PH) with standard and oversized holes for the poison fuel tubes and DFCs. The first top and bottom end support disks are thicker than the intermediate support disks to accommodate postulated rubblized fuel in the 32 DFCs. The basket top and bottom weldments are fabricated from Type 304 stainless steel. The tie rods and spacer sleeves are also fabricated from Type 304 stainless steel. The fuel assemblies are contained in fuel tubes. The MPC-LACBWR fuel tubes are fabricated from stainless steel with stainless steel clad covered BORAL sheets on defined outside surfaces of the fuel tube.

The dimensions of the model are presented in Table A.5-1. Plan and isometric views of the MPC-LACBWR canister are shown in Figure A-5.1.

## A-5.2 Damaged Fuel

Reference 1 considered loss of pitch control, loss of cladding, missing fuel rods, and completely rubblized fuel for potential degradations of scenarios. Reference 1 published the results of the aforementioned degradation scenarios in Tables 6.A.4-8–6.A.4-10. Based on those results, the bounding credible damaged fuel configuration is an unclad 3.94 w/o enriched Allis-Chalmers fuel assembly with a pitch of 0.5999 inches and a single missing rod. The location of the missing rod was not specified; however, it only resulted in a 0.00121 increase in reactivity. The missing rod will be removed from one of the middle four rods because it is likely that it will increase reactivity the most, and the reactivity impact is small. The damaged fuel assembly type has been entered in UNF-ST&DARDS as XLC10ALC.

## A-5.3 Model Verification

Two calculations were performed to validate the canister and fuel assembly models. The first calculation used Exxon fuel, and the second used Allis-Chalmers fuel. The results of the calculations are presented in Table A-5.2 and show good agreement with the licensing calculations in Reference 1.

## A-5.4 References

1. *Final Safety Analysis Report for the MPC-LACBWR*, Volume 2 of 2. ADAMS Accession number ML110250205.
2. ADAMS accession number ML090270151.
3. *Storage and Transportation Cask Data For Used Commerical Nuclear Fuel* - 2013 U.S. Edition, ATI-TR-13047.
4. "Submittal of NAC International Responses to NRC Request for Additional Information for Review of Amdnedment No. 6 to Certificate of compliance No. 1025 for the NAC-MPC Storage System Requesting Approval to Incorporate La Crosse Boiling Water Reactor (LACBWR) Assemblies as Approved Contents." ADAMS accession number ML092680315.

**Table A-5.1. Dimensions used in building the SCALE criticality model for the MPC-LACBWR canister model**

| Canister | Size (cm) | Reference |
|---|---|---|
| Inner canister diameter | 177.8381 | Reference 3 Pg. 106 |
| Outer canister diameter | 179.4256 | Reference 3 Pg. 106 |
| Canister Inner Height | 274.447 | Calculated from Table 6.A.3-5 of Reference 1 |
| **Basket** | | |
| Inner Cell Dimension – Standard Cell | 14.6151 | Reference 1 Figure 6.A.3-1 |
| Inner Cell Dimension – Damaged Fuel Cell | 15.25016 | Reference 1 Figure 6.A.3-1 |
| Cell Thickness | 0.12192 | Reference 1 Figure 6.A.3-1 |
| Fuel Tube Height | 249.301 | Reference 1 Table 6.A.3-2 |
| Radial Layout of Fuel Tubes | See Ref | Reference 1 Figure 6.A.3-2 |
| **Boral Specifications** | | |
| Poison | | |
| Core Thickness | 0.127 | Reference 4 Figure 6.4-A com |
| Cladding | 0.03175 | Calculated from Reference 4 Figure 6.4-A values. |
| Width | 13.1826 | Reference 1 Figure 6.A.3-1 |
| Height | 243.5352 | Reference 1 Table 6.A.3-2 |
| Areal Density before 25% reduction (g/cm$^2$) | 0.02 | Reference 2 B. 3.2.1 item 3 number densities are taken from Reference 4 6.4-A |
| Sheathing thickness | 0.04572 | Reference 1 Figure 6.A.3-1 |
| Distance from bottom of basket to bottom of Boral plate | | Assumed to be axially centered |
| **Disk Specification** | | |
| Support Disk Height | 1.5875 | Reference 1 Page 5.A.6-14 |
| Support Disk Radius | 88.1380 | Reference 1 Page 5.A.6-14 |
| Support Disk Material | SS | Reference 1 |
| Heat Transfer Disk Height | 1.27 | Reference 1 Page 5.A.6-14 |
| Heat Transfer Disk Radius | 87.7951 | Reference 1 Page 5.A.6-14 |
| Heat Transfer Disk Material | Al | Reference 1 |

**Table A-5.2 Model verification results for the MPC-LACBWR**

| Fuel Type | Reference 2 $k_{eff}$ | Calculated $k_{eff} \pm \sigma$ | $\Delta k_{eff}$ |
|---|---|---|---|
| Allis-Chalmers | 0.88983 | 0.89168 ± 0.00044 | 0.00185 |
| Exxon | 0.84195 | 0.84506 ± 0.00044 | 0.00311 |

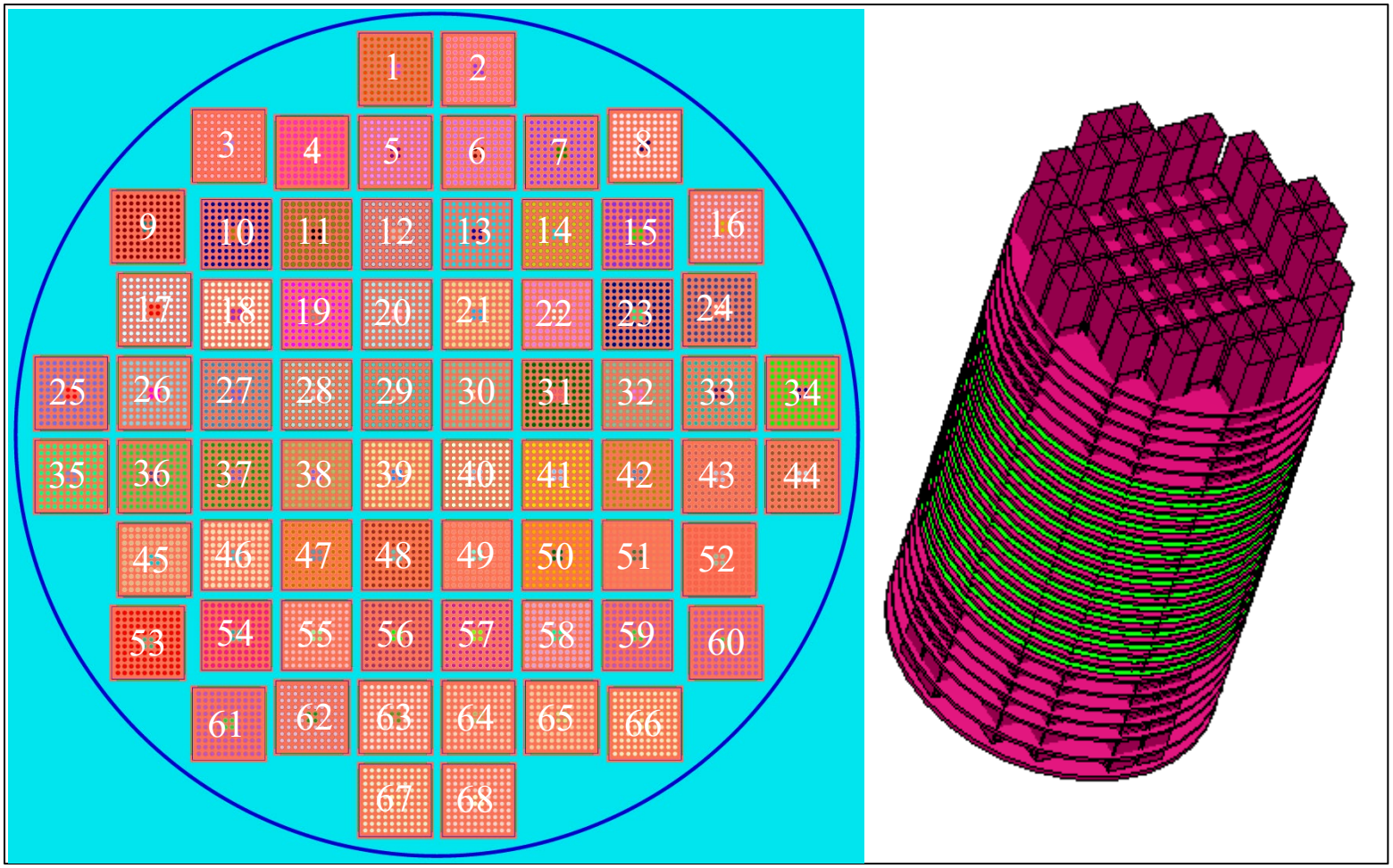


**Fig. A-5.1. Plan view (left) and isometric view (right) of the MPC-LACBWR canister.**

# A-6. MPC-24

## A-6.1 Canister

The MPC-24 is a flux trap design storage and transportation canister that is part of the Holtec International (HI)-STAR and HI-STORM 100 storage and transportation canister family. The canister is similar in design to the Trojan MPC-24 E/EF; however, the neutron absorber panels contain a lower $^{10}B$ loading, and the basket dimensions are slightly different. The dimensions used in the criticality model are listed in Table A-6.1, and a plan view with basket cell numbering scheme is provided along with an isometric view of the basket with the canister wall removed in Figure A.6-1.

## A-6.2 Damaged Fuel

No damaged fuel modeling is available at this time.

## A-6.3 Model Verification

Verification of the MPC-24 CSAS6 model was performed by comparison to the SAR analysis corresponding to the 17×17A01 case from Table 6.2.17 [1]. The case was modeled used the fuel dimensions from Table 6.2.17 and a 4.0 w/ enrichment, with all of the fuel assemblies centered in the basket cells. The results of the model verification calculation are presented along with those from Reference [1] in Table A.6-2 and show good agreement with the SAR value.

## A-6.4 References

1. HI-STAR SAR, Rev. 10, Report HI-951251.

**Table A.6-1. Dimensions used in the CSAS6 criticality model for the MPC-24 canister**

| Canister | Size (cm) | Reference |
|---|---|---|
| Inner canister radius | 85.725 | 1, page 154 |
| Outer canister radius | 86.995 | 1, page 154 |
| Inner canister height (cavity, top baseplate to bottom lid) | 452.91375 | 1, page 154 |
| Bottom plate thickness | 6.35 | 1, page 154 |
| Lid thickness | 24.13 | 1, page 154 |
| Total height (bottom baseplate to top lid) | 482.44125 | 1, page 154 |
| Center column width | 6.985 | 1, page 166 |
| **Basket** | | |
| Cell basket height | 448.31 | 1, page 166 |
| Cell spacer length | 164.30625 | 1, page 166 |
| Cell spacer thickness | 0.79375 | 1, page 166 |
| Cell inner side | 22.6568 | 1, page 167 |
| Flux trap width | 1.09 | 1, page 167 |
| Width cell spacer #1 | 164.338 | 1, page 167 |
| Width cell spacer #2 | 159.0802 | 1, page 167 |
| Width cell spacer #3 | 116.84 | 1, page 167 |
| Width cell spacer #4 | 60.452 | 1, page 167 |

**Table A.6-1. Dimensions used in the CSAS6 criticality model for the MPC-24 canister (continued)**

| | | |
|---|---|---|
| Distance from symmetry plane to center of first cell location | 13.85062 | 1, page 167 |
| **Boral** | | |
| Boral thickness | 0.1397 | 1, page 166, note 1,2 |
| Boral width (wide panel) | 19.05 | 1, page 166, note 1 |
| Boral width (narrow panel) | 15.875 | 1, page 166, note 2 |
| Boral height | 396.24 | 1, page 166, note 1,2 |
| Sheathing thickness | 0.05969 | 1, page 166, note 1,2 |
| Clearance gap thickness | 0.00889 | 1, page 1433 |
| Boral clad (aluminum) | 0.0254 | 1, page 1433 |
| Distance from bottom of basket to bottom of boral plate | 7.3025 | 1, page 166 |

**Table A-6.2. Model verification results for the MPC-24**

| Reference 2 $k_{eff}$ | Calculated $k_{eff} \pm \sigma$ | $\Delta k_{eff}$ |
|---|---|---|
| 0.9325 ± 0.0008 | 0.93017 ± 0.00022 | 0.00233 |

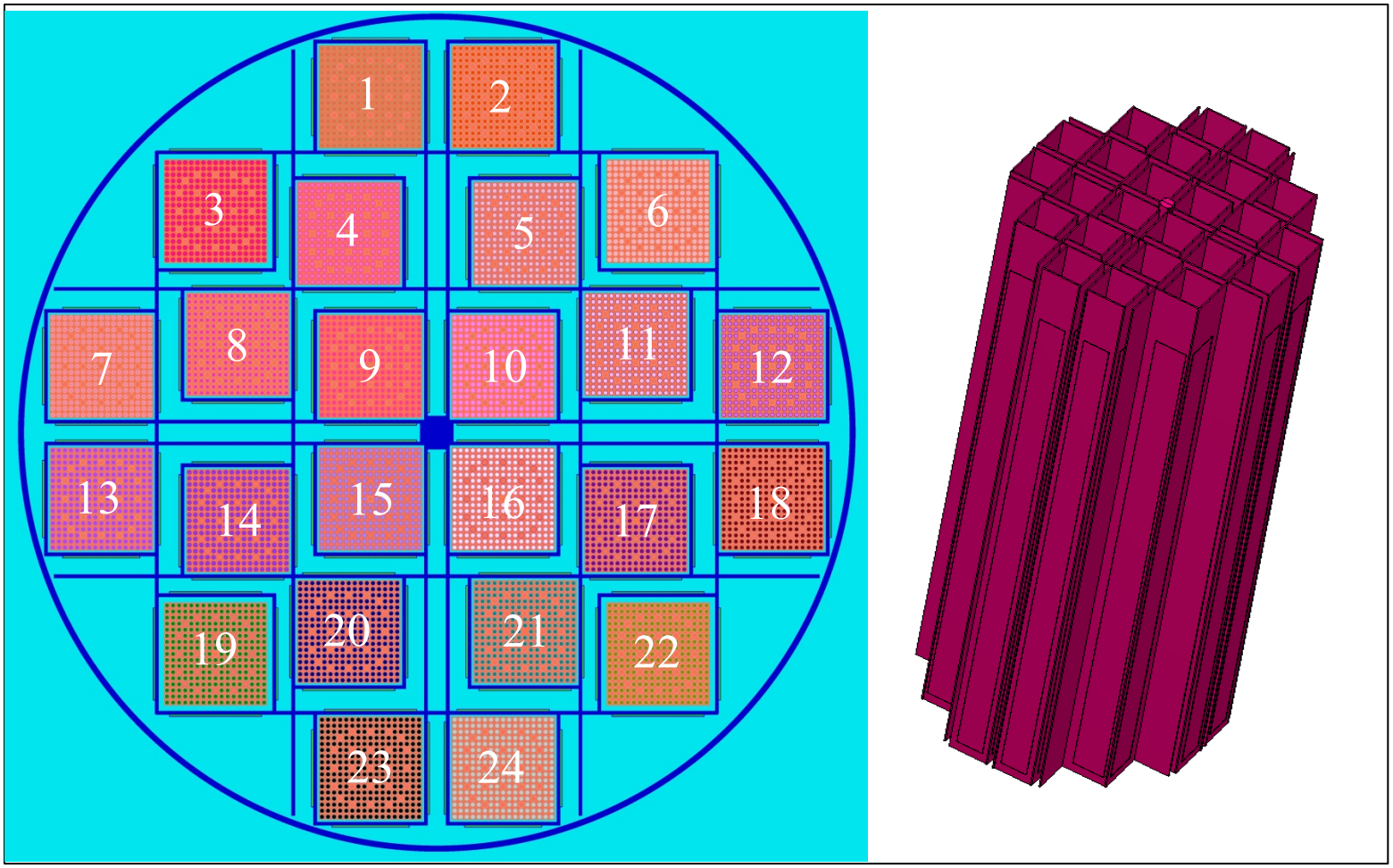


**Fig. A-6.1. Plan view (left) and isometric view (right) of the MPC-24 canister.**

# A-7. Trojan MPC-24 E/EF

## A-7.1 Canister

Portland General Electric's Trojan site uses a variation of Holtec's MPC-24E/EF canister for spent nuclear fuel (SNF) storage. The MPC-24E/EF canister has 24 locations that can host intact spent fuel assemblies, or, in 4 of these locations, damaged fuel assemblies or fuel debris. The Trojan version of this canister has some differences when compared to the standard MPC-24E/EF cask, such as the heights for canister and basket and the dimensions for the special damaged fuel locations.

Table A.7-1 presents the dimensions used to build the CSAS6 template for UNF-ST&DARDS. Figure A.7-1 shows a horizontal cross-sectional view of the SCALE model together with the storage location numbering conventions as well as an isometric view of the outside of the basket with the canister wall removed.

## A-7.2 Damaged Fuel

Damaged fuel for the Trojan MPC-E/EF is modeled as an array of optimally moderated bare fuel rods. The bounding fuel model was determined by varying the number of fuel rods in a square array constrained by the DFC. The calculated $k_{eff}$s were plotted against the linear $UO_2$ density in Figure 6.4.12 of Reference 2. These calculations were performed for the maximum, minimum, and typical pellet diameters. The maximum $k_{eff}$ occurred for the minimum pellet diameter at a linear density of 3.5 kg $UO_2$/inch. A linear density of 3.5 kg $UO_2$/inch corresponds to a 14×14 array of fuel rods with a 0.625 inch pitch. The Reference 2 analysis also uses bounding values of 150 inches and 4.0 w/o for fuel length and enrichment respectively.

## A-7.3 Model Verification

The model was benchmarked using 3.7 w/o, a fuel corresponding to the W1717WL design basis fuel type specified in Reference 3. The calculated results are presented in Table A-7.2 and show good agreement with the results in Table 6.C.1 from Reference 3.

## A-7.4 References

1. Holtec International, *Holtec International Final Safety Analysis Report for HI-STORM 100 Cask System*, USNRC Docket No. 72-1014, Rev. 9, February 13, 2010.
2. Holtec International, *HI-STAR SAR Report HI-951251*, USNRC Docket No. 72-1014, Rev. 15, October 11, 2010.

**Table A-7.1. Dimensions used in the CSAS6 criticality model for the MPC-24 E/EF canister**

| Canister | Size (cm) | Reference |
|---|---|---|
| Inner canister radius | 85.725 | 2, page 154 |
| Outer canister radius | 86.995 | 2, page 154 |
| Inner canister height (cavity, top baseplate to bottom lid) | 430.022 | 2, page 154, note 2 |
| Bottom plate thickness | 6.35 | 2, page 154 |
| Lid thickness | 24.13 | 2, page 154 |
| Total height (bottom baseplate to top lid) | 460.502 | 2, page 154, note 1 |
| Center column width | 6.985 | 2, page 162 |
| **Basket** | | |
| Cell basket height (except locations 3,6,19,22) | 424.815 | 2, page 162, note 3 |
| Cell basket height (locations 3,6,19,22) | 414.655 | 2, page 162, note 3 |
| Cell spacer length | 163.195 | 2, page 162 |
| Cell spacer thickness | 0.79375 | 2, page 162 |
| Cell inner side (square, except locations 3,6,19,22) | 22.225 | 2, page 163 |
| Cell inner side (square, locations 3,6,19,22) | 23.622 | 2, page 163, note 1 |
| Flux trap width (except locations 3,6,19,22) | 2.73304 | 2, page 163 |
| Flux trap width (locations 3,6,19,22) | 1.33604 | 2, page 163, note 2 |
| Width cell spacer #1 | 163.1442 | 2, page 163 |
| Width cell spacer #2 | 159.0802 | 2, page 163 |
| Width cell spacer #3 | 116.84 | 2, page 163 |
| Width cell spacer #4 | 60.4266 | 2, page 163 |
| Distance from symmetry plane to center of first cell location | 13.77569 | 2, page 163 |
| **Boral** | | |
| Boral thickness | 0.25654 | 2, page 162, note 1,2 |
| Boral width (wide panel) | 19.05 | 2, page 162, note 1 |
| Boral width (narrow panel) | 15.875 | 2, page 162, note 2 |
| Boral height | 396.24 | 2, page 162, note 1,2 |
| Sheathing thickness | 0.1524 | 2, page 162, note 1,2 |
| Clearance gap thickness | 0.00889 | 2, page 1433 |
| Boral clad (aluminum) | 0.0254 | 2, page 1433 |
| Distance from bottom of basket to bottom of boral plate | 4.445 | 2, page 162, note 5 |

**Table A-7.2. Comparison of results calculated for the MPC-24 E/EF with those presented in [1]**

| Reference 2 $k_{eff}$ | Calculated $k_{eff} \pm \sigma$ | $\Delta k_{eff}$ |
|---|---|---|
| 0.9187 | 0.90060 ± 0.00026 | 0.0181 |

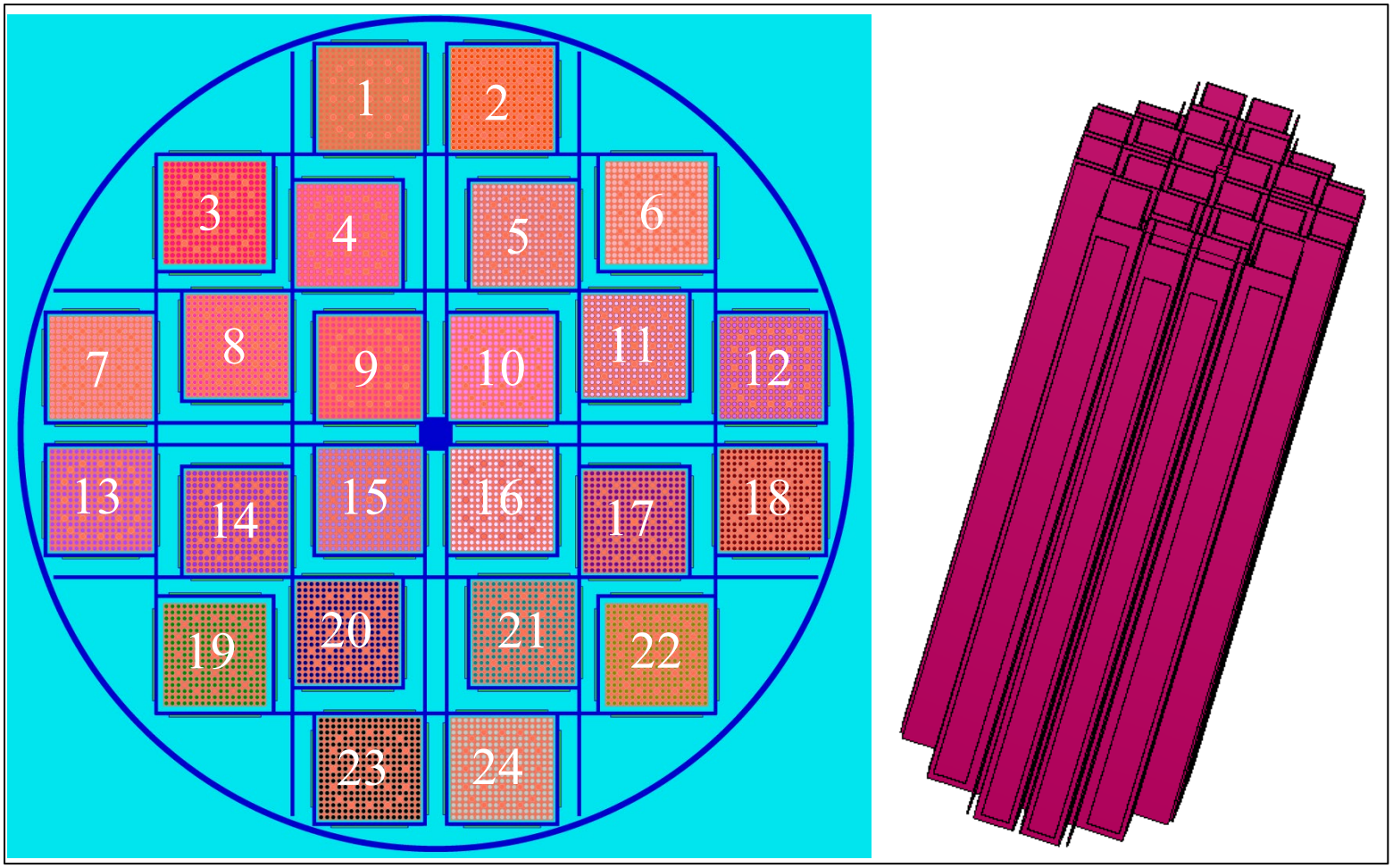


**Fig. A-7.1. Plan view (left) and isometric view (right) of the MPC-24 E/EF canister.**

# A-8. MPC-32

## A-8.1 Canister

The MPC-32 canister has 32 locations that can host intact or damaged spent fuel assemblies. Like the MPC-68 and MPC-HB, the MPC-32 uses a "developed cell" design, which uses a series of fuel tubes that are welded together at the corners. Figure A-8.1 shows a horizontal cross-sectional view of the SCALE model built from the Ref. [1] description with the storage location numbering conventions overlaid on it, as well as an isometric view of the basket structure with canister wall removed. The dimensions used to build the CSAS6 model are shown in Table A-8.1.

## A-8.2 Damaged Fuel

No damaged fuel modeling performed to date.

## A-8.3 Model Verification

No model verification has been performed to date.

## A-8.4 References

1. Holtec Final Safety Analysis Report for the HI-STORM 100 Cask System, Revision 9, February 13, 2010. ADAMS Accession Number ML101400161.

**Table A-8.1. Dimensions used in the CSAS6 criticality model for the MPC-32 canister**

| Canister | Size (cm) | Reference 1 Page Number |
|---|---|---|
| Inner canister radius | 85.725 | Pg. 154 |
| Outer canister radius | 86.995 | Pg. 154 Detail D |
| Canister height (Basket only) | 448.31 | Pg. 170 |
| **Basket** | | |
| Inner Cell Dimension | 22.7076 | Pg. 171 |
| Cell Thickness | 0.714375 | Pg. 170 |
| **Boral Specifications** | | |
| Boral thickness | 0.25654 | Pg. 1435 |
| Boral width | 19.05 | Pg. 1435 |
| Boral height | 396.24 | Pg. 170 |
| Boral clad thickness (aluminum) | 0.0254 | Pg. 1435 |
| Gap Width | 0.01397 | Pg. 1435 |
| Sheathing thickness | 0.1905 | Pg. 1435 |
| Distance from bottom of basket to bottom of boral plate | 7.3025 | Pg. 170 |

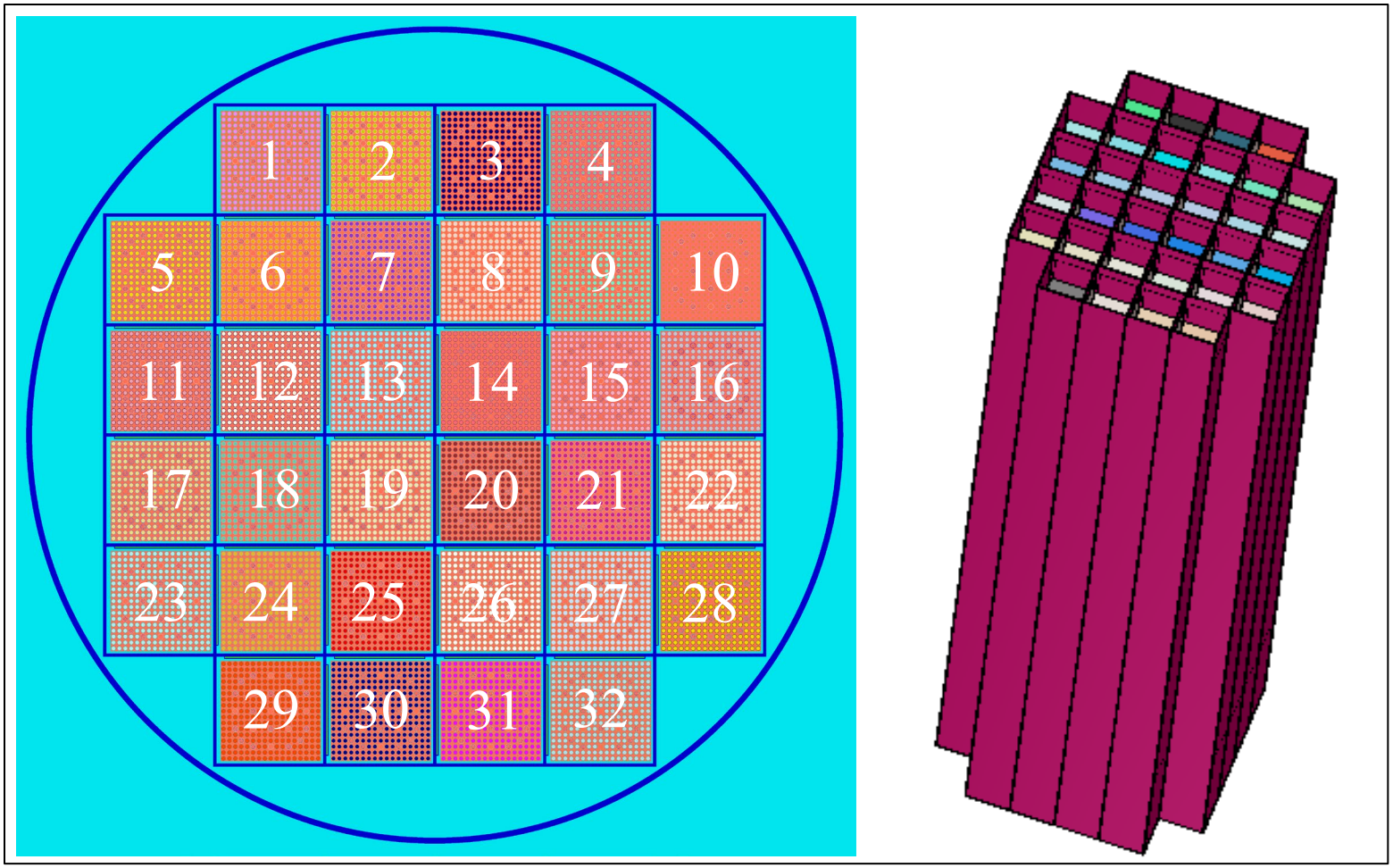


**Fig. A-8.1. Plan view (left) and isometric view (right) of the MPC-32 canister.**

# A-9. MPC-68

## A-9.1 Canister

The MPC-68 canister has 68 locations that can host intact or damaged spent fuel assemblies. Like the MPC-32 and MPC-HB, the MPC-68 uses a "developed cell" design, which uses a series of fuel tubes that are welded together at the corners. Figure A-9.1 shows a horizontal cross-sectional view of the SCALE model built from the Reference 1 description with the storage location numbering convention overlaid on it, as well as an isometric view of the basket structure with the canister wall removed. The dimensions used to build the CSAS6 model are shown in Table A-9.1.

## A-9.2 Damaged Fuel

No damaged model has been developed for the MPC-68 at this time.

## A-9.3 Model Verification

A model verification calculation was developed using the first case from Table 6.2.22 [1]. The calculation used the assembly designated as 8×8C01 from [1] with an enrichment of 4.2 w/o. The results of the benchmark calculation are presented in Table A.9-2 and show good agreement with the calculations presented in [1].

## A-9.4 References

1. *Holtec Safety Analysis Report for the HI-HI-STAR 100 Cask System*, Rev. 10, February 13, 2010.

**Table A-9.1. Dimensions used in the CSAS6 criticality model for the MPC-68 canister**

| Canister | Size (cm) | Reference 1 Page Number |
|---|---|---|
| Inner canister radius | 85.725 | Pg. 204 |
| Outer canister radius | 86.995 | Pg. 204 Detail D |
| Canister height (Basket only) | 448.31 | Pg. 204 |
| **Basket** | | |
| Inner Cell Dimension | 15.8496 | Pg. 214 |
| Cell Thickness | 0.635 | Pg. 214 |
| **Boral Specifications** | | |
| Boral thickness | 0.25654 | Pg. 1252 |
| Boral width | 12.065 | Pg. 1252 |
| Boral height | 396.24 | Pg. 170 |
| Boral clad thickness | 0.0254 | Pg. 1252 |
| Gap Width | 0.01397 | Pg. 1252 |
| Sheathing thickness | 0.1905 | Pg. 1252 |
| Distance from bottom of basket to bottom of boral plate | 7.3025 | Pg. 170 |

**Table A-9.2. Model verification results for the MPC-68**

| Fuel Type | Reference 1 $k_{eff}$ | Calculated $k_{eff} \pm \sigma$ | $\Delta k_{eff}$ |
|---|---|---|---|
| 8×8C01 | 0.9273 | 0.92740 ± 0.00026 | 0.00010 |

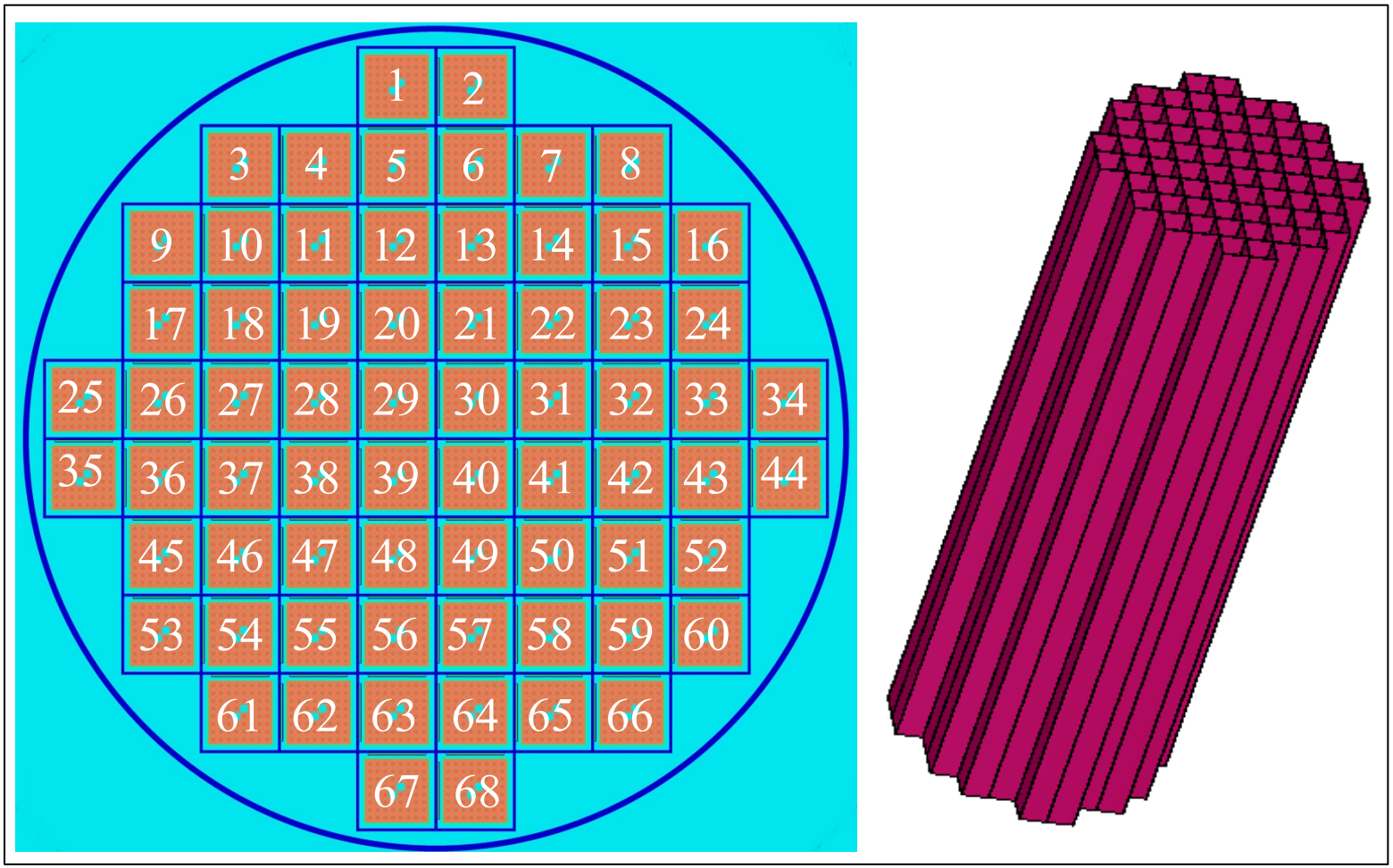


**Fig. A-9.1. Plan view (left) and isometric view (right) of the MPC-68 canister.**

# A-10. MPC-HB

## A-10.1 Canister

The Humboldt Bay (HB) site uses Holtec's MPC-HB canister for SNF storage. The MPC-HB fits within the HI-STAR 100-HB cask system, which is radially identical to the HI-STAR 100 system, but shorter. The canister has the same external diameter as the as the MPC-68 but takes advantage of the smaller size of the Humboldt Bay fuel assemblies to allow storage and transportation of 80 bundles per canister, up to 40 of which may be damaged. Similar to other Holtec canisters like MPC-68 and MPC-32, the MPC-HB incorporates a "developed cell" basket design which is formed by welding fuel tubes together at the corners to make additional storage locations. The MPC-HB also uses single Metamic$^{TM}$ neutron absorber panels between storage locations to ensure criticality control.

The dimensions and material properties important to criticality are listed in Table A-10.1 along with drawing numbers from Reference 2. The radial and isometric layouts of the MPC-HB canister are shown in Figure A-10.1.

## A-10.2 Damaged Fuel

The damaged fuel for the MPC-HB is modeled as a 2.6 w/o enriched GE 7×7 fuel assembly with the cladding removed with a 0.488 inch outer diameter. This fuel has been entered into UNF-ST&DARDS as XHB07G2HB.

## A-10.3 Model Verification Calculations

In order to show that the model was built appropriately from licensing materials, it is necessary to compare the calculated $k_{eff}$s to published values. Calculations were performed for the GE 6×6 and GE 7×7 fuel assemblies with the fuel centered in the storage cells. Holtec uses a conservative version of the assembly in which the mechanical tolerances on the assembly have been applied to increase its reactivity for licensing purposes. In order to replicate their results as closely as possible, the fuel dimensions from Table 6.I.2 of Reference 1 were used in the calculations. A planar average enrichment of 2.6 w/o $^{235}$U and a fuel density of 10.522 g/cm$^3$ were used for the calculations. The results are presented in Table A-10.2 and show acceptable agreement with the "Intact, Standard" results contained in Table 6.I.4 of Reference 1.

## A-10.4 References

1. *Holtec Final Safety Analysis Report for the HI-STAR 100 Cask System – Non-Proprietary version*, Rev. 15, February 11, 2010. ADAMS Accession Number ML102871084.
2. Holtec Drawing package from Steve Maheras of PNNL. (http://curie.ornl.gov/content/hi-star-100-hb-drawing-package)

**Table A-10.1. Dimensions used in the CSAS6 criticality model for the MPC-HB canister**

| Canister | Size (cm) | Reference |
|---|---|---|
| Inner canister diameter | 171.1325 | Shell is ½ in. thick per DETAIL D Drawing 4530 sheet 11 |
| Outer canister diameter | 173.6725 | Holtec Drawing 4530 sheet 11 |
| Canister height (Basket only) | 246.38 | Holtec Drawing 4529 sheet 9 |
| **Basket** | | |
| Inner Cell Dimension | 14.478 | Drawing 4529 Sheet 2 |
| Cell Thickness | 0.47625 | Drawing 4529 Sheet 2 (3/16 in.) |
| **Metamic Specifications** | | |
| Poison | | |
| Thickness | 0.127 | Drawing 4529 Sheet 2 |
| Width | 10.16 | Drawing 4529 Sheet 2 |
| Height | 223.52 | Drawing 4529 Sheet 2 |
| Areal Density (g/cm$^2$) | 0.01 | Concentrations taken from Reference 1 Table 6.I.3 |
| Sheathing thickness | 0.0889 | Drawing 4526 Sheet 2 |
| Sheathing Width | 12.065 | Drawing 4526 Sheet 2 |
| Sheathing Length | 225.7245 | Drawing 4526 Sheet 2 |
| Distance from bottom of basket to bottom of Metamic plate | Assumed to be axially centered | |

**Table A-10.2. Comparison of results calculated for the MPC-HB with those presented in Reference 1**

| Fuel Type | Reference 1 $k_{eff}$ | Calculated $k_{eff} \pm \sigma$ | $\Delta k_{eff}$ |
|---|---|---|---|
| GE 6×6 | 0.8318 | 0.83313 ± 0.00034 | 0.00133 |
| GE 7×7 | 0.8237 | 0.82498 ± 0.00031 | 0.00128 |

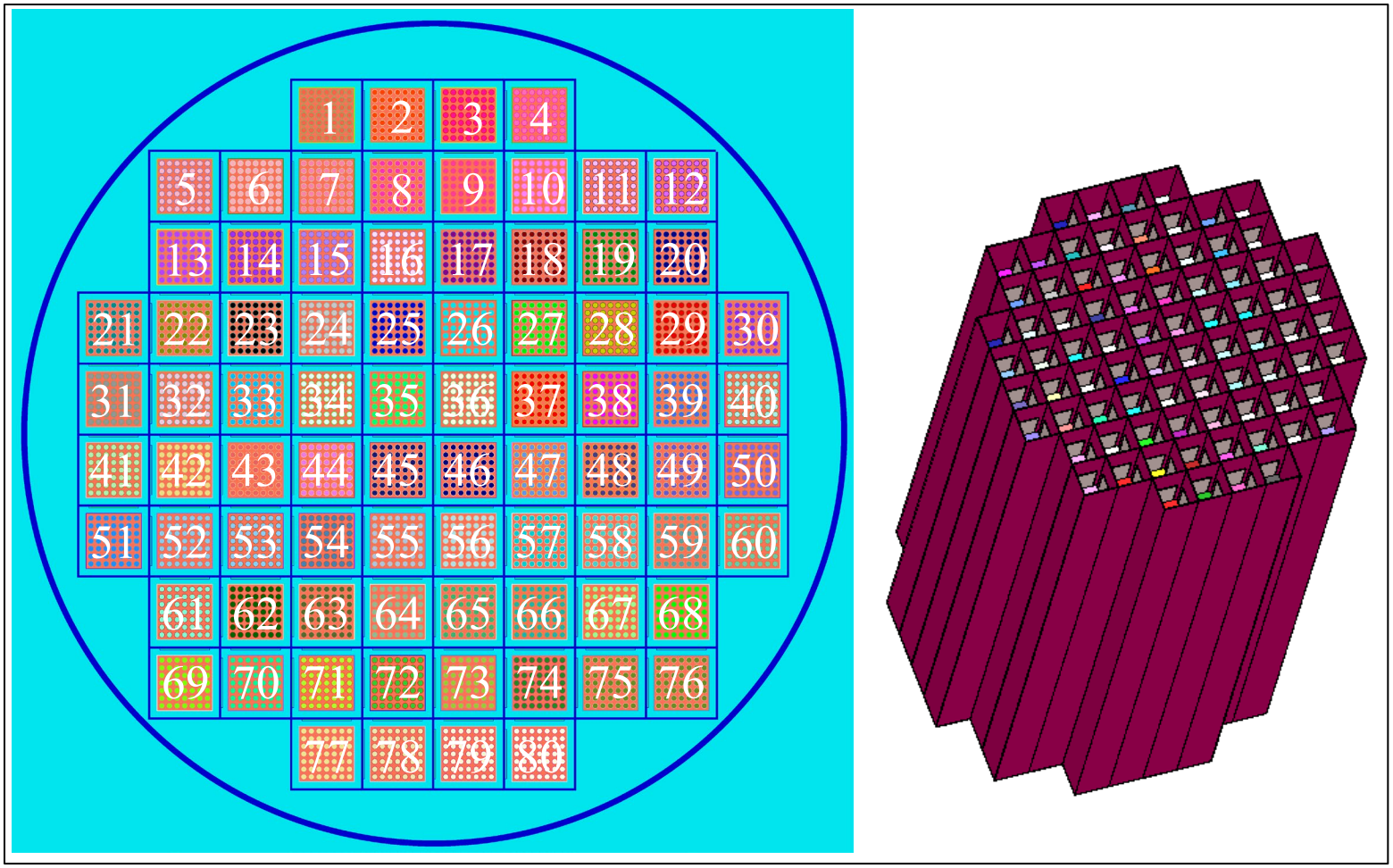


**Fig. A-10.1. Plan view (left) and isometric view (right) of the MPC-HB canister.**

# A-11. FO-DSC, FC-DSC, and FF-DSC

## A-11.1 Canisters

The Rancho Seco site uses three canisters that are specific to the site: the Fuel Only (FO)-Dry Shielded (DSC) Canister, the Fuel and Component (FC)-DSC, and the Failed Fuel (FF)-DSC. The PWR assembly capacity for these DSCs is 24 for FO/FC-DSC and 13 for FF-DSC. All three canisters have the same outer diameter and fit into the same horizontal storage module and transportation overpacks. The canisters use a tube and disk design which uses several support disks, which provide lateral support of the fuel tube. Because the FO-DSC and FC-DSC only vary in terms of above the neutron absorbing material, which has no effect on the criticality analysis, a single CSAS6 model is used to represent both canisters. The FF-DSC contains only failed fuel. In order to conservatively account for presence of failed fuel in all locations the licensing dimensions are used for the DSC-FF canister.

The nominal dimensions for the FO-DSC and FC-DSC are presented in Table A-11.1, and the licensing dimensions for the FF-DSC are presented in Table A-11.2. Figure A-11.1 shows the plan and isometric views of the FO/FC-DSCs and Figure A-11.2 shows the plan and isometric view of the FF-DSC. Both plan views show the basket cell numbering scheme for the DSCs.

## A-11.2 Damaged Fuel

Although the FC-DSC and FO-DSC are not certified for loading damaged assemblies, six assemblies with minor cladding flaws were loaded in five FC DSCs. These six damaged assemblies are conservatively modeled as fresh design basis assemblies. All of the fuel within the DSC-FF is declared as damaged and modeled as the design basis fuel assembly. The design basis fuel assembly for the FO-DSC, FC-DSC, and FF-DSC is a 3.43 w/o B1515B fuel assembly.

## A-11.3 Model Verification Calculations

A benchmark calculation was performed with the licensing assumptions presented in [1] and a uniform loading of the 3.43 w/o B1515B fuel assemblies in the FO/FC-DSC model. The results are presented in Table A-11.3. No benchmark calculations have been performed to date for the FF-DSC.

## A-11.4 References

1. *SMUD – Rancho Seco Independent Spent Fuel Storage Installation Final Safety Analysis Report*, Rev. 0, US NRC, Docket No. 72-11, 11/21/2000.
2. *Transnuhclear NUHOMS-MP187 Multi Purpose Cask Safety Analysis Report*, Revision 17, Transnuclear, Inc. (Vendor Provided Proprietary Safety Analysis Report).
3. Drawing NUH-05-4004, Rev. 16.
4. Drawing NUH-05-4005, Rev. 14.

**Table A-11.1. Dimensions used in the CSAS6 criticality model for the FO-DSC and FC-DSC canisters**

| Canister | Size (cm) FO-DSC | Size (cm) FC-DSC | Reference |
|---|---|---|---|
| Inner canister radius | 83.82 | 83.82 | 1, page 26 |
| Outer canister radius | 85.4075 | 85.4075 | 1, page 26 |
| Inner canister height (inner cavity length) | 424.180 | 439.42 | 2, page 80 ([B-3]) |
| Thickness of outer bottom cover | 4.445 | 1.905 | B-2, page 83 ([B-3]) |
| Thickness of inner bottom cover | 1.905 | 1.905 | B-2, page 83 ([B-3]) |

**Table A-11.1. Dimensions used in the CSAS6 criticality model for the FO-DSC and FC DSC canisters (continued)**

| Canister | Size (cm) FO-DSC | Size (cm) FC-DSC | Reference |
|---|---|---|---|
| Thickness of bottom plug top casing | | 1.905 | 2, page 83 ([B-3]) |
| Thickness of bottom plug side casing | | 1.27 | 2, page 83 ([B-3]) |
| Thickness of bottom shield plug | 15.875 | | 2, page 83 ([B-3]) |
| Thickness of bottom lead shielding | | 9.525 | 2, page 83 ([B-3]) |
| Thickness of lid - inner top cover plate | 1.905 | 1.905 | 2, page 83 ([B-3]) |
| Thickness of lid - outer top cover plate | 3.175 | 3.175 | 2, page 83 ([B-3]) |
| Thickness of lid - top plug top casing | | 0.9652 | 2, page 83 ([B-3]) |
| Thickness of lid - top shield plug | 20.955 | | 2, page 83 ([B-3]) |
| Thickness of lid - top lead shielding | | 10.4648 | 2, page 83 ([B-3]) |
| Thickness of lid - top plug side casing | | 1.27 | 2, page 83 ([B-3]) |
| Thickness of lid - top plug bottom casing | | 1.27 | 2, page 83 ([B-3]) |
| Height | 472.948 | 472.948 | 2, page 80 ([B-3]) |
| **Fuel can** | | | |
| Inner size (square) | 22.606 | 22.606 | 2, page 84 ([B-3]) |
| Internal cavity length | 410.972 | 410.972 | 2, page 82 ([B-3]) |
| Distance from bottom of basket to bottom of absorber sheath | 1.905 | 1.905 | 2, page 82 ([B-3]) |
| Thickness of guide sleeve | 0.3048 | 0.3048 | 2, page 82 ([B-3]) |
| **Boral** | | | |
| Boral thickness | 0.2159 | 0.2159 | 2, page 82 ([B-3]) |
| Boral width (wide panel) | 21.463 | 21.463 | 2, page 82 ([B-3]) |
| Boral height | 389.26 | 389.26 | 2, page 82 ([B-3]) |
| Sheathing thickness | 0.0452 | 0.0452 | 2, page 82 ([B-3]) |
| Sheathing width | 22.098 | 22.098 | 2, page 82 ([B-3]) |
| Sheathing height | 392.13 | 392.13 | 2, page 82 ([B-3]) |
| **6.1.1.1 Support rod** | | | |
| Radius | 3.81 | 3.81 | 2, page 82 ([B-3]) |
| Spacer disc radius | 83.2612 | 83.2612 | 2, page 81 ([B-3]) |
| Spacer disc thickness | 3.175 | 3.175 | 2, page 82 ([B-3]) |

**Table A-11.2. Licensing dimensions used in the CSAS6 criticality model for the FF-DSC canister**

| Canister | Size (cm) | Reference (Transnuclear Drawing Number) |
|---|---|---|
| Inner canister radius | 83.74 | 2, page 87 ([B-4]) |
| Outer canister radius | 85.344 | 2, page 87 ([B-4]) |
| Inner canister height (inner cavity length) | 439.42 | 2, page 85 ([B-4]) |
| Thickness of outer bottom cover | 1.905 | 2, page 87 ([B-4]) |
| Thickness of inner bottom cover | 1.905 | 2, page 87([B-4]) |
| Thickness of bottom plug top casing | 1.905 | 2, page 87 ([B-4]) |

**Table A-11.2. Licensing dimensions used in the CSAS6 criticality model for the FF-DSC canister (continued)**

| | | |
|---|---|---|
| Thickness of bottom plug side casing | 1.27 | 2, page 87 ([B-4]) |
| Thickness of bottom lead shielding | 9.525 | 2, page 87 ([B-4]) |
| Thickness of lid - inner top cover plate | 1.905 | 2, page 87 ([B-4]) |
| Thickness of lid - outer top cover plate | 3.175 | 2, page 87 ([B-4]) |
| Thickness of lid - top plug top casing | 0.9652 | 2, page 89 ([B-4]) |
| Thickness of lid - top lead shielding | 10.4648 | 2, page 89 ([B-4]) |
| Thickness of lid - top plug side casing | 1.27 | 2, page 89 ([B-4]) |
| Thickness of lid - top plug bottom casing | 1.27 | 2, page 89 ([B-4]) |
| Height | 472.948 | 2, page 85 ([B-4]) |

**Table A-11.3. Comparison of results calculated for the FO/FC-DSC model with those presented in Reference 1**

| Reference 1 $k_{eff}$ | Calculated $k_{eff} \pm \sigma$ | $\Delta k_{eff}$ |
|---|---|---|
| 0.92033 ± 0.00026 | 0.93159 | 0.01126 |

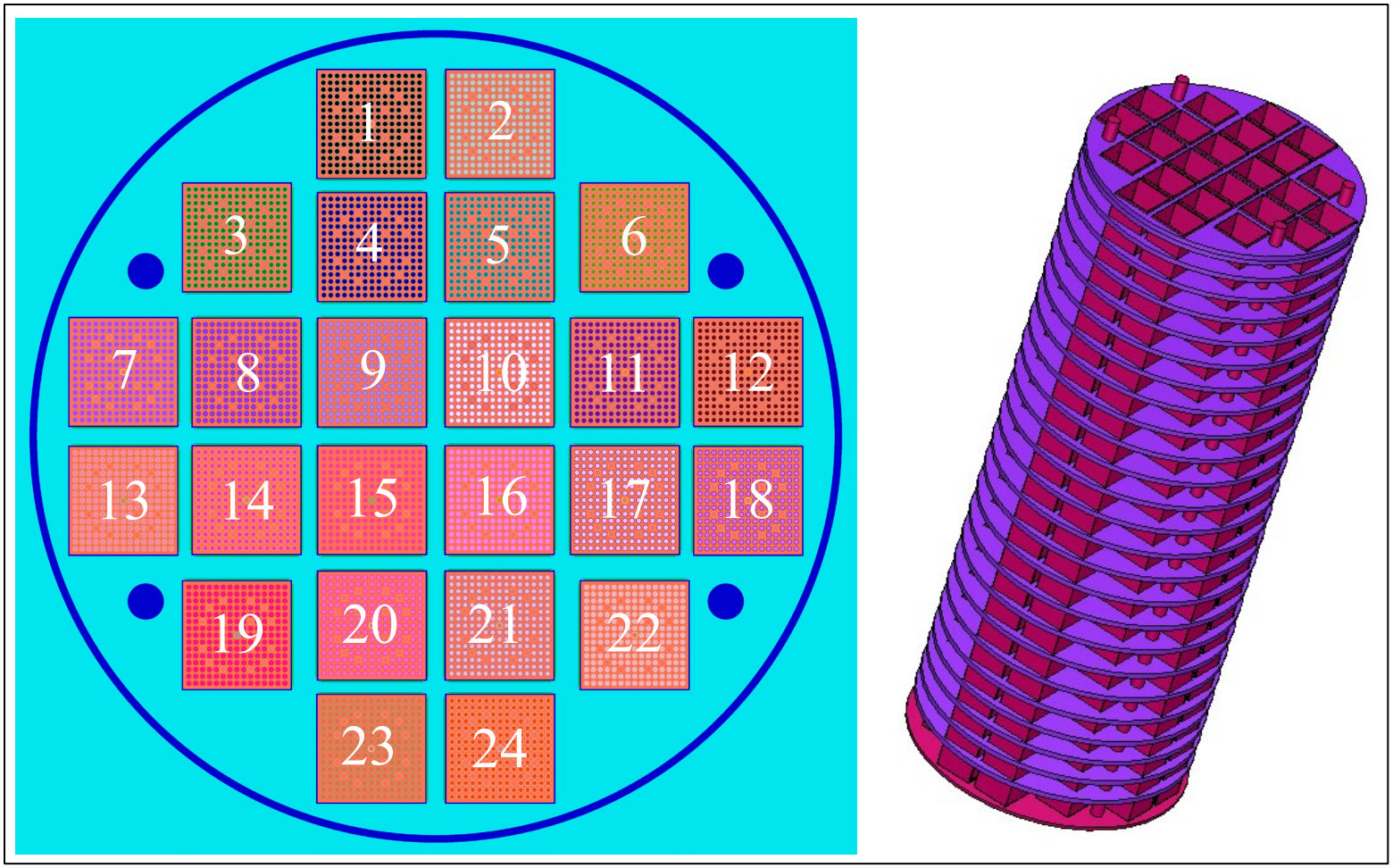


**Fig. A-11.1. Plan view (left) and isometric view (right) of the FO/FC-DSC canister.**

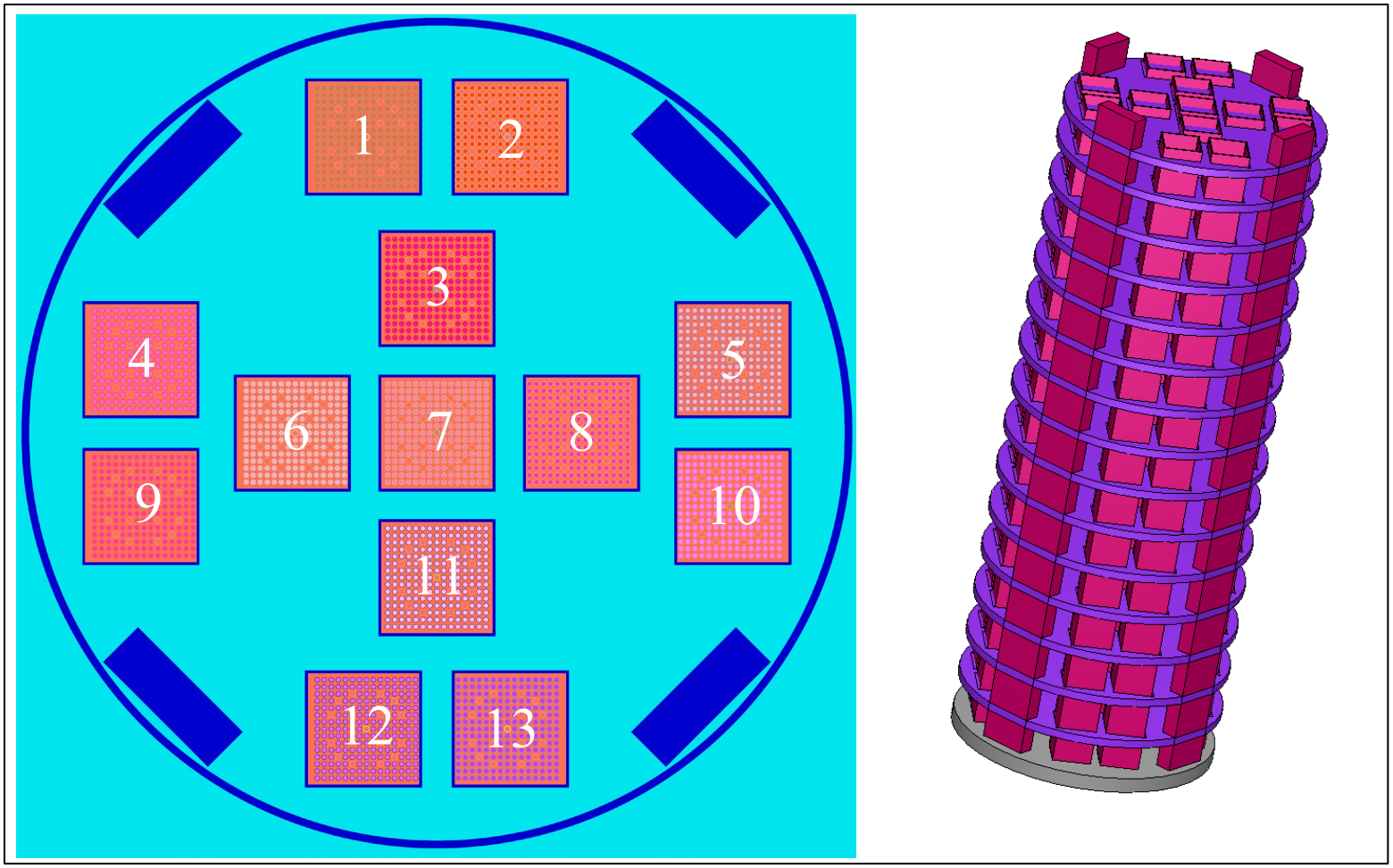


**Fig. A-11.2. Plan view (left) and isometric view (right) of the FF-DSC canister.**

# A-12. W74

## A-12.1 Canister

The W74 canister includes two stackable basket assemblies with a capacity to accommodate up to 64 Big Rock Point fuel assemblies. Each basket includes 37 cell locations, with the center five cell locations mechanically blocked to prevent fuel loading in these locations. The W74 uses a tube and disk design that consists of a series of circular spacer plates that are positioned and supported by four support tubes that run through the spacer plates and support sleeves between the spacer plates. Each basket cell location, with the exception of the four support tubes and the five blocked-out center cells, contains a guide tube assembly. The W74 guide tube assemblies include borated stainless steel neutron absorber sheets on either one side or two opposite sides. The guide tubes are arranged in the basket to position at least one poison sheet between adjacent fuel assemblies, with the exception of intact fuel assemblies placed in the support tubes.

There are two different varieties of the W74 canister, the W74M (Multipurpose Canister) and the W74T (Transportable Storage Canister). The primary difference between the W74M and the W74T is that the W74M includes additional spacer disk with respect to the W74T. The criticality evaluation provided in Reference 1 determined that the additional neutron absorbing nature of the steel disks outweighed the water displacement in the flux traps so the W74T was chosen for incorporation into the UNF-ST&DARDS because it is slightly more reactive than the W74M.

The dimensions of the model are presented in Table A-12.1. Radial and isometric views of the model are shown in Figure A-12.1.

## A-12.2 Damaged Fuel

The design basis fresh 4.10 w/o 11×11 ANF assembly was shown in [1] to be more reactive than any of the MOX fuel assemblies and may therefore be substituted for any of the MOX fuel assemblies used at Big Rock Point. It should be modeled as fresh rather than at the declared burnup.

Damaged fuel at Big Rock Point is analyzed in [1] as either partial fuel or damaged fuel. The licensing analysis [1] optimized the partial fuel models such that the pitch selected yielded the maximum $k_{eff}$ in full density water. This analysis showed that a 3.55 w/o enriched GE 9×9 fuel assembly with a pin pitch of 0.741 inches was the most reactive fuel configuration to still be confined within the envelope of the intact assembly (Table 6.6-12, [1]). The GE 9×9 partial fuel assembly was more reactive than the GE 11×11 partial assembly, both in the absolute sense and when considering margin to the upper subcritical limits in Table 6.6-13 of [1]. There were multiple pellet arrays modeled for the damaged fuel inside the DFC, which was placed in each of the support tubes in the model. The $k_{eff}$ calculated for a canister with all of the guide tubes filled with the limiting partial assembly and support tubes fill with the limiting damaged fuel array (Table 6.6-20) was lower than the $k_{eff}$ calculated with all guide and support tubes filled with the limiting partial fuel assembly (Table 6.6-12). It is therefore simple and conservative to model all damaged fuel at Big Rock Point as fresh GE 9×9 fuel with a pitch of 0.741 inches and an enrichment of 3.55 w/o. No DFC should be modeled with this damaged fuel type.

**Model Verification Calculations**

The criticality analysis [1] does not publish a $k_{eff}$ value for the condition of nominal basket design with all assemblies centered in the storage cells as is typically modeled in the UNF-ST&DARDS project. In order to appropriately benchmark the model being placed into UNF-ST&DARDS, it was necessary to show that one of the Reference 1 design basis calculations could be replicated by perturbing the template model. The Siemens 11×11 fuel assembly was used for the calculation because it is the design basis fuel assembly for the W74 canister. All of the mechanical tolerances listed in Table 6.3-1 of Reference 1 were applied to basket dimensions and the relocation of the fuel and guide tubes “Normal Transport

Conditions" in the directions shown in Figure 6.3-12 of Reference 1. The results of the benchmark calculations are presented in Table A-12.2.

**References**

1. *FuelSolutions W74 Canister Transportation SAR* - Revision 3.

**Table A-12.1. Dimensions used in the CSAS6 criticality model for the W74 canister**

| Canister | Size (cm) | Reference 1 Location |
|---|---|---|
| Inner Canister Radius | 82.2325 | Table 1.2-1 |
| Outer Canister Radius | 83.82 | Table 1.2-1 |
| Canister Cavity Height | 439.42 | Table 1.2-1 |
| **Basket** | | |
| Inner Cell Dimension – Standard Cell | 17.526 | DWG W74-122 (pg. 111)/ Table 1.2-1 |
| Cell Thickness – Standard Cell | 0.2286 | Table 1.2-1 |
| Cell Height – Standard Cell | 214.63 | DWG W74-122 |
| Inner Cell Dimension – Support Tube Cell | 18.796 | DWG W74-120 Table 1.2-1 |
| Cell Thickness – Standard Cell – Support Tube Cell | 1.6002 | Table 1.2-1 |
| Cell Height - Support Tube Cell | 216.535 | DWG W74-120 |
| Radial Layout of Fuel Tubes | See Reference | DWG W74-121 |
| **Borated Stainless Steel** | | |
| **Poison** | | |
| Thickness | 0.1905 | Table 1.2-1 |
| Width | 16.256 | DWG W74-122 |
| Height | 212.09 | DWG W74-122 |
| Number Densities | See Reference | Tables 6.3-7 and 6.3-8 |
| **Support Plate Specification** | | |
| Axial placement of support plates | See Reference | DWG W74-120 (2 sheets) |
| Engagement disk thickness | 5.08 | Table 1.2-1 |
| Spacer disk thickness | 1.905 | Table 1.2-1 |

**Table A-12.2. Comparison of results calculated for the W74 canister model with those presented in Reference 1**

| Model Type | Reference 2 $k_{eff}$ | Calculated $k_{eff} \pm \sigma$ | $\Delta k_{eff}$ |
|---|---|---|---|
| Normal Transport Conditions | 0.93831±0.00088 | 0.94072±0.00044 | 0.00241 |

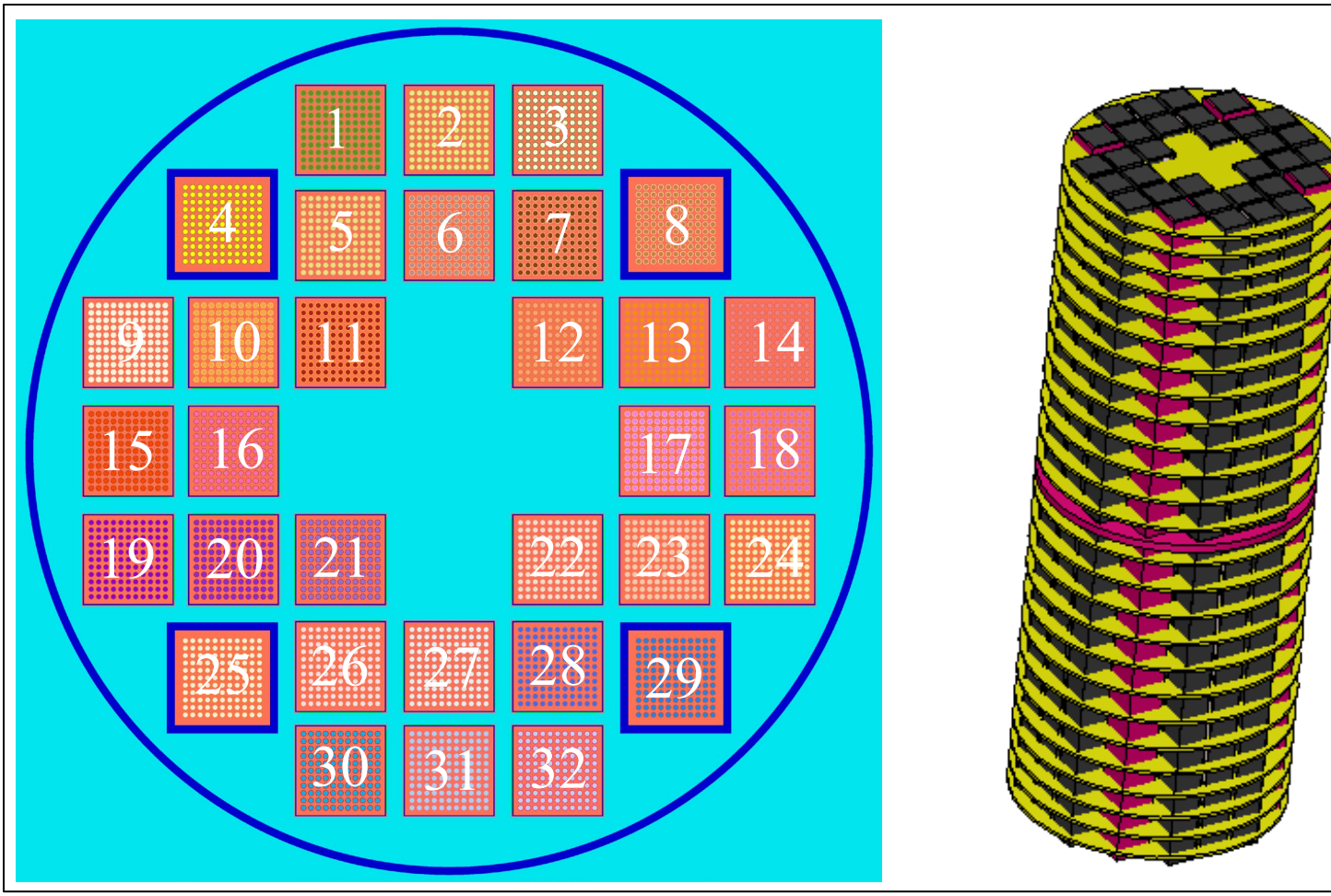


**Fig. A-12.1. Plan view (left) and isometric view (right) of the W74 canister.**

# A-13. NUHOMS® 61BT/BTH-DSC

## A-13.1 Canister

The NUHOMS® 61BT-DSC and NUHOMS® 61BTH-DSC canisters each provide 61 locations that can host intact BWR fuel assemblies or up to 16 BWR damaged fuel assemblies. These canisters are constructed of tubes which contain the fuel assemblies, referred to as *fuel compartments*. The fuel compartments are joined together into four and nine compartment assemblies. The neutron absorber material is installed between the fuel compartments within the compartment assemblies and in between the compartment assemblies. Damaged fuel assemblies must be loaded in the 2 × 2 cluster of fuel compartments closest to each corner of the basket. The NUHOMS® DSC-61BTH-DSC differs from the 61BT-DSC in that it can accommodate a higher heat load with the addition of rails that allow for better thermal coupling of the basket to the shell of the DSC. From the perspective of criticality analysis, there is no difference between the 61BT-DSC and the 61BTH Type 1-DSC. The NUHOMS® DSC-61BTH Type 2-DSC requires a slightly higher boron content, but the difference is negligible. Model dimensions are withheld from this section of the document because the models have been derived from proprietary documents.

## A-13.2 Damaged Fuel

Damaged fuel modeling is enabled with the can inner diameter being set to the inner dimension of the fuel compartment.

## A-13.3 Model Verification

A model verification calculation was developed using the "Most Reactive Fuel Analysis" model from [1] and comparing the calculations to the GE12 fuel type limiting case provided in [1], Table 6-6, for the DSC-61BT. The calculation was performed using a fuel enrichment of 3.7 wt. % and a $^{10}B$ loading of 0.021 g/cm$^2$. The results of the benchmark calculation are presented in Table A-13.1 and they show good agreement with the calculations presented in [1].

## A-13.4 References

1. *MP197 Transportation Packaging Safety Analysis Report*, Rev. 12, February, 2012.

**Table A-13.1. Model verification results for the DSC-61BT\BTH**

| Fuel Type | Reference[a] $k_{eff}$ | Calculated $k_{eff} \pm \sigma$ | $\Delta k_{eff}$ |
|---|---|---|---|
| GE 14 (10x10) | 0.9095±0.0013 | 0.91211 ± 0.00016 | 0.00261 |

[a][1], Table 6-6, GE12 fuel type limiting case.

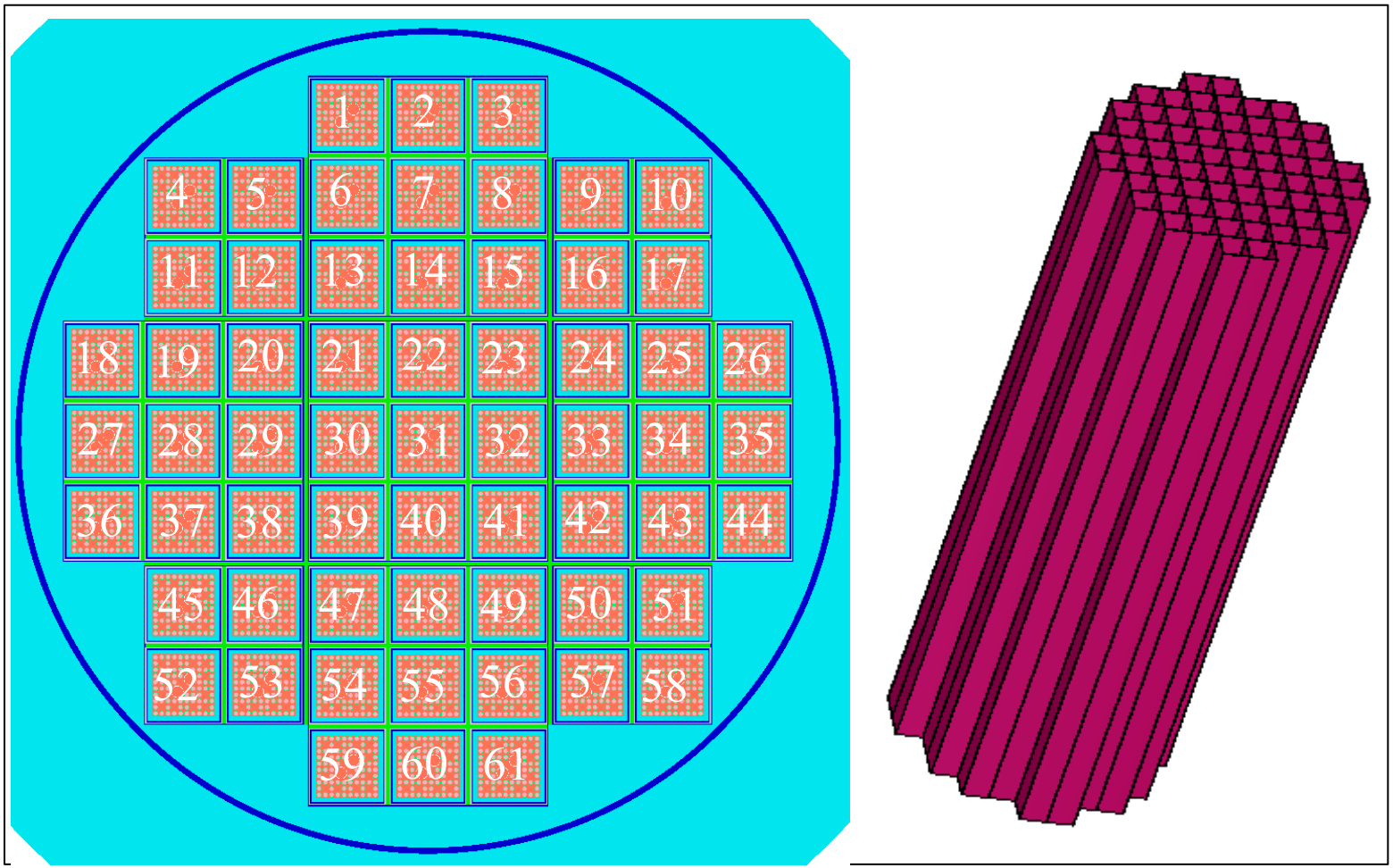


**Fig. A-13.1. Plan view (left) and isometric view (right) of the DSC-61BT\BTH canister.**

# A-14. NUHOMS® 32PTH/PTH1-DSC

## A-14.1 Canister

The NUHOMS® 32PTH-DSC and NUHOMS® 32PHT Type 1-DSC (32PTH1) canisters each provide 32 locations that can host intact PWR fuel assemblies or up to 16 PWR damaged fuel assemblies. The fuel compartment tubes are arrayed in an "egg-crate" plate design. The egg-crate design holds the fuel compartments between aluminum basket plates. The neutron poison, which may be either borated aluminum or Boral is sandwiched between the fuel compartments and the basket plates. The entire basket is affixed to the outer shell of the DSC via transition rails. The documentation for the NUHOMS® 32PTH-DSC and NUHOMS® 32PTH1-DSC criticality analysis is contained in Section A.6.5.4 of the MP197 SAR [1]. The NUHOMS® 32PTH1-DSC comes in three lengths, designated as NUHOMS® 32PTH1-S, M, and L. the NUHOMS® 32PTH1-S DSC is identical in length to the shortest NUHOMS® 32PTH-DSC. Comparison of the loading curves and neutron absorber $^{10}B$ loading requirements indicates that the canisters are identical from a criticality safety perspective. The templates developed here vary the length of the canister automatically in order to account for the variant, as identified in the UDB. Model dimensions are withheld from this section of the document because the models have been derived from proprietary documents.

## A-14.2 Damaged Fuel

Damaged fuel modeling is enabled with the fuel can inner dimensions being used for the lattice pitch expansion.

## A-14.3 Model Verification

A model verification calculation was developed using results from Table A.6.5.4-10 from [1] and comparing the calculations to a UNF-ST&DARDS calculation with normal storage and transportation conditions with a W1717WO fuel assembly. The results of the calculations are compared with a Westinghouse 17 × 17 OFA (W1717WO) fuel type limiting case from Table 6.5.4-10 for the 32PTH-DSC using a Type C basket. The calculation was performed using fresh fuel with a fuel enrichment of 1.75 wt. % and a $^{10}B$ loading of 0.018 g/cm$^2$. The results of the benchmark calculation are presented in Table A-14.1.

## A-14.4 References

1. *MP197 Transportation Packaging Safety Analysis Report*, Rev. 12, February, 2012.

**Table A-14.1. Model verification results for the 32PTH/PTH1-DSC canister**

| Fuel Type | Reference 1 $k_{eff}$ | Calculated $k_{eff} \pm \sigma$ | $\Delta k_{eff}$ |
|---|---|---|---|
| W1717WO | 0.9361 | 0.92417 ± 0.00063 | 0.0119 |

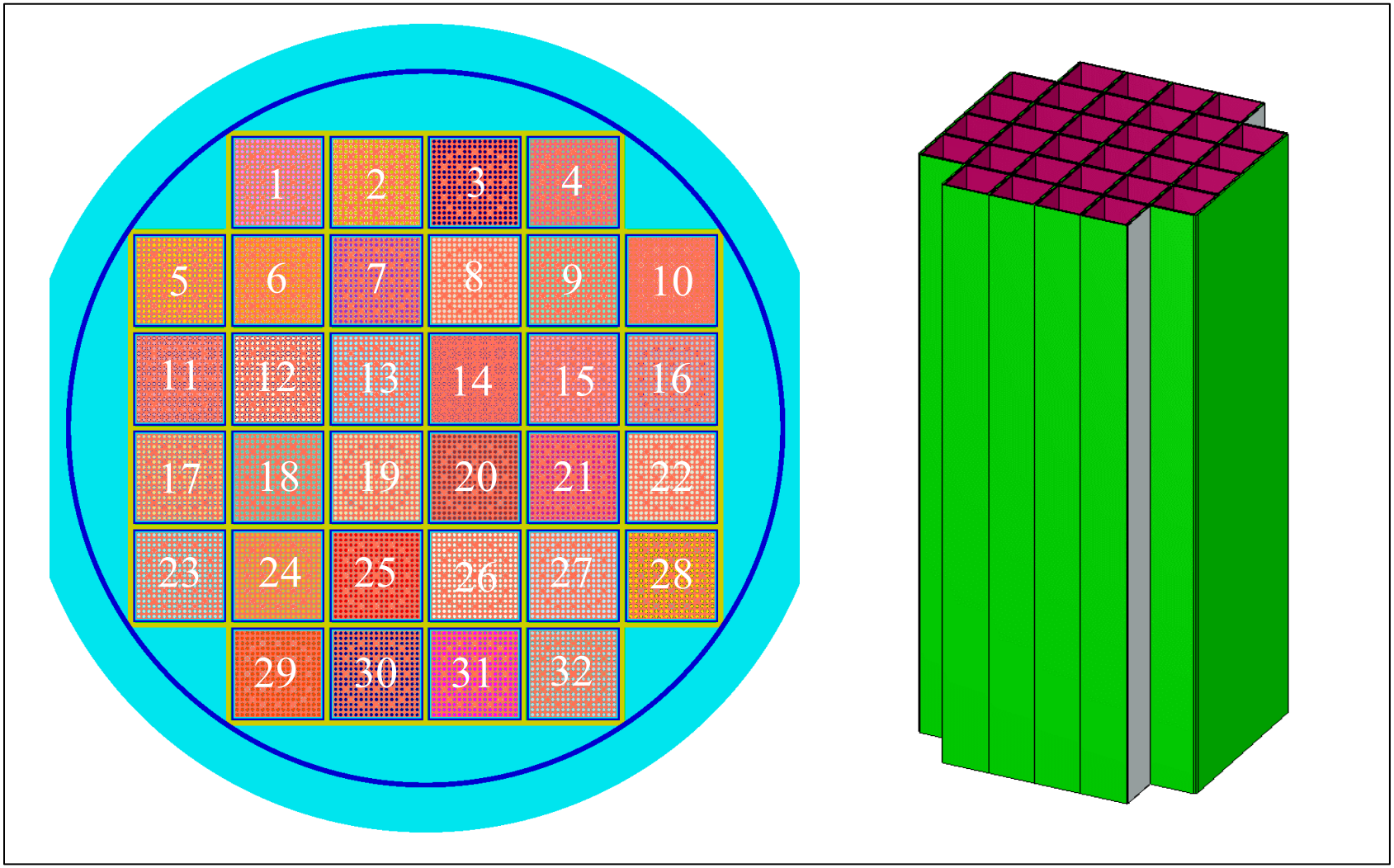


**Fig. A-14.1. Plan view (left) and isometric view (right) of the DSC-32PTH\PTH1 canister.**

# Appendix B

# Results of the FY 2019 Criticality Calculations

This appendix of the report presents the query used to retrieve $k_{eff}$ results from the UDB. The query presented in Table B.1 retrieves the $k_{eff}$ results and the standard deviation of the $k_{eff}$ for each canister and evaluation date combination. The query in Table B.1 also allows for the selection of either the normal storage and transportation case (ccb.crit_analysis_type_id = 1) or disposal condition (ccb.crit_analysis_type_id = 2). The nuclide sets that are used are a function of analysis type, the normal storage and transportation nuclide set is indicated by ccb.nuclide_category_id = 6 and the disposal isotope set is indicated by ccb.nuclide_category_id = 5.

**Table B-1. Query to retrieve $k_{eff}$ results from the UDB**

```
SELECT
   cr.id,
   cbfc.canister_id,
   cr.analysis_date,
--   YEAR(ccb.evaluation_date),
   cr.keff,
   cr.uncertainty_1_sigma,
   cr.crit_analysis_type_id,
   cr.nuclide_category_id,
   zcr.modified,
   f.name
FROM
   critiality_results cr
      LEFT JOIN
   canister_barefuelcask cbfc ON cbfc.id = cr.canister_barefuelcask_id
      LEFT JOIN
   canister_barefuelcask_inventory ci ON ci.canister_barefuelcask_id = cbfc.id
      LEFT JOIN
   assembly_location_dry ald ON ald.id = ci.assembly_location_dry_id
      LEFT JOIN
   zref_criticality_results zcr ON zcr.id = cr.id
      LEFT JOIN
     facility f on f.id = ald.facility_id


WHERE
   cr.crit_analysis_type_id = 2
      AND f.name LIKE 'Humbold%'
      AND zcr.modified > '2016-02-20'
   GROUP BY cbfc.canister_id , cr.analysis_date
   ORDER BY cbfc.canister_id , cr.analysis_date;
```

# Appendix C

# As-Loaded BWR Criticality Analysis Approach within UNF-ST&DARDS

# C-1. Introduction

This appendix documents work performed supporting the US Department of Energy (DOE) Nuclear Energy (NE) Fuel Cycle Technologies Nuclear Fuels Storage and Transportation (NFST) Planning Project under work breakdown structure element 1.02.09.01.05 - CX, "Characterization and Assessment." In particular, this appendix fulfills the M3 milestone, M3FT- 16OR090105016, "UNF-ST&DARDS Criticality Model Development and Implementation" within work package FT-16OR09010501, "Characterization and Assessment -ORNL."

This appendix documents justification of the various modeling approaches used within UNF-ST&DARDS to take credit for the reduced reactivity associated with the burnup of BWR fuel for as-loaded criticality analysis. In the absence of detailed BWR fuel and reactor operational data, these as-loaded BWR criticality analysis approaches are meant to be conservative. However, no attempt is taken to establish the most limiting as-loaded BWR burnup credit approaches. For the past several years, burnup credit has been used for the storage (both wet and dry), transportation, and disposal of PWR SNF fuel. However, the fresh fuel assumption has historically been applied to the BWR SNF criticality analyses for dry storage and transportation, and the peak reactivity method of burnup credit has been applied to pool storage. The fresh fuel assumption ignores the credit for the gadolinium burnable absorbers in the fuel, as well as the burnup of the fuel and is therefore extremely conservative. Peak reactivity methods are less conservative than the fresh fuel assumption because they take credit for the reactivity associated with depletion of the fuel to the point at which the limiting lattice reaches its highest reactivity. While the peak reactivity method allows for demonstration of more credit than the fresh fuel assumption, it still ignores credit for the actual burnup of the SNF assemblies.

This work follows the framework traditionally used for PWR burnup credit analyses, and it uses available data and recently published regulatory guidance to justify an approach to model the as-loaded burnup and enrichment of SNF assemblies in dry casks. Unlike licensing evaluations—which are designed to cover a broad range of SNF characteristics—cask-specific as-loaded criticality analysis is performed without establishing bounding parameters and conditions. Conservatisms from the safety analysis reports (SARs) are retained for cases in which information is insufficient to justify a change in the criticality analysis that incorporates additional detail in the model. For example, damaged fuels are modeled using the limiting geometric configuration from the SAR and with fresh fuel compositions. If these types of analyses are used to support future licensing activities, additional validation and assessment of the applicable biases uncertainties may be required to verify the safety margins. The BWR criticality analysis approach discussed in this appendix will be refined in the future as more data become available.

UNF-ST&DARDS uses the declared burnups and enrichments from DOE fuel inventory surveys [13] to perform criticality safety calculations that take full burnup credit (actinides and fission products) for BWR fuel bundles loaded in SNF storage and transportation canisters. Justification for the following features of the criticality analysis approach are presented in this appendix.

- Selection of axial burnup profiles for BWR fuel from publicly available sources using methods derived from recently published regulatory guidance.
- Justification of the selected axial burnup profiles as relevant to all types of BWR fuel.
- Comparison of the axial features of the fuel from which the profiles were selected with the range of axial features of the population of fuel present at the SNF storage sites.
- Justification for modeling the fuel assemblies with a uniform axial and radial enrichment. (BWR fuel typically has a number of different enrichments which vary within a single axial segment (also known as lattice) and as a function of elevation.)
- Justification for modeling the axial void profile as a single nominal value that does not change with elevation or time, and using the margin associated with the bounding depletion

assumption that control blades are fully inserted throughout the entire irradiation history of the fuel assembly.

The modeling parameters used to perform as-loaded BWR criticality analysis within UNF-ST&DARDS are summarized in Table C-2.

**Table C-2. Fuel assembly classes, RW-859 codes, and number of fuel assemblies in the database for SLU fuel.**

| Parameter | Value |
|---|---|
| Fuel rod mixture | $UO_2$ |
| Fuel density (g/cm$^3$)a | 10.741 |
| Specific power (MW/MTU) | 22.38 |
| Fuel temperature (K) | 1200 |
| Moderator temperature (K) | 560.7 |
| Moderator density (g/cm$^3$) | 0.3 |
| Absorber exposure | $Gd_2O_3$ admixed with fuel pellet in small number of rods based on fuel type and full-length control blade exposure. |
| Axial burnup profiles | Listed in Table C-6 |

Section C-2 of this appendix discusses the characteristics and evolution of BWR fuel within the context of how the fuel features affect a criticality analysis. Section C-3 discusses the origin and features of the KENO models that were used to perform the criticality sensitivity calculations to justify as-loaded analysis approach. Section C-4 discusses the guidance, data, and methodology associated with selection of axial burnup profiles, as well as the justification of those burnup profiles for all of the fuel types considered in this report. Section C-5 justifies the use of a single enrichment to model fuel with axial and radial enrichment gradients. Section C-6 justifies using the depletion assumptions that went into developing the cross section libraries used to deplete the fuel. Section C-7 presents the conclusions drawn from this work and discusses potential future work in this area.

## C-2. BWR Fuel Characteristics and Evolution

In order to justify a burnup credit approach for BWR fuel, it is important to understand the characteristics of the fuel to be analyzed. BWR fuel assemblies represent a significant increase in complexity in the way the fuel is arranged and the way reactors are operated when compared to PWR fuel assemblies. This section of the appendix discusses the structures of the different BWR fuel types as they have evolved over the years, dividing the fuel types into three categories based on their axial features for future discussions.

Early generation BWR fuel used a single axial enrichment and lattice at all elevations, had few-to-no nonfuel locations within the fuel lattice, and used a small number of low concentration gadolinium-bearing rods. Having a single axial enrichment and a single lattice, this fuel design is referred to as *single lattice unblanketed (SLU)* fuel. The SLU fuel assembly population includes assemblies from the single unit early BWR designs (Dresden 1, Big Rock Point, Humboldt Bay, La Crosse), all of the 7 × 7 fuel, and the early 8 × 8 fuel designs. All 8 × 8 fuel that is not considered *single lattice blanketed (SLB)* fuel is categorized as SLU fuel. The fuel designs, the fuel assembly identifiers from the RW-859, and the number of SLU fuel assemblies in the assembly inventory are documented in Table C-3.

The second generation of BWR fuel designs also used a single lattice for all elevations but began incorporating multiple axial enrichments, used water holes as part of the fuel assembly lattice, and a had a larger number of higher concentration gadolinium-bearing fuel rods. While there is some non-blanket axial variation in the enrichment of these fuel assemblies, the primary enrichment change is the universal inclusion of natural uranium axial blankets in these fuel types. Because these fuel assemblies began

including natural uranium blankets but did not change the geometry of the fuel lattice with elevation, these designs are referred to as *single lattice blanketed (SLB) fuel*. SLB fuel assemblies consist of all 8 × 8 fuel designs except the early designs, which are SLU fuel types, and all of the Advanced Nuclear Fuel (ANF) 9 × 9 fuel types. The characteristics database (Ref. C-5, Table 2.2.4) indicates that the GE-5 fuel design was the first by that vendor to implement natural blankets. Because there is no evidence of reversion to unblanketed fuel, and because natural blankets are universal among BWR fuel assemblies today, it is assumed that all subsequent GE fuel designs also used natural blankets. There is no information on the axial features for the ANF and Westinghouse designs in Ref. C-5; however, the ANF pre-pressurized fuel assembly is assumed to be similar to the GE version. The Westinghouse 8 × 8 assembly design was introduced in 1987, long after the introduction of natural blankets in 1975. Therefore, both of those designs are categorized as SLB fuel. The fuel designs, the fuel assembly identifiers from the RW-859, and the number of SLB fuel assemblies in the assembly inventory are documented in Table C-4.

The third and most modern generation of BWR fuel assemblies includes those that continue to use natural uranium axial blankets, that have expanded the usage of water holes and gadolinium (both in number of rods and concentration), and that have also incorporated the use of part-length fuel rods which terminate mid-way up the assembly. This leaves a "vanished" lattice in the upper portion of the fuel assembly. Because these fuel assemblies can be uniquely identified by the presence of at least two unique lattices, these fuel types are referred to as *multi-lattice (ML)* fuels. Table 2.2.4 of Ref. C-5 directly states that fuel designs GE-11 through GE-13 incorporate part-length rods, and the GE-14 and GNF-2 designs are assumed to continue that practice due to the trend towards using part-length rods. Reference C-11 documents the inclusion of 8 part-length rods in the ATRIUM-10 for the first time by Areva. Reference C-12 shows that the SVEA-96 fuel designs have multiple sets of part-length rods. The fuel designs, the fuel assembly identifiers from the RW-859, and the number of ML fuel assemblies in the assembly inventory are documented in Table C-3.

In order to understand the near-term needs of the UNF-ST&DARDS criticality analysis process, it is important to examine the prevalence of the various fuel types within the general population of fuel assemblies, within the population of fuel assemblies currently in dry storage, and within the analyzable population of fuel assemblies. Reference C-13 contains the number of assemblies and their locations reported by utilities as of June 2013. The information from Ref. C-13 was incorporated into the UDB, and the database was queried to generate Figs. C-1 through C-3. These figures contain plots of the total number of assemblies in each fuel category present in (1) the population of discharged fuel assemblies, (2) within the population of fuel assemblies in dry storage, and (3) within the population of fuel assemblies that have been analyzed. Figure C-1 shows slightly more discharged SLB fuel assemblies (64,645) than ML fuel assemblies (51,151) in the overall population of fuel assemblies. These totals are considerably larger than the number of SLU fuel assemblies (24,521). Figure C-2 shows that there are far more SLB fuel assemblies (21,785) in dry storage than SLU fuel assemblies (5,988) or ML fuel assemblies (4,501). Figure C-3 shows that the population of fuel assemblies analyzed to date is comprised of 7,302 SLB assemblies, 4,768 SLU assemblies, and 2,521 ML assemblies. Because UNF-ST&DARDS analyzes casks, the immediate need is to have methods tailored to the analysis of SLB fuel. Although SLU makes up a considerable portion of the fuel that has been analyzed, using modeling approximations for SLU fuel that are overly bounding in many cases may be acceptable because that population of assemblies is limited and will be fixed or decreasing with time. Additionally, the SLU fuel assemblies are typically very low enriched and inherently have substantial margin to criticality. However, longer term goals should focus on effective analysis of ML fuel because (1) there are a large number of ML fuel assemblies in wet storage being irradiated, and (2) all projected future fuel assemblies will be of the ML design.

**Table C-3. Fuel assembly classes, RW-859 codes, and number of fuel assemblies in the database for SLU fuel**

| Fuel assembly class | Fuel assembly RW-859 codes | Number of assemblies in database |
|---|---|---|
| Big Rock Point | XBR09G, XBR11G, XBR11N, XBR09A, XBR11A | 527 |
| Dresden 1 | XDR06A, XDR06U, XDR06G3F, XDR063B, XDR06G5 | 892 |
| Humboldt Bay | XHB06G, XHB07G2, XHB06A | 390 |
| La Crosse | XLC10L, XLC10A | 334 |
| ANF 7 × 7 | G2307A | 152S |
| ANF 8 × 8 | G2308A | 1,517 |
| GE-2 | GE2307G2A, GE2307G2B, GE4607G2 | 7,862 |
| GE-3 | G2308G3, G4608G3A, G4608G3B | 5,331 |
| GE-4 | G2308G4, G4608G4A, G4608G4B | 7,516 |

**Table C-4. Fuel assembly classes, RW-859 codes, and number of fuel assemblies in the database for SLB fuel**

| Fuel assembly class | Fuel assembly RW-859 codes | Number of assemblies in database |
|---|---|---|
| GE-5 | G2308G5, G4608G5 | 5,127 |
| GE Pre-pressurized | G2308GP, G4608GP | 15,923 |
| GE Barrier | G2308GB, G4608GB | 11,613 |
| GE-7 | G2308G7 | 164 |
| GE-8 | G2308G8A, G2308G8B, G4608G8A, G4608G8B | 6,608 |
| GE-9 | G2308G9, G4608G9 | 8,054 |
| GE-10 | G2308G10, G4608G10 | 5,242 |
| ANF Pre-pressurized | G2308AP, G2308AP | 1,921 |
| ANF 9 × 9 | G2309A, G4609A, G2309AIX, G4609A5, G4609AIX, G4609AX+, | 9,985 |
| Quad + | G4608W | 8 |

**Table C-5. Fuel assembly classes, RW-859 codes, and number of fuel assemblies in the database for ML fuel**

| Fuel assembly class | Fuel assembly RW-859 codes | Number of assemblies in database |
|---|---|---|
| GE-11 | G2309G11, G4609G11 | 15,085 |
| GE-12 | G4610G12 | 460 |
| GE-13 | G4609G13 | 2,060 |
| GE-14 | G2310G14, G4610G14 | 21,038 |
| GNF-2 | GNF2 | 40 |
| SVEA 96 | G2310W, G4610C | 2,474 |
| ATRIUM 10 | ATRIUM 10, G4610A, G4610AIX, G4610AXM | 9,994 |

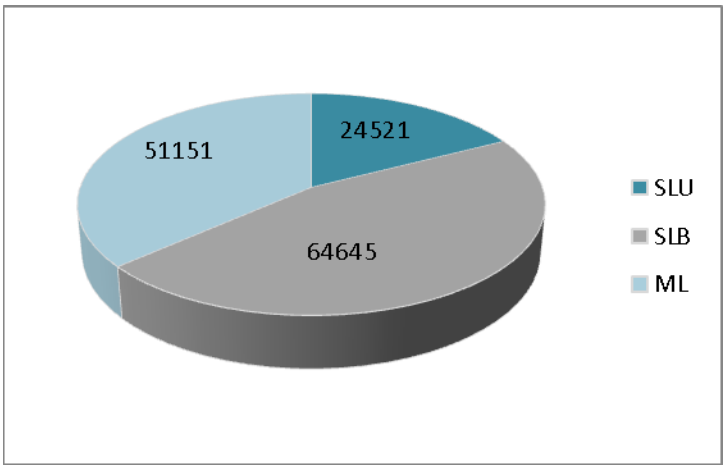


**Fig. C-1. Distribution of assemblies by fuel type in the discharged SNF inventory.**

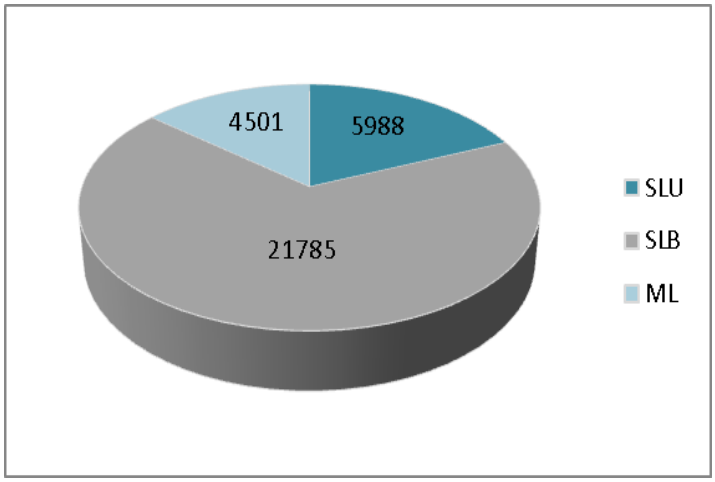


**Fig. C-2. Distribution of assemblies by fuel type in the discharged SNF inventory that are currently in dry storage.**

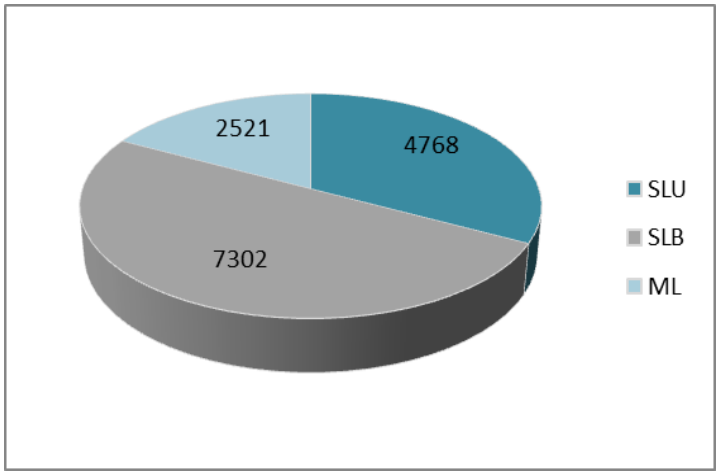


**Fig. C-3. Distribution of assemblies by fuel type in the discharged SNF inventory that are currently in dry storage.**

## C-3. Modeling Techniques

To study the effects of the parameters important to burnup credit, an appropriate criticality model is necessary. The model must capture the features of a canister important to reactivity, and it must represent canisters used to store, transport, and dispose of SNF. For the purposes of this work the MPC-68 canister manufactured by Holtec International as part of the HI-STORM 100/ HI-STAR 100 cask systems has been chosen. A full canister version of the MPC-68 KENO-VI model is shown in Sect. A-9 of this report, along with the appropriate description of the material properties and basket dimensions. Because all of the sensitivity studies presented in this work assume a radially uniform loading of assemblies throughout the basket, the model was trimmed to a single basket cell with periodic boundary conditions on all sides. There are two feet of water above and below the fuel assembly to provide axial decoupling of the top fuel zones from the bottom fuel zones for the sensitivity studies.

There are two fuel models used within the MPC-68 canister model. The first model is used for profile selection and to investigate the effects of control blade insertion and moderator void profiles. The first model has an 8 × 8 fuel assembly divided into 25 equally spaced axial nodes. The second model, which is used to investigate the effect of axially distributed enrichments, uses a second set of rods to allow for modeling of the gadolinium compositions. Only four gadolinium-bearing rods are modeled because this represents the minimum number used in any SLB fuel assembly found in the CRC data. The modeling of gadolinium to offset the effects of the GC-859 uniform axial enrichment reporting is discussed in further detail in Sect. C-5.2. The radial views of the non-gadolinium–bearing and gadolinium-bearing fuel models are presented in Fig. C-4. An axial representation of the various models is presented in Fig. C-10 in Sect. C-5.2, along with an explanation of its use.

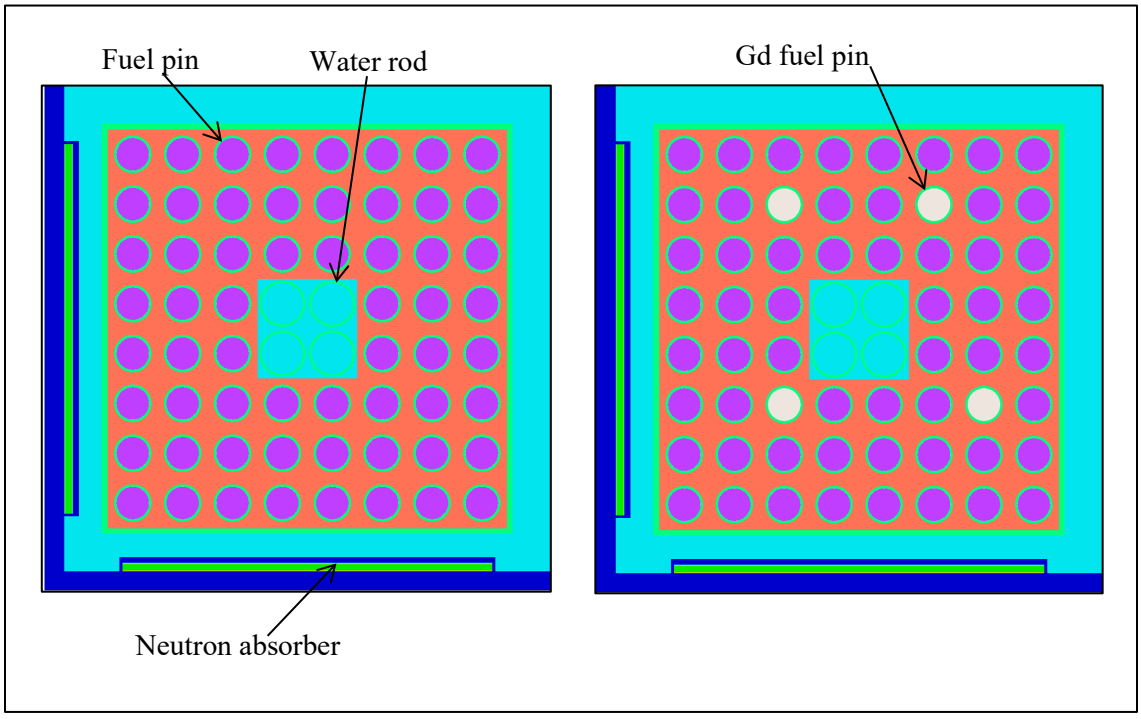


**Fig. C-4. Radial view of the MPC-68 KENO criticality model with examples of the fuel assembly with and without gadolinium.**

## C-4. Axial Burnup Profiles

It is a well-established phenomenon that the asymmetric axial accumulation of burnup during irradiation results in the ends of the fuel receiving less burnup than the center portion. Because the water is heated along the length of the core, and all US cores are required to have a negative moderator density coefficient, the upper portion of the fuel assemblies receive even less burnup than the lower portion of the assemblies. At some point in the burnup history of the fuel assembly, the upper portion of the assembly will become so underburned relative to the middle that it will dominate the reactivity of the assembly and cause the assembly to be more reactive than if it had been modeled with a uniform axial burnup profile. This increase in reactivity from the uniform axial profile is termed the *end effect* and must be appropriately captured in a burnup credit analysis. This section of the report discusses the guidance, data, and calculations used to determine an appropriate set of axial burnup profiles for use in the UNF-ST&DARDS criticality analysis process for BWR fuels.

### C-4.1 Regulatory Guidance for Axial Burnup Profile Selection

The guidance on axial burnup profiles used in this report is from NUREG-7224, *Technical Basis for the Use of Axial Moderator Density Distributions, Control Blade Usage, and Axial Burnup Distributions in Extended BWR Burnup Credit Analyses* [C-3]. Reference C-3 uses typical BWR core follow data from a recent cycle of a BWR core that contained four different modern BWR fuel assembly designs: GE14, GNF2, SVEA-96 Optima 2, and ATRIUM-10 (all ML fuel assembly types). The data from the core simulator model has 25 axial nodes at 240 different time/burnup points throughout the cycle. Variables such as the moderator density, power level, exposure, and control state were extracted from the simulated data for analysis. The extracted core follow data were then used to perform sensitivity studies to show what fuel and operational characteristics lead to selection of bounding values pertinent operating parameters. Because the data from Ref. C-3 are proprietary in nature, they are not used directly in this report. The identified limiting data and conclusions from Ref. C-3 are used to justify the analysis approaches used in this document.

Section 6.2.3 of Ref. C-3 uses the end-of-cycle axial burnup profile data from a core simulator to perform depletion and criticality calculations with all of the axial profiles at burnups of 30, 40, and 50 GWd/MTU. The $k_{eff}$ results of the criticality calculations were plotted versus the sum of the relative burnups for a variable number of top nodes. The number of nodes used included 1, 3, 6, and 11 (out of 25). This process was performed once while assuming a uniform enrichment over the entire axial length of the fuel assembly, and once when considering a 6-inch axial blanket on the top and bottom of the fuel assembly (regardless of whether the blanket length is 6 or 12 inches). The plots were examined for linearity and scatter, especially in the region of low relative burnup sum / high $k_{eff}$. Based on examination of the plots, it was determined that summing the relative burnups over the top three nodes produced the best results for the models with no axial blankets modeled, and summing over the top 6 nodes produced the best results for models which included axial blankets. Fig. C-5 and Fig. C-6 show Figs. 6.14 (models with no blankets) and 6.29 (models with 6-inch blankets) from Ref. C-3. These figures show the clear, well-defined trend in $k_{eff}$ as a function of the sum of the top node-relative burnups.

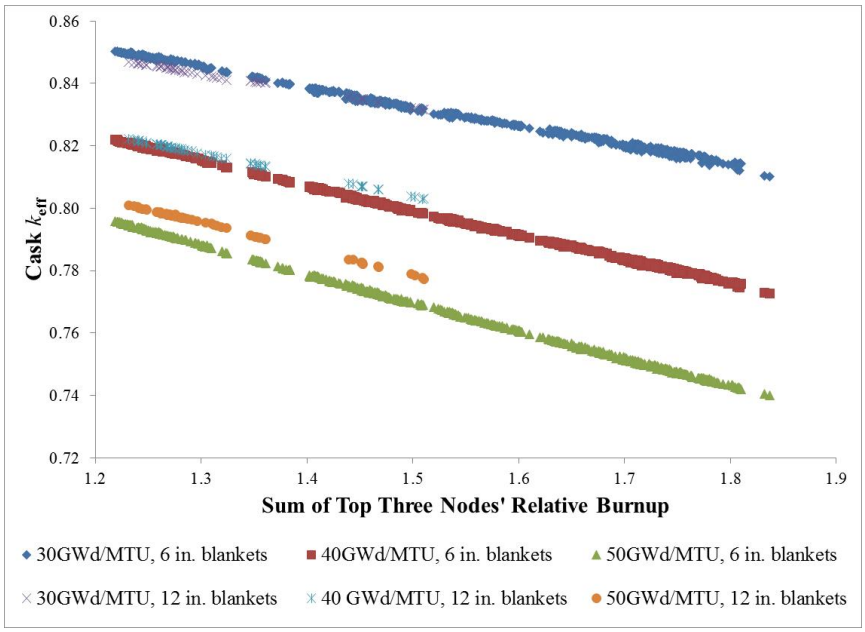


**Fig. C-5. Plot of cask $k_{eff}$ vs. the sum of the top three nodes relative burnup for fuel modeled without axial blankets (reproduced from Fig. 6.14 in Ref. C-3).**

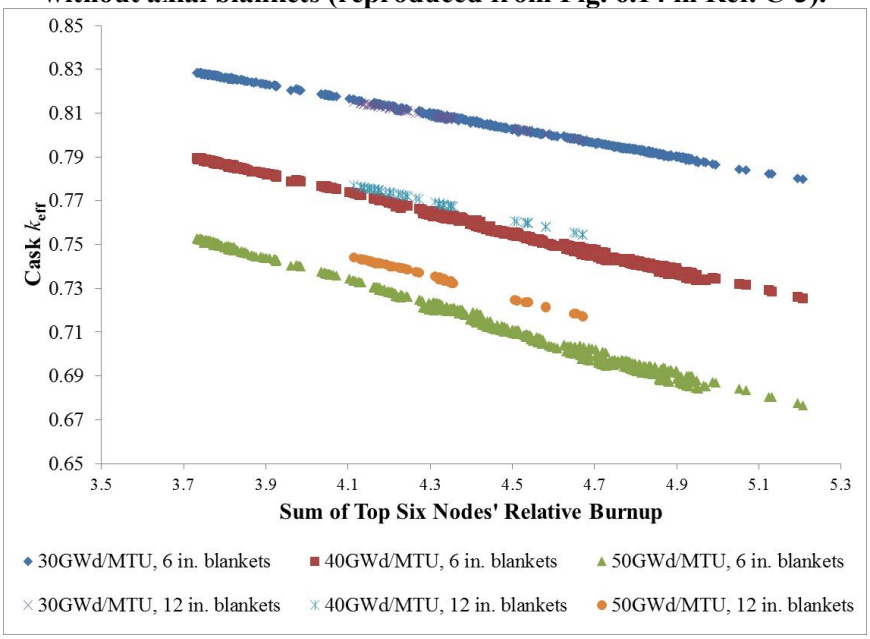


**Fig. C-6. Plot of cask $k_{eff}$ vs. the sum of the top six nodes relative burnup for fuel modeled with six-inch natural uranium axial blankets (reproduced from Fig. 6.29 in Ref. C-3).**

## C-4.2 Sources of Data

The best source of publicly available data for BWR core operations is the commercial reactor critical (CRC) benchmark evaluations. Initially envisioned as a means of using reactor core state-points as a means of validating burnup credit calculations, the CRC summary reports contain the detailed fuel and operational information necessary to construct both depletion and Monte Carlo models. The CRC data from the three sites used here are discussed below.

### C-4.2.1 La Salle

Reference C-7 provides information for Cycles 4–8 of the LaSalle Unit 1 reactor. Material and geometry data for the fuel assembly components are included. The fuel assembly designs used at La Salle for the cycles in question were the GE-5, GE-Barrier, GE-Pre-pressurized, GE-8, GE-9, GE-10, and ANF 9 × 9 designs, which are all SLB designs. The assembly average enrichment ranges between 3.007–3.430 weight percent (w/o) $^{235}U$ for the fuel used at La Salle Unit 1 in Cycles 4–8, and the gadolinium loading ranges from 7 rods at an average of 3.5 w/o to 11 rods at an average of 4.5 w/o.

### C-4.2.2 Quad Cities

Reference C-8 provides information for Cycles 9–14 of the Quad Cities Unit 2 reactor. Material and geometry data for the fuel assembly components are included. The assembly designs used at Quad Cities Cycles 9–14 include the GE-Barrier, GE-Pre-pressurized, GE-8, GE-9, and GE-10 (all SLB designs). This report provides fuel assembly design information, including material and geometry data for the fuel assembly components. The fuel assembly enrichments for the Quad Cities Unit 2 CRC data range from 2.986–3.16 w/o $^{235}U$, and gadolinium loading ranges from 7–9 rods at an average of 3.0 w/o.

### C-4.2.3 Grand Gulf

This report (Ref. C-9) provides fuel assembly design information for Cycles 2–8 of the Grand Gulf Unit 1 reactor. Material and geometry data for the fuel assembly components are included. The fuel assembly $^{235}U$ w/o enrichments and gadolinia ($Gd_2O_3$) enrichments for each fuel design of Cycles 2–8 are also presented. The fuel assembly designs used during those cycles included the ANF Pre-pressurized, ANF 9 × 9, and GE Pre-pressurized. All of the assembles from Ref. C-9 were of the SLB design class.

### C-4.2.4 Axial Burnup Profile Selection

The selection process to determine BWR axial burnup profiles used for criticality analysis within UNF-ST&DARDS uses in the regulatory guidance and axial burnup profile data sources discussed above. The data from La Salle 1, Quad Cities 2, and Grand Gulf 1 were conveniently tabulated by Wimmer in Ref. C-10, which groups the 2,213 burnup profiles into burnup groupings of <6 GWd/MTU, > 46 GWd/MTU, and burnup ranges of every 4 GWd/MTU from burnups of 6 GWd/MTU to 46 GWd/MTU. Each profile was segmented into 25 six-inch nodes. Wimmer selected profiles for use in the Yucca Mountain Project, but they only extended to a maximum burnup of 22 GWd/MTU, and they were selected considering axial blankets, while UNF-ST&DARDS does not currently have a means of modeling axial blankets. Wimmer also provided plots only and did not report the selected axial profiles in a tabular manner.

The guidance in Ref. C-3 indicates that the sum of the relative burnup in either the top 3 or top 6 nodes is most highly correlated with canister $k_{eff}$, depending on the presence of axial blankets in the model. Profiles with minimum burnups in both the top 3 nodes and top 6 nodes were selected because, even though the current modeling approach is to uses with a single axially constant enrichment, it may be advantageous to include axial blankets where appropriate in the future (ML and SLB fuel types). The profiles with the minimum burnups summed over both the top 3 and top 6 nodes were down-selected from each of the burnup ranges provided in Ref. C-10. For all burnup ranges except the <6, 22–26, 34–38, and 42–46 GWd/MTU burnup ranges, the profiles selected were identical. The selected burnup profiles were then grouped into burnup ranges of 0–6, 6–10, 10–18, 18–34, and >34 GWd/MTU to align with the burnup ranges used for other analysis sequences within UNF-ST&DARDS. Depletion calculations were

then performed with ORIGAMI using the selected profiles. The assemblies were depleted to the highest burnup corresponding to each of the UNF-ST&DARDS burnup ranges (i.e., 6, 10, 18, 34), as well as a burnup of 45 GWd/MTU for >34 GWd/MTU range. The upper end of the burnup range was selected to maximize the difference in $k_{eff}$ because the profiles should be separated the most at higher burnups. The depleted fuel isotopic compositions were then brought into the single cell MPC-68 model described in Sect. C-3 so that the $k_{eff}$ of each profile could be calculated. The profiles that calculated the highest $k_{eff}$ for each burnup are the limiting profiles for use in the UNF-ST&DARDS criticality analysis methodology and are presented in Table C-6. The uniform axial burnup profile was considered for all ranges and found to be non-limiting in all cases. It is possible that the uniform burnup profile would be limiting or that different burnup profiles would be limiting if axial blankets were considered in the modeling. Future efforts will examine this when UNF-ST&DARDS becomes capable of modeling multiple axial enrichments.

**Table C-6. Limiting relative burnup profiles with the burnup range over which they are applicable**

| | Burnup range (GWd/MTU) | | | | |
|---|---|---|---|---|---|
| Axial node number | 0–6 | 6–10 | 10–18 | 18–34 | >34 |
| 25 | 0.095 | 0.121 | 0.086 | 0.103 | 0.160 |
| 24 | 0.157 | 0.186 | 0.166 | 0.198 | 0.258 |
| 23 | 0.451 | 0.483 | 0.457 | 0.537 | 0.571 |
| 22 | 0.561 | 0.642 | 0.597 | 0.694 | 0.746 |
| 21 | 0.645 | 0.788 | 0.671 | 0.784 | 0.876 |
| 20 | 0.714 | 0.916 | 0.744 | 0.858 | 0.960 |
| 19 | 0.779 | 1.004 | 0.813 | 0.917 | 1.013 |
| 18 | 0.829 | 1.067 | 0.884 | 0.971 | 1.062 |
| 17 | 0.894 | 1.113 | 0.955 | 1.021 | 1.106 |
| 16 | 0.973 | 1.148 | 0.968 | 1.021 | 1.076 |
| 15 | 1.111 | 1.180 | 1.038 | 1.070 | 1.116 |
| 14 | 1.176 | 1.212 | 1.107 | 1.120 | 1.152 |
| 13 | 1.250 | 1.247 | 1.175 | 1.167 | 1.185 |
| 12 | 1.301 | 1.283 | 1.257 | 1.214 | 1.215 |
| 11 | 1.342 | 1.318 | 1.311 | 1.264 | 1.241 |
| 10 | 1.393 | 1.351 | 1.352 | 1.300 | 1.261 |
| 9 | 1.439 | 1.350 | 1.386 | 1.328 | 1.274 |
| 8 | 1.483 | 1.346 | 1.415 | 1.355 | 1.286 |
| 7 | 1.525 | 1.362 | 1.444 | 1.380 | 1.296 |
| 6 | 1.553 | 1.371 | 1.480 | 1.402 | 1.301 |
| 5 | 1.532 | 1.347 | 1.515 | 1.415 | 1.294 |
| 4 | 1.428 | 1.244 | 1.513 | 1.393 | 1.259 |
| 3 | 1.236 | 1.035 | 1.386 | 1.271 | 1.150 |
| 2 | 0.917 | 0.708 | 1.030 | 0.965 | 0.888 |
| 1 | 0.215 | 0.186 | 0.249 | 0.254 | 0.252 |

[a]Node #1 is at the bottom of the BWR fuel assembly.

## C-4.3 Applicability of the Axial Burnup Profiles to Individual Fuel Types

As previously mentioned, all fuel assemblies used to generate the axial burnup profiles considered in the selection of the bounding profiles in Table C-6 are of the SLB fuel type. The SLB fuel type has a single

lattice of fuel rods and natural uranium axial blankets covering at least the top and bottom six inches of the fuel assembly. This section of the report provides justification as to the applicability of those axial profiles to the SLU and ML fuel types. To simplify this evaluation, the comparison of the impacts of using SLB axial burnup profiles and SLU and ML fuel criticality calculations will be treated separately.

Both SLB and SLU fuel use a single lattice for the entire length of the fuel assembly, with the most significant difference between the two fuel types being the absence of natural uranium axial blankets at the ends of SLU fuel and the presence of them at the ends of SLB fuel. Having the natural uranium blankets present in the top of axial profiles generated from the SLB fuel results in a depression of the burnup in the top fuel relative to what would have been generated with SLU fuel. The reduced relative burnups in the upper portion of the assembly will result in higher $k_{eff}$ values than those that would have been calculated if the assembly had the appropriate profile. At this writing there are no known sources of axial burnup profiles for SLU fuel in the open literature. If an open source of SLU axial profiles become available, it will be examined and included if useful.

All ML fuel also has natural uranium blankets and is therefore similar to SLB fuel in that respect. The primary difference between SLB and ML fuel is that ML fuel has at least two distinct radial lattices of fuel rods as a function of the elevation in the fuel assembly. It is not readily apparent what the impact on the axial burnup profile would be based on the inclusion of the lattices with a reduced number of rods in the upper portions of the assembly during depletion. To investigate the effect, the axial burnup profiles provided in Ref. C-3 were used. Reference C-3 provides burnup profiles for one cycle of operation that contained only ML fuel. The data include all of the burnup profiles from the end of cycle and were divided into three groups based on the assembly average burnup: 0– 25 GWd/MTU, 25–40 GWd/MTU, and > 40 GWd/MTU. To evaluate the applicability of the limiting burnup profiles selected in this report, the burnup profiles from Table C-4 were grouped using the same burnup ranges as those in Ref. C-3 and plotted along with the original profiles from Figs. 6.1–6.3 of Ref. C-3. For cases where a burnup group from this report spanned one of the boundaries given in Ref. C-3, the burnup profile was included in both groups. Figures C-7 though C-9 provide plots of the profiles from Table C-4 as black lines along with profiles from Ref. C-3, which are plotted as gray lines.

Examining Figs. C-7 through C-9, it is evident that the axial burnup distributions generated from core simulator models using SLB fuel are more bottom-skewed than the burnup distributions generated from ML fuel. Because the SLB burnup profiles have less burnup in the neutronically important top portion of the fuel assembly, it is reasonable to conclude that the SLB axial burnup profiles will over predict reactivity compared with using the ML axial burnup profiles when considering the same criticality model and are therefore acceptable for use with ML fuel.

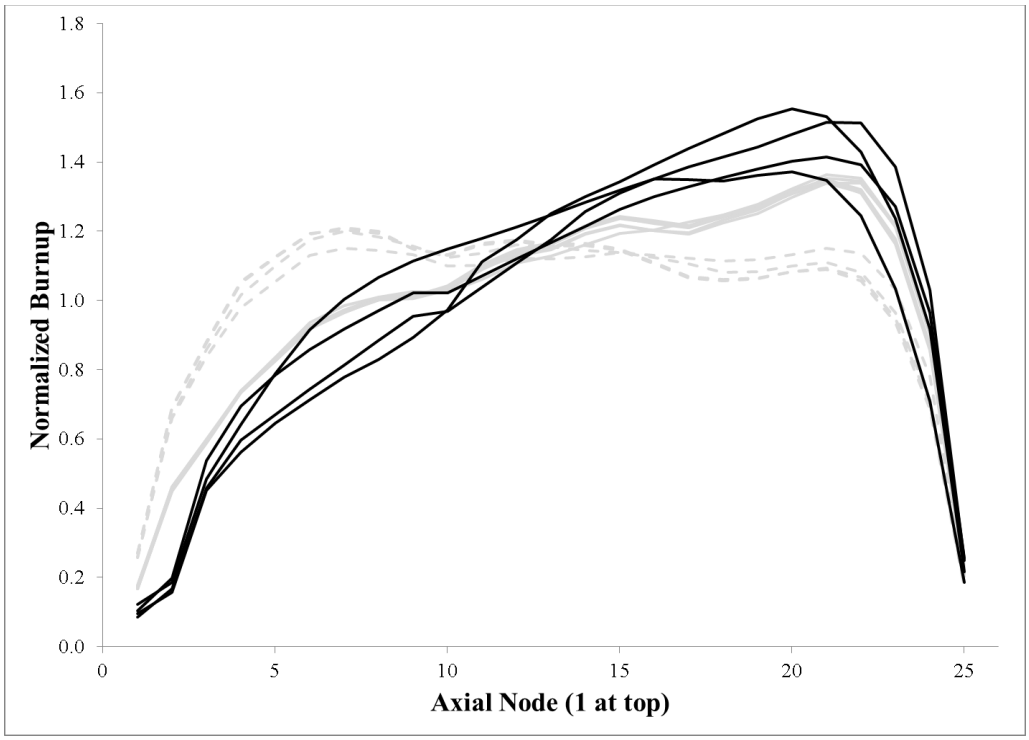


**Fig. C-7. Comparison of burnup profiles from Ref. C-3 (gray) with all limiting profiles generated in this report (black) for burnups less than 25 GWd/MTU.**

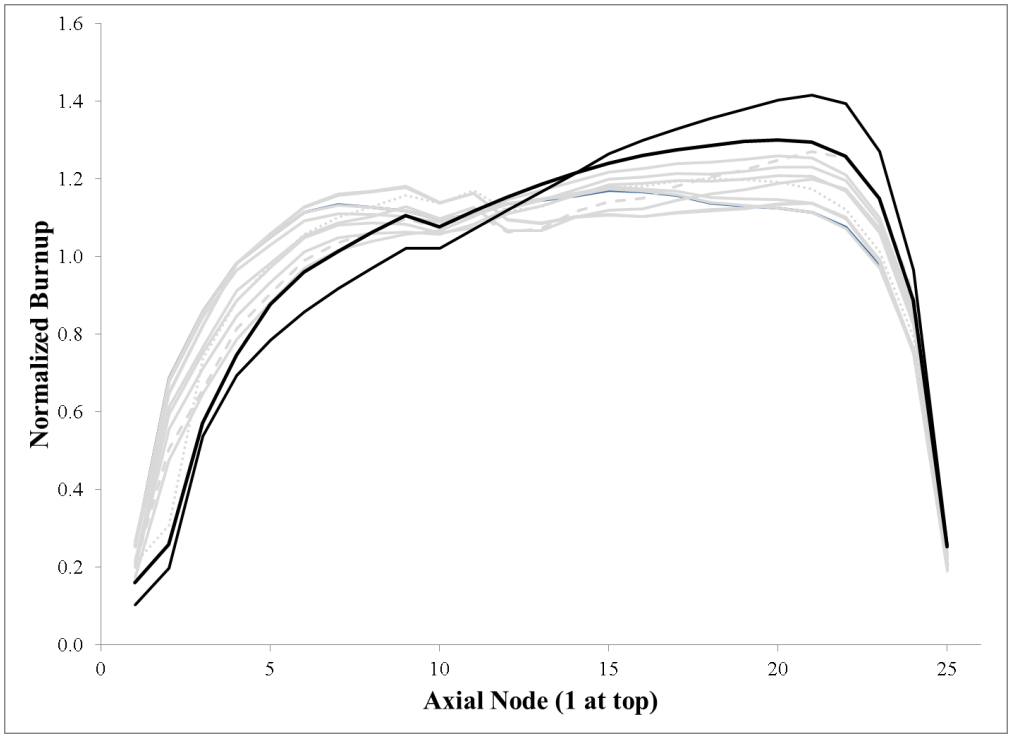


**Fig. C-8. Comparison of burnup profiles from Ref. C-3 (gray) with all limiting profiles generated in this report (black) for burnups greater than 25 GWd/MTU and less than 40 GWd/MTU.**

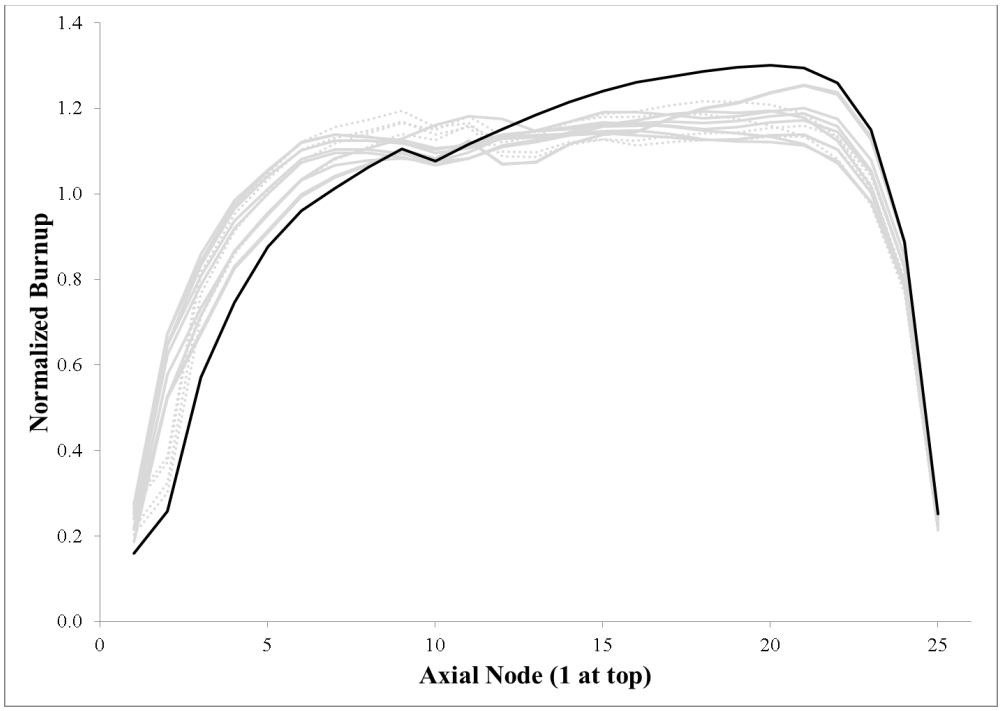


**Fig. C-9. Comparison of burnup profiles from Ref. C-3 (gray) with all limiting profiles generated in this report (black) for burnups greater than 40 GWd/MTU.**

## C-5. Radial and Axial Enrichment Distributions

The fuel enrichment information in UNF-ST&DARDS originates from the GC-859 fuel inventory survey, which provides vague instructions as to how the enrichment of the fuel should be reported. As the predecessor to the GC-859, the RW-859 form defined initial enrichment of the fuel assembly as the "Average enrichment for a fresh fuel assembly as specified and ordered in fuel cycle planning. This average should include axial blankets and axially and radially zoned enrichments." BWR fuel typically uses a significantly larger number of radial enrichments, and virtually all BWR fuel used in the US since approximately 1986 (based on last discharged GE-4 fuel assembly reported in RW-0184) has included axial blankets. Rather than attempt to incorporate a detailed scheme for modeling the radial and axial enrichments, it is logistically desirable to model the fuel with a single enrichment within UNF-ST&DARDS. This section of the report justifies the modeling assumption of a single enrichment for the entire assembly. To simplify analysis of the problem, the justification has been broken down into (1) the justification of using a single radial enrichment and (2) the justification for using a single axial enrichment.

### C-5.1 Radial Enrichment Distribution

As previously mentioned, BWR fuel typically uses significant pin-to-pin variation of enrichment within a given axial elevation. Reference C-2 describes a series of studies to investigate the effect of homogenizing the radially distributed values into a single average enrichment applied across all fuel pins in the lattice for peak reactivity analyses. Reference C-2 studies ran calculations using a range of modeling assumptions, with the most realistic being "Pin-wise Enrichment – Pin-wise Isotopics" (PEPI), and the most approximate being the "Average Enrichment, Average Isotopics" (AEAI). The PEPI technique models each pin in the lattice as having a specified enrichment and tracks the depleted isotopic concentrations for each pin individually throughout the depletion calculations. The AEAI technique models all fuel pins as having radially averaged enrichment and tracks the depleted isotopic concentrations on a lattice average basis.

The study in Ref. C-2 ran both the PEPI and AEAI calculations using burnups of 0 to a maximum of 11 GWd/MTU for the lattice studied. The calculations were repeated for the cases of no gadolinium and light gadolinium loading (typical of peak reactivity analyses). In all cases, it was shown that the AEAI method used for this work resulted in a conservatism of approximately 0.00300 to 0.00500 $\Delta k_{eff}$. The maximum burnup range considered is small relative to the burnups credited within UNF-ST&DARDS calculations. Reference C-2 calculations were 2-D calculations, whereas the UNF-ST&DARDS calculations are 3-D calculations, which use an axial burnup profile. 3-D criticality calculations using an axial burnup are most sensitive to the under depleted top nodes which are typically one quarter to one half of the assembly average burnup. While not ideal, it is reasonable to conclude that the radially averaged enrichment assumption is acceptable for the UNF-ST&DARDS criticality calculations.

## C-5.2 Axial Enrichment Distribution

The database of fuel assembly characteristics used for this effort only has a single average value for the fuel enrichment. All SLB and ML SNF assemblies have natural uranium blankets. Because the natural uranium enrichment of 0.71 w/o was averaged into the assembly enrichment, it is possible that modeling the bulk of the assembly as having a slightly reduced enrichment could be non-conservative for criticality analysis. It is also possible that not modeling the natural uranium blanket in the neutronically important upper portion of the fuel assembly could result in an excessively conservative estimation of $k_{eff}$, which might be desirable to capture more accurately with more detailed modeling. It is noted that SLU fuel is exactly modeled in the axial dimension by the UNF-ST&DARDS criticality modeling approach.

To assess the impact of using only a single average enrichment to model the entire fuel assembly, three sets of calculations were performed. This first set of calculations uses the current UNF-ST&DARDS modeling approach, which models 25 axial elevations with the same enrichment but with axially varying burnups corresponding to the bounding profile for burnup range of 10–18 GWd/MTU multiplied by the assembly average burnup. The burnup profile is used in order to give a similar importance to each axial node in sensitivity study as would be experienced in typical burnup credit calculation, though capturing the exact burnup profile for all burnup ranges is not necessary for a sensitivity study. The second set of calculations uses the same modeling assumptions, except that the top and bottom nodes are modeled as having an enrichment of 0.71 w/o, and the remainder of the assembly is modeled with an enrichment that is increased by a factor large enough to preserve the assembly length averaged enrichment from the fuel database. The third set of calculations is the same as the second set except that residual gadolinium is modeled in the central 21 nodes of the four pins (minimum number of pins from CRC data). The residual gadolinium model uses the same isotopics for all of the non-gadolinium–bearing fuel rods and the cutback and blanket zones in the gadolinium rods, as does the blanketed model. The gadolinium-bearing model includes the depleted isotopic concentrations from an ORIGAMI model with 3.0 w/o $Gd_2O_3$ (minimum loading from CRC data), including the residual Gd-155 and Gd-157 number densities. The residual gadolinium ORIGAMI model conservatively showed a radially flat power distribution that did not account for the power suppression that would occur in a lattice with poisoned and unpoisoned fuel rods. Physically, the gadolinium bearing rods would burn more slowly than the non-gadolinium pins, resulting in additional gadolinium being present in the assembly at higher burnups than was modeled. Fig. C-10 shows the three different models used in the calculations discussed. The different regions are color coded according to the fuel composition. The blue region corresponds to the axially averaged fuel assembly enrichment that UNF-ST&DARDS would normally use, the yellow region corresponds to the natural uranium blankets, the red region corresponds to the fuel that has been adjusted to preserve the assembly average enrichment while accounting for the blankets, and the green region is the same as the red region except with the presence of residual gadolinium in four rods.

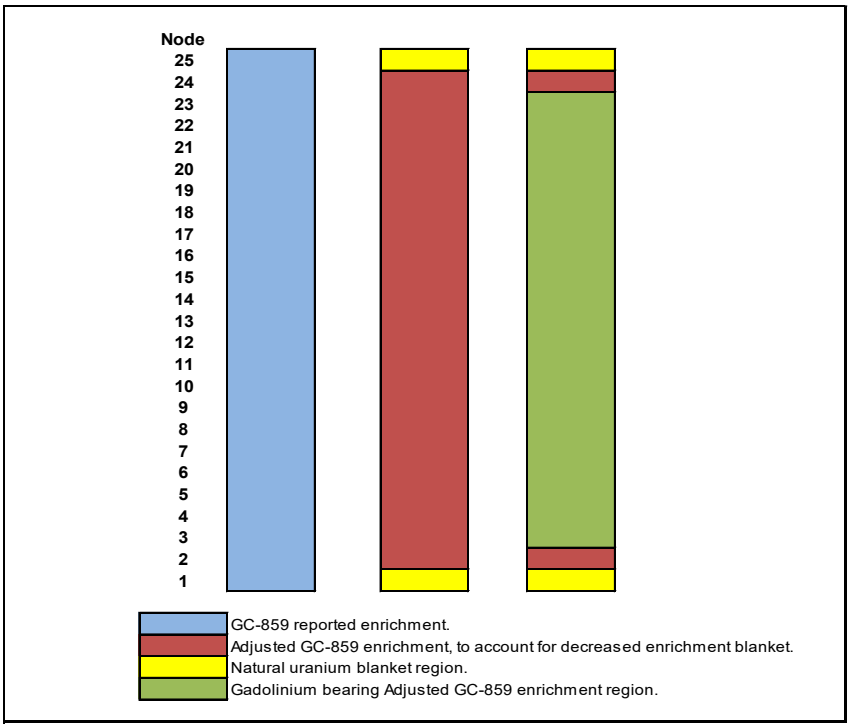


**Fig. C-10. Axial depiction of the three models used in the axial enrichment sensitivity study. Left most model is the UNF-ST&DARDS single axial enrichment model, the middle model contains 6-inch natural uranium blankets on top and bottom and central portion of the fuel assembly has an enrichment that has been increased to preserve the average. The right most model is the same as the middle model, except that residual gadolinium is modeled in 4 pins in the middle 21 nodes of the model.**

The calculations were performed for the three types of models discussed above to determine if axially averaged enrichments are appropriate for criticality calculations. The results of the calculations are plotted in Fig. C-11 for 2 w/o enriched fuel and Fig. C-12 for 4 w/o fuel. Examining Fig. C-11 and Fig. C-12, it can be seen that the distributed enrichment case is more reactive than the average enrichment case over the early portion of the assembly's irradiation history, but the reactivities converge and cross over between 15 GWd/MTU and 22 GWd/MTU, depending on the average enrichment. This indicates that early in the irradiation history, the increased enrichment in the central portion of the assembly overcomes the blanket because the flux distribution is predominantly located in the middle elevations of the assembly. As the assembly burnup increases, the flux shifts to the upper portion of the assembly, where the decreased enrichment at the top of the assembly decreases the reactivity of the distributed case below that of the average enrichment case. To show that axially averaged enrichment case is conservative with respect to a realistic model of a fuel assembly, it is important to consider the gadolinium neutron absorber added to the fuel rods. Surveying the population of fuel assemblies available publicly, the lowest amount of gadolinium found to have been used in SLB fuel (or more recently) was 4 rods with 3 w/o $Gd_2O_3$. It is also noted that the nodes immediately adjacent to the blanket nodes are modeled in the same way that the original distributed calculations were modeled. The distributed enrichment calculations with a conservative representation of gadolinium show that there is sufficient reactivity suppression below the burnup where the average enrichment and distributed enrichment cases cross over to offset the assembly average enrichment modeling assumption. At burnups beyond the cross over, UNF-ST&DARDS over predicts the reactivity of the system.

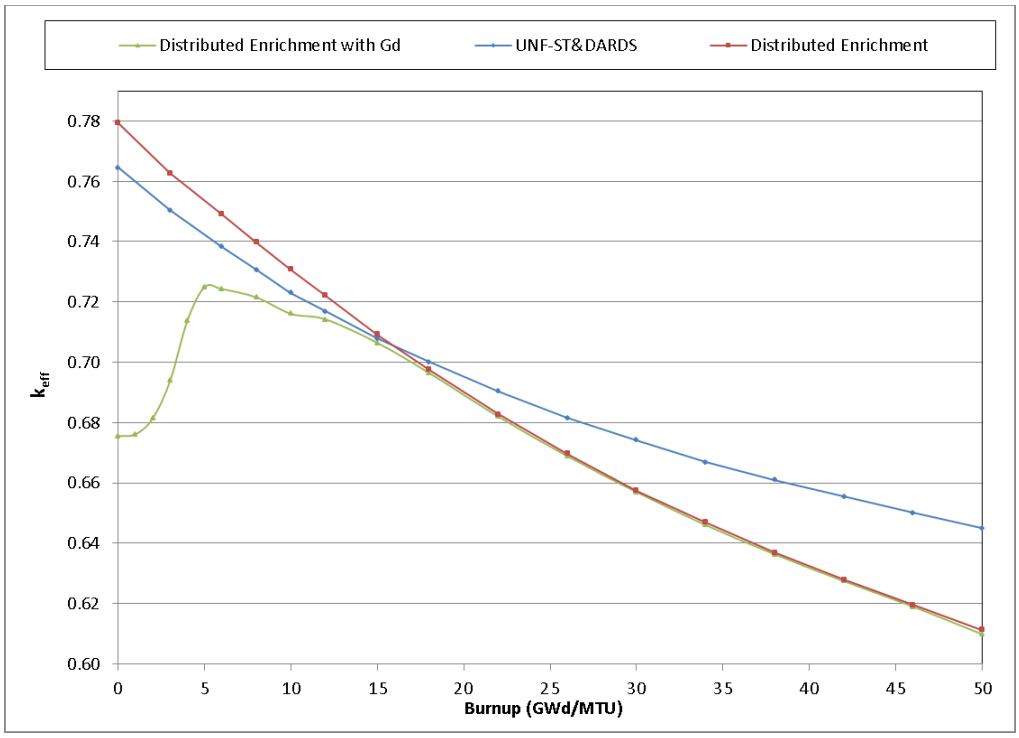


**Fig. C-11. Results of the 2 w/o axial enrichment sensitivity study. The results show that gadolinium is sufficient to overcome the distributed enrichment reactivity increase over the average enrichment at low burnups.**

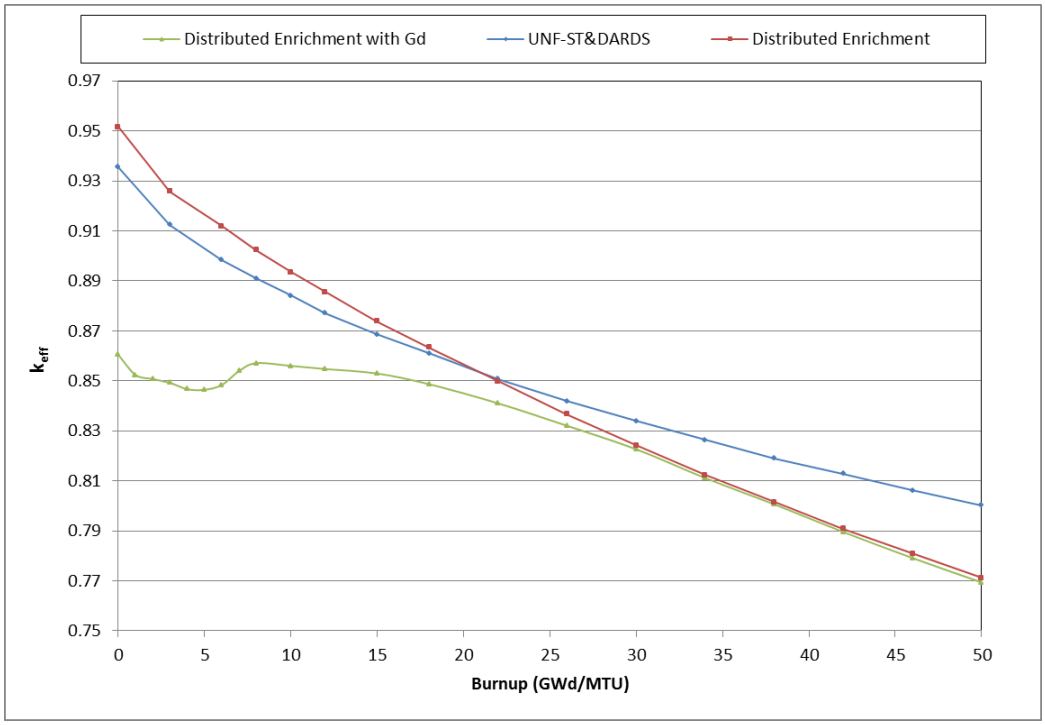


**Fig. C-12. Results of the 4 w/o axial enrichment sensitivity study. The results show that gadolinium is sufficient to overcome the distributed enrichment reactivity increase over the average enrichment at low burnups.**

## C-6. Control Blades and Axial Void Profiles

Phenomena that displace moderator and insert thermal neutron absorbing poisons into the fuel lattice harden the neutron energy spectrum and result in the increased buildup rate of plutonium isotopes during irradiation. The increased generation of plutonium in fuel exposed to these phenomena leads to increased discharged reactivity. For BWR fuel, the two parameters that most dramatically increase reactivity and therefore must be accounted for are the void fraction of the coolant and the amount of control blade insertion that occurs during operation. UNF-ST&DARDS uses depletion calculations that model control full-length axial control blade insertion for the entire assembly life and an axially and temporally uniform moderator density of 0.3 g/cc during depletion. While the 0.3 g/cc moderator density is not a bounding assumption, full control blade insertion for the entire burnup history is an extremely bounding assumption resulting in sufficient margin to offset the non-bounding void profile. This section documents sensitivity studies performed based on the guidance and data presented in Ref. C-3 to show that the presence of control blades in the calculations for the full duration of the burnup is sufficient to offset the use of a non-limiting axial void profile.

Unlike PWRs, BWRs boil the water in the core to generate steam, which is directly used by the turbine to generate power. The process of boiling water in the core leads to significant void formation and water density reduction. Fuel depleted with a lower moderator density will experience a more rapid generation of plutonium compared to fuel depleted with a higher moderator density. This effect is compounded by the fact that the moderator density is at its minimum at the top of the fuel assembly, which has the lowest relative burnup compared to the rest of the assembly, and therefore dominates the reactivity of the fuel assembly as discussed in Sect. C-4. An additional operational difference from PWRs is that BWRs also typically use their control blades as a means of reactivity control and power shaping during operation, resulting in a higher probability of control blade exposure. The control blades are a thermal neutron-absorbing structure, and also displace moderator when present in fuel assemblies and therefore would increase discharge reactivity for exposed portions of the assembly. However, the control blades are mounted on the bottom of the reactor and inserted through the bottom of the core, so control blade insertion into the neutronically important upper portion of the assemblies for extended periods of time is not common.

Similar to the selection of axial burnup profiles, Ref. C-3 provides guidance on the appropriate modeling of axial moderator profiles and blade rod insertion. The temporal variation study performed in Ref. C-3 showed that it was acceptable to use a cycle average moderator density profile to represent the irradiation history of a fuel assembly. Reference C-3 also provided a profile that contains the minimum cycle average moderator density for each of the axial nodes across all of the 624 fuel assemblies in the cycle considered (see Table 4.3 in Ref. C-3). The bounding cycle average moderator density profile is repeated here in Table C-7. With regard to control blade usage, Ref. C-3 investigated the effects of modeling realistic control blade histories. Considering all of the control blade histories for the cycle analyzed, it was shown that an increase in reactivity of up to 1.2% $\Delta k_{eff}$ over ignoring the presence of the control blades was possible.

Three sets of calculations were performed to assess the relative effects of control blade insertion and void profiles. Each set of calculations used ORIGAMI to develop depleted fuel isotopic concentrations that were then placed into a KENO model to determine the reactivity effects. In order to approximately weight the importance of each axial node in the criticality model, a uniform axial enrichment and the axial burnup profile for 10–18 GWd/MTU from Table C-6 were used for all calculation sets. The first set of calculations determined the baseline from which reactivity increases were calculated. The baseline calculations used the default ORIGEN libraries from Scale 6.2, which do not model control blade insertion, with an axially uniform 0.3 g/cc moderator density. The second set of calculations determined the impact of the limiting axially distributed moderator density profile from Ref. C-3. The moderator density profile calculations also used the ORIGEN libraries from Scale 6.2, however, they modeled each axial node as having the moderator density corresponding to the entries in Table C-7. The third set of

calculations determined the impact of control blade insertion. The control blade calculations used ORIGEN libraries generated specifically for UNF-ST&DADS, which used a moderator density of 0.3 g/cc and control blade insertion throughout life for each axial node. The results of the baseline calculations were subtracted from both the moderator density calculations and the control blade calculations to generate the $k_{eff}$ increases from each of the phenomena. The calculations were performed for 2 w/o and 4 w/o fuel from burnups of 0 to 50 GWd/MTU. The results of the studies are presented in Fig. C-13 for 2 w/o fuel and Fig. C-14 for 4 w/o fuel. The results of the sensitivity study in Fig. C-13 and Fig. C-14 show that for both enrichments considered, the full control blade insertion case bounds the bounding moderator density profile case in terms of reactivity increase above the uniform 0.3 g/cc baseline base case. The 2 w/o case showed that the control blades were worth 0.03178 $\Delta k_{eff}$ more than the void profile at 30 GWd/MTU and were worth 0.03976 $\Delta k_{eff}$ more at 50 GWd/MTU. For the 4 w/o case the control blade case was 0.00937 $\Delta k_{eff}$ more reactive at 30 GWd/MTU and 0.01472 $\Delta k_{eff}$ more reactive at 50 GWd/MTU.

The sensitivity studies in this section show that there is a significantly larger reactivity increase caused by full control blade insertion than by the bounding moderator density profile for all cases at reasonable discharge burnups (>30 GWd/MTU). When considering that potential increase of 0.01200 $\Delta k_{eff}$ associated with realistic control blade histories found by Ref. C-3, the effect would be offset (difference between the two lines greater) completely for the 2w/o case for reasonable discharge burnups by the lifetime insertion assumption. The 4 w/o case shows that there are points in life where the lifetime control blade insertion may not be sufficient to offset the entire 0.01200 $\Delta k_{eff,}$ however, it is unlikely that an assembly would experience both a limiting axial void profile and a limiting control blade insertion simultaneously. Additionally, it is not necessary for the UNF-ST&DARDS analytical approaches to bound all parameters, since it is used to obtain realistic margin estimates rather bounding values.

**Table C-7. Limiting axial moderator densities used for sensitivity studies**

| Node | Minimum moderator density (g/cc) |
|---|---|
| 25 | 0.1208 |
| 24 | 0.1077 |
| 23 | 0.1186 |
| 22 | 0.1298 |
| 21 | 0.1238 |
| 20 | 0.1471 |
| 19 | 0.1427 |
| 18 | 0.1497 |
| 17 | 0.1698 |
| 16 | 0.1668 |
| 15 | 0.1871 |
| 14 | 0.2083 |
| 13 | 0.2120 |
| 12 | 0.2389 |
| 11 | 0.2640 |
| 10 | 0.2778 |
| 9 | 0.3209 |
| 8 | 0.3591 |
| 7 | 0.4007 |
| 6 | 0.4657 |
| 5 | 0.5391 |
| 4 | 0.6275 |
| 3 | 0.7065 |
| 2 | 0.7445 |
| 1 | 0.7548 |

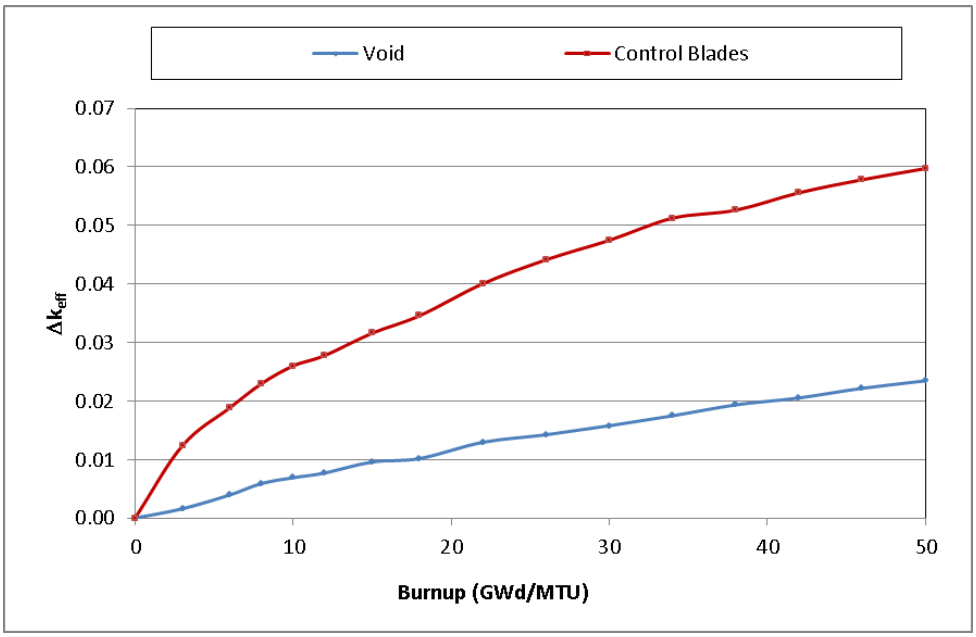


**Fig. C-13. Comparison of the increase in reactivity associated with full cycle control blade insertion and limiting void profile compared to a base case with a 0.3 g/cc moderator density for 2 w/o enriched 8 × 8 fuel.**

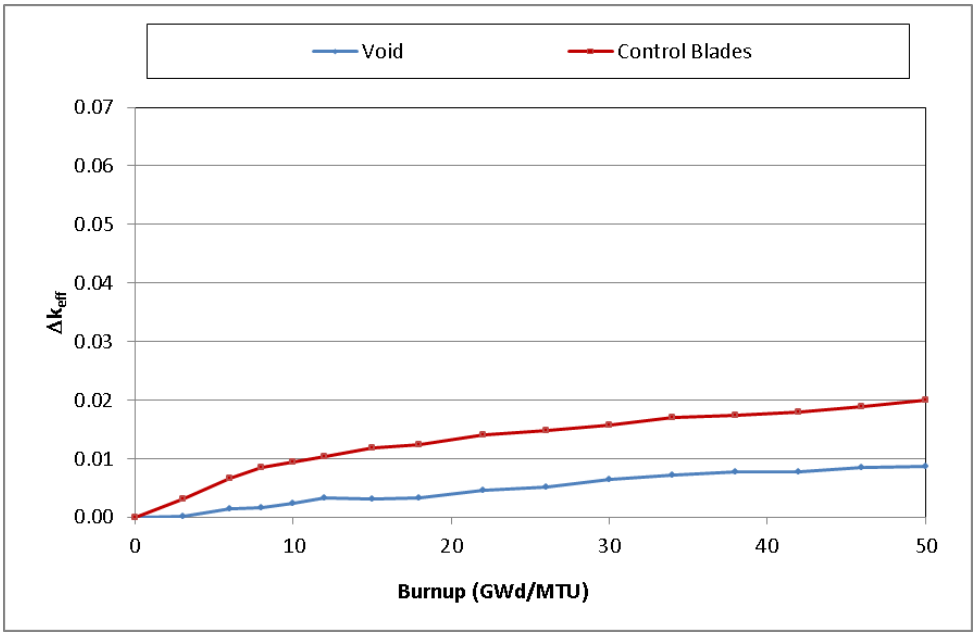


**Fig. C-14. Comparison of the increase in reactivity associated with full cycle control blade insertion and limiting void profile compared to a base case with a 0.3 g/cc moderator density for 4 w/o enriched 8 × 8 fuel.**

## C-7. Conclusions and Future Work

This appendix of the UNF-ST&DARDS criticality analysis report identifies the various BWR fuel types currently present in the current SNF inventory and groups them into the SLU, SLB, and ML categories. Bounding axial burnup profiles are developed using a set of axial burnup profiles from three plants using all SLB fuel. The SLB axial burnup profiles are also shown to be acceptable for use with both SLU and ML fuel assembly types. Modeling of the axial and radial enrichment distributions are also shown to be exact for SLU fuel types, given their lack of natural uranium axial blankets, and are reasonable for SLB and ML fuel, when the presence of gadolinium is considered at lower burnups. Additionally, it is shown that depletion with full control blade insertion throughout life and a moderator density of 0.3 g/cc is sufficient to account the spectral hardening effect introduced by a bounding moderator density profile and a bounding realistic control blade insertion history.

This work uses a number of conservative assumptions or approximations that will show less calculated margin than is possible to demonstrate with a more refined approach. The first item to be improved is to model the axial enrichment modeling for SLB and ML fuel to account for axial blankets. Accounting for axial blankets could result in an additional margin of 0.03500 $\Delta k_{eff}$ for high burnup assemblies. Additionally, axial-dependent geometry modeling should be included to capture the geometry of the ML fuel assemblies more accurately. It would also be advantageous to incorporate Ref. C-3 profiles for the ML fuel assembly designs and/or obtain axial burnup profile data for SLU fuel. It may also be possible to show more margin by incorporating a more refined approach to include the control blade insertion history and moderator density profile effect in the UNF-ST&DARDS ORIGEN libraries.

## C-8. References

1. D. E. Mueller, S. M. Bowman, W. J. Marshall, and J. M. Scaglione, *Prioritization of Technical Issues Related to Burnup Credit for BWR Fuel*, NUREG/CR 7158, ORNL/TM-2012/261, US Nuclear Regulatory Commission, Oak Ridge National Laboratory (2013).
2. W. J. Marshall, B. J. Ade, S. M. Bowman, I. C. Gauld, G. Ilas, U. Mertyurek, G. Radulescu, *Technical Basis for Peak Reactivity Burnup Credit for BWR Spent Nuclear Fuel in Storage and Transportation Systems*, NUREG/CR-7194 (ORNL/TM-2014/240), prepared for the US Nuclear Regulatory Commission by Oak Ridge National Laboratory, Oak Ridge, Tenn. (April 2015).
3. W. J. Marshall, B. J. Ade, and S. M. Bowman, *Technical Basis for the Use of Axial Moderator Density Distributions, Control Blade Usage, and Axial Burnup Distributions in Extended BWR Burnup Credit Analyses*, NUREG/CR-7224 (ORNL/TM-2015/544), Oak Ridge National Laboratory (2015).
4. J. C. Wagner, M. D. DeHart, and C. V. Parks, *Recommendations for Addressing Axial Burnup in PWR Burnup Credit Analyses*, NUREG/CR-6801 (ORNL/TM-2001/273), Oak Ridge National Laboratory (2002).
5. "Characteristics of Potential Repository Wastes," DOE/RW-0184-R1, ORNL, Oak Ridge, Tenn. (July 1992).
6. *RW-859 Nuclear Fuel Data* (survey form), US Department of Energy, EIA, Washington, DC (October 2004).
7. D. P. Henderson, *Summary Report of Commercial Reactor Criticality Data for LaSalle Unit 1*, B00000000-01717-5705-00138 REV 00, Civilian Radioactive Waste Management System M&O Contractor (September 1999).
8. D. P. Henderson, *Summary Report of Commercial Reactor Criticality Data for Quad Cities Unit 2*, B00000000-01717-5705-00096, Rev. 01, Civilian Radioactive Waste Management System M&O Contractor (September 1999).
9. M. K. Punatar, *Summary Report of Commercial Reactor Criticality Data for Grand Gulf Unit 1*, TDR-UDC-NU-000002, Rev. 00C, Bechtel SAIC Company, LLC (September 2001).
10. L. B. Wimmer, *BWR Axial Burnup Profile Evaluation*, 32-5045751-00, Framatome ANP (July 2004).
11. P. Urban and D. Bender, *Advanced Fuel Assemblies for Economic and Flexible Operation of Light Water Reactors*, Framatome Advanced Nuclear Power (2001).
12. *Reference Fuel Design SVEA OPTIMA 3*, WCAP-17769-NP, Westinghouse Electric Company (November 2013).
13. "Nuclear Fuel Data Survey," Form GC-859, EIA, Washington, DC (July 2012).